ALKANE OXIDATION USING METALLOPHTHALOCYANINE AS HOMOGENEOUS CATALYSTS

THESIS

Submitted to

Rhodes University

In fulfillment of the requirements for the degree of

MASTERS DEGREE OF SCIENCE

By

NATASHA DENISE GROOTBOOM

January 2002

Department of Chemistry

Rhodes University

Grahamstown

In Memory

Of my late grandparents,

Gorden Howard,

Daniel and Ann Grootboom

Acknowledgements

I would like to thank my supervisor, Prof. T. Nyokong for her guidance and support throughout the duration of this project and the writing-up of this manuscript.

I would also like to thank my mom, Patricia, for all the sacrifices she had made for me, the support she has given me and for her constant encouragement. For having taught me that scarifies have to be made in order to be successful in life and just for being my mom, thank you, Mommy!!!!!!!

To my dad, Dennis, for the financial scarifies he had made for me and the support he has given me.

My brothers Edward and Denzil for a good laugh.

My grandparents, Julia and Andrew, aunts, Sister 'Rose', Beryl, Melinda, Tisha, Lorna, Nicolette and uncles Glen and Joseph for their hospitality throughout my stay in Grahamstown and their support.

To my boyfriend, Max thank you for listening to me during stressful times and for proof reading this manuscript.

To Dr. Mattys Janse van Vuuren for enriching my insight on alkane oxidation chemistry.

To Mr. Sonnamen, thank you for your assistance with the GC.

To Sasol for there generous financial support.

And to the Lord, for having carried me during times of discouragement.

Abstract

Iron polychlorophthalocyanine ($FePc(Cl)_{16}$) and tetrasulfophthalocyanine ($[M^{II}TSPc]^{4-}$) complexes of iron, cobalt and manganese are employed as catalysts for the oxidation of cyclohexane using *tert*-butyl hydroperoxide (TBHP), chloroperoxybenzoic acid (CPBA) and hydrogen peroxide as oxidants. Catalysis using the $FePc(Cl)_{16}$ was performed in a dimethylformamide:dichloromethane (3:7) solvent mixture. For the $[Fe^{II}TSPc]^{4-}$, $[Co^{II}TSPc]^{4-}$ and $[Mn^{II}TSPc]^{4-}$catalysts, a water:methanol (1:9) mixture was employed. The products of the catalysis are cyclohexanone, cyclohexanol and cyclohexanediol. The relative percentage yields, percentage selectivity and overall percentage conversion of the products depended on types of oxidant, or catalyst, concentrations of substrate or catalysts and temperature. TBHP was found to be the best oxidant since minimal destruction of the catalyst and higher selectivity in the products were observed when this oxidant was employed. Of the four catalysts investigated $[Fe^{II}TSPc]^{4-}$ yielded the highest overall percentage conversion of 20%.The mechanism of the oxidation of cyclohexane in the presence of the $FePc(Cl)_{16}$ and $[M^{II}TSPc]^{4-}$ involves the oxidation of these catalysts, forming an Fe(III) phthalocyanine species as an intermediate.

Electrocatalysis using $[Co^{II}TSPc]^{4-}$ as catalyst, employed an aqueous pH 7 buffer medium for electro-oxidation of 4-pentenoic acid. An enone is suggested as the only oxidation product of 4-pentenoic acid. No degradation of $[Co^{II}TSPc]^{4-}$ was observed during the electrocatalytic process. In this process water was used as a source of oxygen therefore eliminating the production of by-products from oxidant as in the case of TBHP and

CPBA. This system was studied in an attempt to set up conditions for alkane electrocatalytic oxidation.

Table of Contents

List of Abbreviations

Abbreviation

Cp	=	cyclopentadienyl
CPBA	=	chloroperoxybenzoic acid
CT	=	charge transfer
Cum	=	cumyl
CV	=	cyclic voltammertry
Fe(F_{20}Tpp)	=	meso-tetrakis(pentaflourophenyl-porphinato)iron(III)
Fe(O)	=	iron-oxo-ferryl-intermediate
HOMO	=	highest occupied molecular orbital
LMCT	=	ligand to metal charge transfer
LUMO	=	lowest unoccupied molecular orbitals
M-C	=	metal carbon
Me	=	methyl
MLCT	=	metal to ligand charge transfer
M(TMP)	=	metal tetramesitylporphyrin

M(TNP)	=	metal tetranaphthylporphyrin
M(TPP)	=	metal tetrapheylporphyrin
$[MTSPc]^{4-}$	=	metal tetrasulfopthalocyanine
M(TTP)	=	metal tetra-o-tolylporphyrin
MPc	=	Metallophthalocyanine
NADH	=	Dihydronicotinamide Adenine Dinucleotide
NADPH	=	Dihydronicotinamide Adenine Dinucleotide Phosphate
OTTLE	=	Optically Transparent Thin Layer Electrochemistry
P	=	Porphyrin dianion
Pc	=	Phthalocyanine dianion
RS^+ or RSH	=	cysteine
TBHP	=	*tert*-butylhydroperoxide
UV/Visible	=	ultra violet and visible spectroscopy

List of Symbols

Symbol

A = electrode surface area

C = concentration of electroactive species in solution

D = diffusion coefficient

$E^{o'}$ = formal potential

$E_{1/2}$ = half wave potential

E_f = final potential

E_i = initial potential

E_{pa} = anodic peak potential

E_{pc} = cathodic peak potential

ΔE_p = potential difference

F = Faraday constant

i_{pa} = anodic peak current

i_{pc} = cathodic peak current

n = number of electrons

R = gas constant

v = scan rate

List of figures

Page

List of schemes

Page

List of tables **Page**

1. Introduction

1.1 Alkanes, as alternative starting materials

A large percentage of petroleum industries employ alkenes and aromatic compounds as starting materials. These traditional starting materials posses "activated" H atoms and are therefore susceptible to H atom abstraction under appropriate conditions. Thus the functionalization of these compounds occur with relative ease. Another reason for the popularity of these starting materials is that they are readily available from petrochemical processes [1].

Alkanes are as readily available as alkenes, but are less toxic and a much cheaper alternative to alkenes. The direct oxidation of alkanes offers an attractive cut in process costs. The conversion of naphtha to acetic acid is a good example to illustrate this point, **Scheme 1** [1].

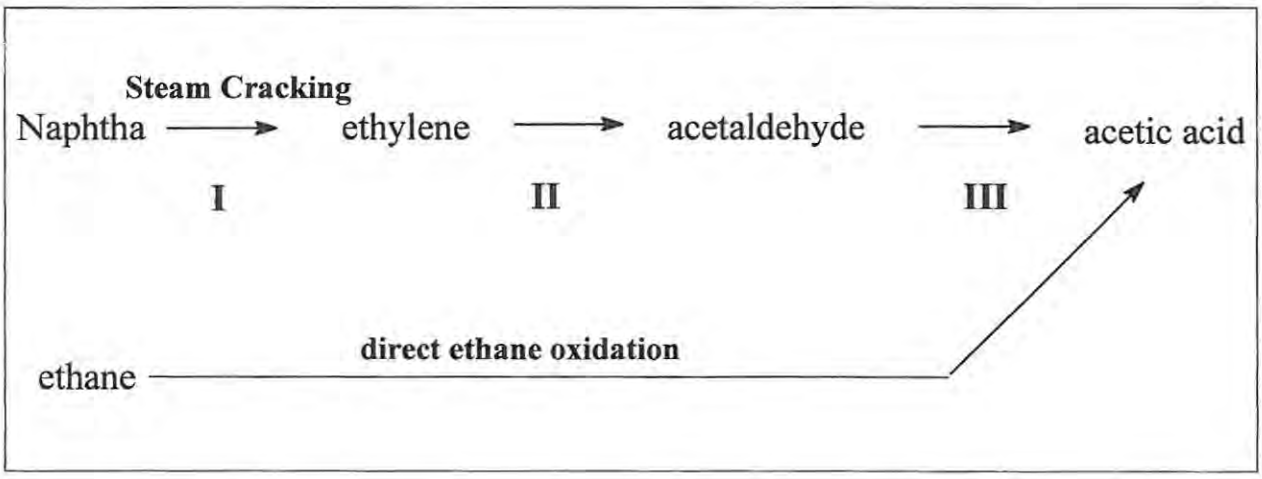

Scheme 1 The formation of acetic acid from naphtha or ethane

For step **I** to proceed (in **Scheme 1**) energy needs to be supplied into the system and a total of three steps (i.e. **I** to **III**) are required to obtain the product of interest. When ethane is directly oxidized the end product is also acetic acid. No energy is required to initiate the latter one step process reaction. Thus one advantage of employing ethane as opposed to naphtha as a starting material is that the former results in a more cost-effective process with production of no unwanted intermediates.

The second advantage for using ethane as a starting material is also due to the environmental regulations cutting down the light alkane content in petroleum. Thus a large amount of research has gone into systems employing alkanes as starting materials [1]. The alkane systems, which are currently under investigation as potential starting materials, are shown in **Table 1**.

Table 1 Alkane systems under current investigation with a potential for use in direct oxidation processes

Alkanes	**Products**
Methane	Formaldehyde or ethene
Methane	Vinyl chloride in the presence of hydrocarbons
Propane	Acrylic acid
n-Butane	Maleic anhydride
Cyclohexane	Cyclohexanol and cyclohexanone

By the 1960's the advances in the catalytic and co-ordination chemistry had achieved functionalization of many compounds such as hydrogen, olefins, aromatics, carbon monoxide and molecular nitrogen. No one had yet attempted to functionalize alkanes and most of this avoidance was due to alkanes' inherent inability to be reactive; its old name is paraffin which means "without affinity". The inherent inability to react is due to the lack of multiple bonds, electron lone pairs and also due to strong C-C and C-H bonds [2].

It however became evident to researchers that if it was possible to activate σ – bonds of H_2, it should be possible to activate σ – bonds of C-H since the bond strength of the latter is weaker than that of σ – bonds of H_2. Metal complexes had the ability to interact with "activated" C-H bonds (i.e. aromatic C-H or C-H α–positioned to double bonds in non-aromatic compounds) resulting in the cleaving of the C-H bond and the formation of a metal-C bond. This indicated that it should be possible for metal complexes to interact with the C-H bonds of alkanes since the bond energies of aromatic and alkene C-H are higher than that of the alkanes [2].

$[PtCl_4]^{2-}$ was shown [2] to be able to catalyze the hydrogen-deuterium exchange not only of the C-H bond attached to the aromatic ring but also the C-H bond belonging to the side chain attached to the aromatic ring. This revealed that Pt(II) complexes could have the ability to attack non-activated C-H (i.e. H atoms in alkanes) bonds. This theory was proven when methane and ethane showed the ability to catalytically exchange their H atoms for deuterium of the solvent. Other ligands and metals proved to be inefficient and non-catalytic at times. It was found [2] that Pt(IV) complexes could oxidize alkanes to chlorides and alcohols in the presence of Pt(II). **Equation 1** and **2** show the formation of methyl chloride and methanol from methane [2].

$$H_2PtCl_6 + CH_4 \xrightarrow[Pt(II)]{} H_2PtCl_4 + CH_3Cl + HCl \quad \text{.....(1)}$$

$$H_2PtCl_6 + CH_4 + H_2O \xrightarrow[Pt(II)]{} H_2PtCl_4 + CH_3OH + 2HCl \quad \text{.....(2)}$$

When cyclohexane was employed in the system above, dehydrogenation occurred instead of oxidation.

It has also been shown [2] that methane could be activated in the presence of a hydrocarbon solvent and catalyst combination systems. In a study using heptane as the solvent, CD_4 as the substrate and catalyst systems such as $TiCl_4 + AlMe_2Cl$; $VCl_3 + AlMe_2Cl$ and $(\eta^5\text{-}C_5H_5)_2TiCl_2 + AlMe_2Cl$ it was shown that CD_4 had the ability to exchange deuterium with the hydrogens of the methyl group of the $AlMe_2Cl$ component of the catalyst (where Me = methyl) [2].

Addition of methane to a multiple bond via a process called hydromethylation, has also been described [2]. Hydromethylation of ethylene and acetylene produced propane and propylene, respectively [2]. These reactions are however not homogeneous and therefore require high temperatures and pressures which could result in the formation of unwanted by-products.

Hydromethylation of carbon monoxide resulted in the formation of acetaldehyde in a system employing Cp_2TiCl_2 - $AlMe_2Cl$ as catalysts (where Cp = cyclopentadienyl). This reaction is however thermodynamically not favourable [2].

1.2 Models for the biological oxidation of alkanes

Mother nature has been known to overcome the most difficult challenges, including the activation of hydrocarbons. Monooxygenases are enzymes responsible for catalyzing the insertion of one atom of molecular oxygen into a C-H bond, generating water.

Oxygen insertion reactions are imperative in organisms for the elimination of harmful hydrophobic compounds such as steroid precursors and pesticides. It is also important for the up-take of essential vitamins and drugs [2,3]. These reactions are of great interest to many industries in particular the petroleum industry which produces thousands of tons of alkanes per annum.

Diooxygenase enzymes on the other hand catalyze the insertion of both atoms of the molecular oxygen, generating no water. Ketogluterate-dependant diooxygenase is an example and it is responsible for the hydroxylation of the C-H bond with gluterate participating [2].

Majority of the monooxygenase and dioxygenase enzymes have a heme-like active site known as iron porphyrin, **Figure 1.1.**

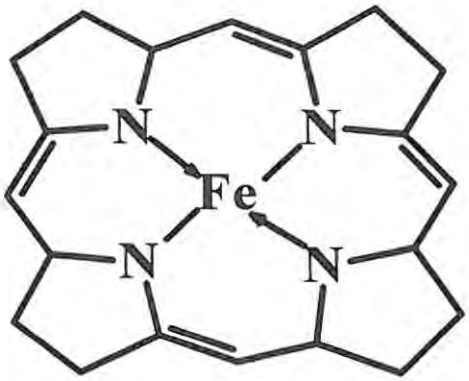

Figure 1.1 Structure of iron porphyrin (PFe)

The porphyrin ring consists of four pyrrol rings linked by methine corners [4]. The monooxygenase enzymes derived from *Pseudomonos oleorans*, have a non-heme active site and are responsible for converting octane to 1-octanol. Monooxygenase enzymes can also transfer oxygen atoms to multiple bonds in alkenes, aromatic compounds, as well as N and S containing compounds [2].

Cytochrome P-450 dependant monooxygenase is an example of a group of monooxygenase enzymes. These enzymes have been known since the early 1950`s. The cytochrome P450-dependant monooxygenases catalyze the oxidation in a coupled process, involving simultaneous oxidation of the hydrocarbon and dihydronicotinamide adenine dinucleotide (NADH) or dihydronicotinamide adenine dinucleotide phosphate (NADPH). **Equation 3** shows the overall oxidation process [2].

$$RH + O_2 + 2e^- + 2H^+ \longrightarrow ROH + H_2O \quad \text{..... (3)}$$

The mechanism of cytochrome P-450 dependant monooxygenase has been well studied and is presented below in **Scheme 2** [2,3].

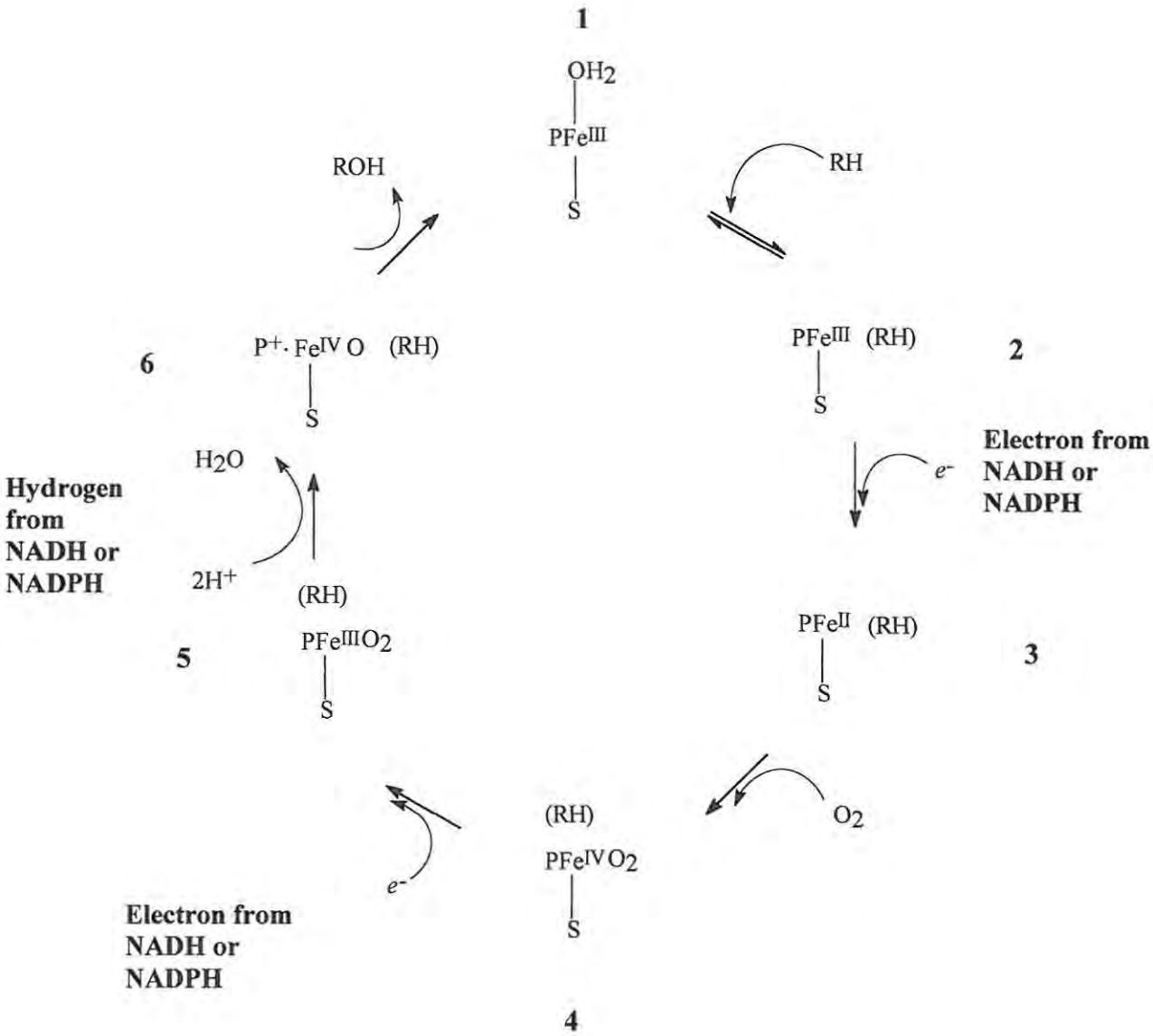

Where
P = Porphyrin

S = cysteine

RH = hydrophobic compound

Scheme 2 The mechanism of cytochrome P-450 enzymes

At the start (**Scheme 2**) the iron porphyrin active site **(1)** is in the +3 oxidation state. An equilibrium exists between this hexa co-ordinated low spin complex **(1)** and the penta co-ordinated (RH does not ligate to the central of the active site of the enzyme but interacts via electrostatic interactions with the hydrophobic "pocket" of the enzyme) high spin complex **(2)**. Complex **(2)** is reduced by electron transfer from NADH or NADPH [2,3].

Binding of oxygen to complex **(3)** leads to the formation of complex **(4)**. Reduction of complex **(4)** by NADH or NADPH gives complex **(5)** which following elimination of water gives the reactive oxygenated complex species **(6)** [2,3]. This reactive species is responsible for a single oxygen insertion to a R- H bond [2,3]. The reactive species are thought to be generated by the heterolytic cleavage of the O-O bond of oxygen from **Scheme 2**.

Ah Lee and Nam [5] studied the oxidation of organic compounds by iron porphyrin catalyst in the presence of labeled water. They reported that (meso-tetrakis(pentaflourophenyl)-porphinato)iron(III) [Fe(F_{20}TPP)] formed the high valent iron oxo porphyrin, Fe(O), at room temperature. At low temperatures, iron porphyrins containing electronegative substituents,

formed the hydroperoxo-iron(III) porphyrin (Fe-OOR) intermediate species, which has the ability to epoxidize alkenes [5]. Many others have recently proposed that the Fe-OOR species also has the ability to hydroxylate alkanes prior to the formation of Fe(O) [6-8]. Nam *et al.* [9] reported for the first time the existence of acylperoxo-iron(III) porphyrin complexes, Fe-OOC(O)R, which are responsible for the hydroxylation of alkanes to alcohols using *m*-chloroperoxybenzoic acid as an oxidant at low temperatures [9].

1.3 Porphyrins as biomimetic complexes

Intensive research has been undertaken during the past few decades in an attempt to mimic cytochrome-P450 and other oxygenases. It started with the oxidation of alkanes using simple metal salts such as Fe^{2+}, Cu^{+} and Sn^{2+} followed by synthetic iron porphyrins [2].

Groves *et al.* [10] were the first to report that iron tetraphenylporphyrin, Fe(TPP), **Figure 1.2**, catalyzes oxygen atom transfer from iodosobenzene to cyclohexane forming cyclohexanol only, at a low yield of 8% (yield based on the iodosobenzene).

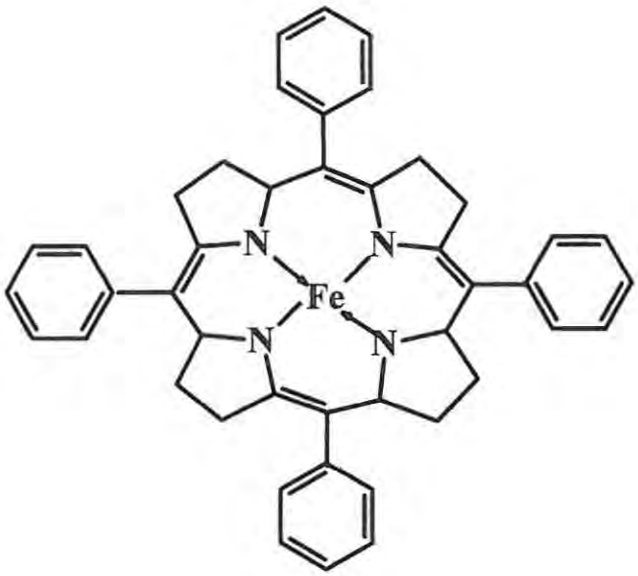

Figure 1.2 Structure of iron tetraphenylporphyrin (FeTPP)

Further oxidation of cyclohexane to cyclohexanone was not observed. Greater success was achieved by oxidizing cyclohexene to cyclohexene oxide and cyclohexenol. Cyclohexadiene was oxidized to a monoepoxide. A mixture of *cis*-stilbene and *trans*-stilbene employing chloro-α,β,γ,δ-tetraphenylporphinatoiron(III) led to an efficient isolation of *cis*-stilbene oxide (82%) and the recovery of *trans*-stilbene. This indicated that the mechanism involved an oxygen transfer step, hence indicating stereo selectivity [10].

Nappa *et al.* [11] reported that a reaction between cyclohexane, iodosobenzene and FeTPP (**Figure 1.2**) in a molar ratio of 1100/20/1 at 25°C, resulted in the formation of a 10% yield of cyclohexanol (yield based on the iodosobenzene) in methylene chloride. Under conditions of high initial cyclohexane concentration, only trace amounts of cyclohexanone were observed.

They had better success with pentane forming a mixture of 1-, 2- and 3-pentanol and trace amounts of 2-, 3-pentanones [11].

Mansuy *et al.* [12] were able to increase the yield of cyclohexanol formation from cyclohexane to 19% yield by changing the solvent from methylene chloride to benzene and increasing the cyclohexane concentration [12]. This agrees with the observations made by Nappa *et al.* [11], that the yield of cyclohexanol is critically dependent on the absolute and relative concentrations of the reactant [11].

Mansuy *et al.* [13] were able to oxidize cyclohexane to cyclohexanol and cyclohexanone by a reaction catalyzed by Fe(TPP) and cumylhydroperoxide. Cyclohexanol (40%) and cyclohexanone (20%) were obtained after 15 min. In the catalytic reaction employing iodosobenzene, 12% cyclohexanol and 1% cyclohexanone were obtained. In this reaction the porphyrin ring is irreversibly oxidized, hence the lifetime of the catalyst is lowered, resulting in diminished yields. Mansuy *et al.* [13] also found that Fe(TPP) and Mn(TPP) were true catalysts when cumylhydroperoxide was employed in that they were unmodified after the reactions. Co(TPP) catalyst gave higher yields and faster reaction times when cumylhydroperoxide was employed, but was found modified at the end of the reaction with a decrease in catalyst activity. It was observed that Cu^{II}, Ni^{II}, Zn^{II}, Mg^{II}, V^{II} and Ti^{II} tetraphenylporphyrins were inactive towards the oxidation of cyclohexane [13].

Groves *et al.* [10,14] also oxidized adamantane to 1-adamantanol, 2-adamantanol and 2-adamantanone employing iodosobenzene as oxidant and Fe(TPP), Fe(TTP) [(5, 10, 15, 20-tetra-

(*o*-tolylporphyrinato)iron(III)] and Fe(TMP) [(5, 10, 15, 20-tetramesitylporphyrinato)iron(III)] catalysts. Oxidation of *cis*-decahydronaphthalene catalyzed by Fe(TPP), Fe(TTP), Fe(TMP) and Fe(TNP) [(5, 10, 15, 20-tetra-1-naphthylporphyrinato)iron(III)], using iodosobenzene as oxidant, gave *cis*-9-decalol, 1-decalol and 2-decalol [10,14].

From here the research of alkane oxidation branched into modification of peripheral substituants on the ring of the porphyrin in the hope of increasing the stability and activity of the catalyst. In 1980 Groves *et al.* [15] reported a 20% yield of cyclohexanol from cyclohexane using iron tetrakis(2-methylphenyl)porphyrin, **Figure 1.3.**

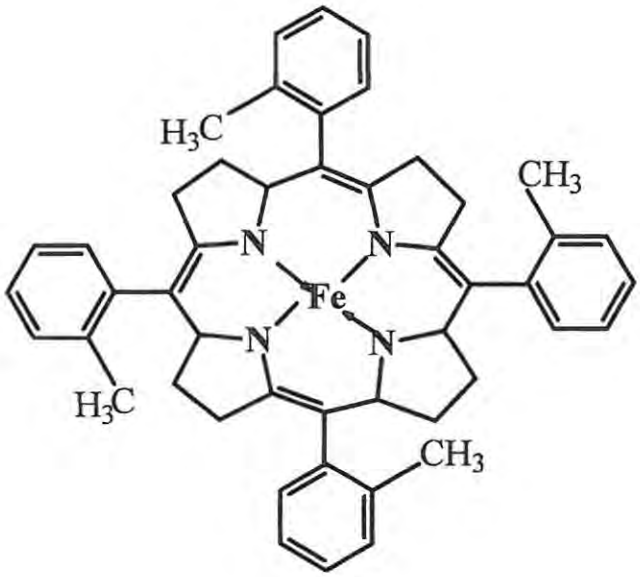

Figure 1.3 Structure of iron tetrakis(2-methylphenyl)porphyrin (FeT $_{2\text{-Me}}$PP)

It was suggested that a steric effect from the 2-methyl substituents was responsible for the higher yield [15]. Chang *et al.* [16], using iron tetrakis(pentafluorophenyl)porphyrin (**Figure 1.4**) and iodosobenzene as oxidant, obtained a high cyclohexanol yield of 71% from cyclohexane oxidation. It was attributed that the increase in yield was due to both steric and electronic effects of the fluorine substituents [16].

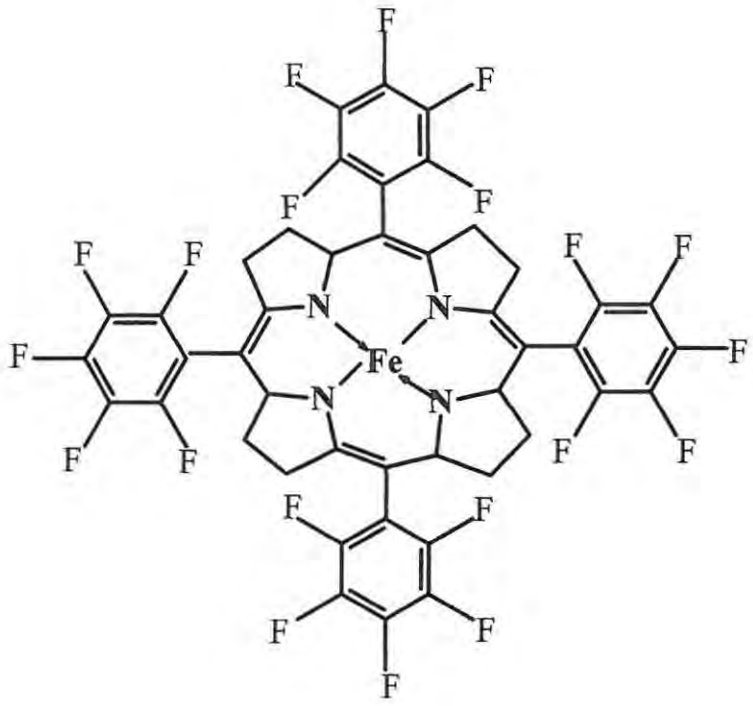

Figure 1.4 Structure of iron tetrakis(pentafluorophenyl)porphyrin ($FeTF_5PP$)

Traylor *et al.* [17] reported that iron tetrakis(2,6-dichlorophenyl)porphyrin, **Figure 1.5**, and pentafluoroiodosobenzene gave a high cyclohexanol yield of 73%.

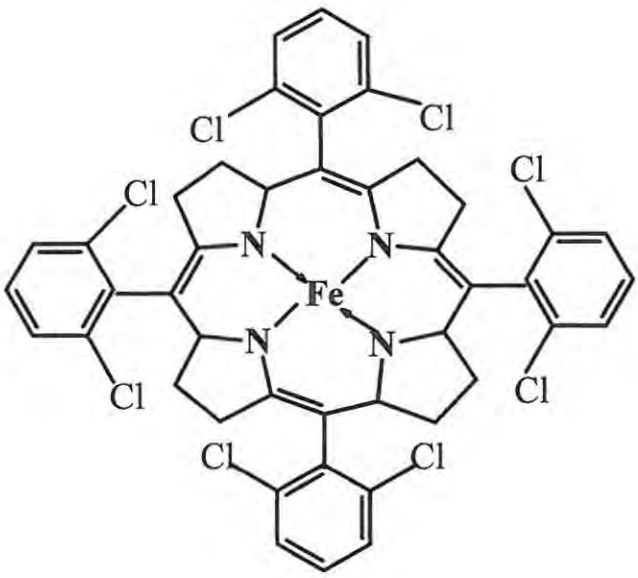

Figure 1.5 Structure of iron tetrakis(2,6-dichlorophenyl)porphyrin ($FeT_{2,6\text{-}Cl}PP$)

It was reported [17] that the chlorine substituents increase the catalyst`s lifetime, thus leading to higher yields [17]. Nappa *et al.* [11] reported that electron-withdrawing groups remove the electron density away from the ring thereby making the porphyrin ring less susceptible to electrophilic attack [11].

At present, a large amount of the research is still focused on different types of electron withdrawing groups on the pyrrol rings of the porphyrin.

1.4 Types of oxidants in biomimetic systems

To mimic the pathway of the cytochrome P-450 using the cheapest and naturally abundant oxygen source, molecular oxygen, is extremely difficult. If molecular oxygen is employed in a system using iron porphyrin for example, it must be accompanied by a reducing agent, to ensure the formation of the highly reactive oxo ferryl intermediate (Fe(O)) [1,2]. Expensive reducing agents such as sodium borohydrides, ascorbic acid, hydrogenated platinum and Zn powder have been employed. The reducing agent, catalyst and substrate occur in the same medium resulting in the reactive Fe(O) being readily reduced before interacting with the substrate [1,2].

The reducing agents, NADPH or NADH in the biological system employing cytochrome P-450, are separated from the active site by a series of proteins to prevent any potentially dangerous biological interaction [3]. This does not occur in biomimetic systems, hence hindering the use of molecular oxygen as a cheap oxidant for complexes aimed at mimicking the cytochrome P-450 enzymes.

In the presence of single oxygen atom donors such as hydrogen peroxide, iodosobenzene and alkylhydroperoxides, iron porphyrins have been shown to form the reactive Fe(O) species without the use of oxygen or NADH and NADPH as reducing agents required by cytochrome P-450. This shortened pathway is known as the "shunt path"[1,2], **Scheme 3**, which bypasses many steps in **Scheme 2.**

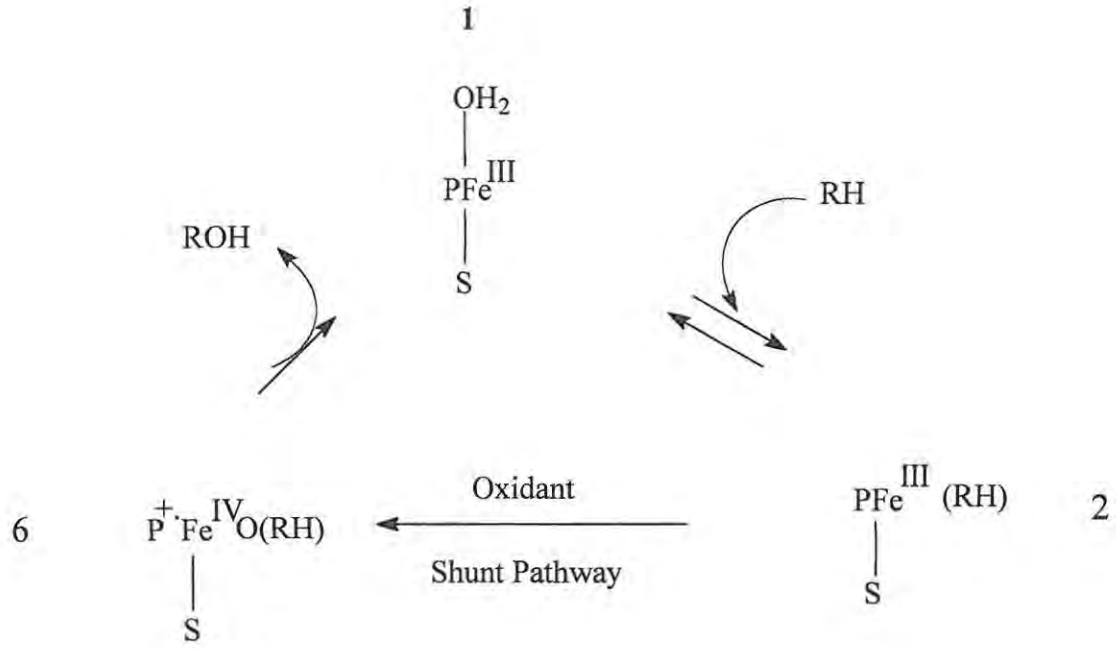

Scheme 3 Mechanism of the "shunt pathway" (numbering as in **Scheme 2**)

It has been reported [2,18] that when cumylhydroperoxide was used as an oxidant in **Scheme 3** the product yield was independent of the nature of the central metal in metal porphyrins, whereas when iodosobenzene was used, the central metal was important. These results suggested that the metal center of the porphyrin is not directly involved in the oxygen atom transfer to the hydrocarbon when cumylhydroperoxide was used. Thus, reactive species in the cumylhydroperoxide system was not the expected Fe(O) reactive species [2,18].

It was suggested [2] that the active species when cumylhydroperoxide was employed as oxidant, alkoxy radical, CumO· (Cum =cumyl), was formed by a "Fenton Type" reaction shown in **Scheme 4**.

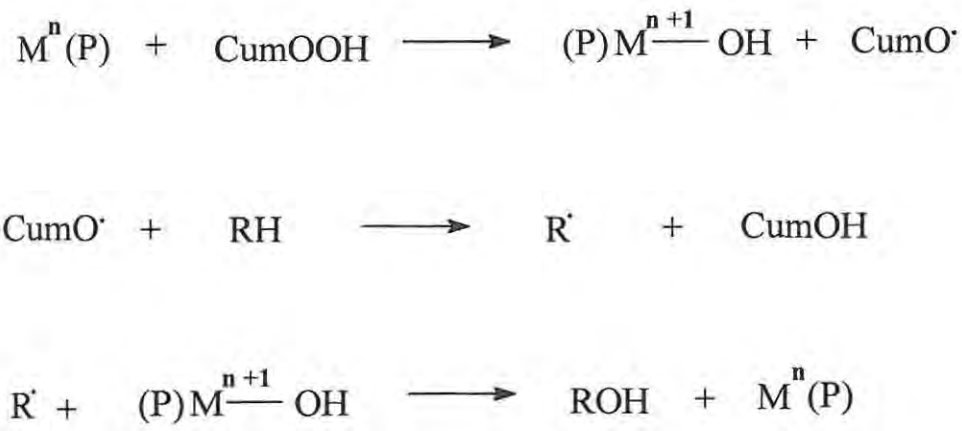

Scheme 4 Mechanism of metalloporphyrin catalysts when cumylhydroperoxide is employed as oxidant

It has also been reported [2] that Fe porphyrins could also heterolytically cleave the O-O bond of alkylhydroperoxide to form the reactive Fe(O) (**6, Scheme 3**). It was found [2] that the oxygen atom transfer to the hydrocarbon was intercepted by the alkylhydroperoxide reacting with the reactive Fe(O) intermediate. This resulted in the formation of ROO·, RO·, ROOR and O_2 within the system.

Hydrogen peroxide (H_2O_2) is suitable as an oxidant from an economical and environmental point of view since it gives rise to water as the only by-product. It is however hazardous to handle in high concentrations or anhydrous form. It is also difficult to employ as an oxidant for organic substrates due to miscibility problem [1].

The use of H_2O_2 in a Fe porphyrin catalyzed system results in rapid dismutation to water and oxygen. The porphyrins also generally decompose with very little oxygen transfer within these systems [2].

Thellend *et al.* [19] reported that in the presence of co-catalysts both Fe and Mn porphyrins catalyzed the oxidation of alkenes and alkanes using H_2O_2 as oxidant. Ammonium acetate proved to be the best co-catalyst. Co-catalysts facilitate the heterolytic cleavage of hydrogen peroxide, with no hydroxyl radical formation, which would decompose porphyrin molecules [19].

Gonsalves and Serra [20] showed in their study that benzoic acid can be used as a co-catalyst in a biphasic system and that it dramatically improved the stability of the porphyrin catalyst in the oxidative media [20]. It has also been reported that the addition of the N-base such as 4-t-butylpyridine enhanced the activity of the investigated metalloporphyrin catalysts. The inhibition of porphyrin oxidative degradation during the course of the reaction was also observed [21].

Most co-catalysts however are also degraded in the oxidative media. Degradation of porphyrins are less when co-catalysts are employed for H_2O_2 oxidation of alkanes [20].

1.5 Metallophthalocyanines as biomimetic catalysts

Metalloporphyrins (MP) are generally unstable and decompose readily in oxidative media [1,22]. The stability of the porphyrins has been increased by ring substitution using halogens. The active

Fe(O) species of porphyrins can be deactivated by the formation of oxo-bridges. Formation of intermediate oxidation states of the porphyrin, which cannot re-enter the oxidation, may also occur [1]. Also porphyrins are not accessible on an industrial scale and are therefore expensive catalysts [1,22].

Metallophthalocyanines (MPc), **Figure 1.6**, overcomes many of the limitations of metalloporphyrins. MPcs are more stable than metalloporphyrins. They are also accessible on an industrial scale and are therefore much cheaper than porphyrins.

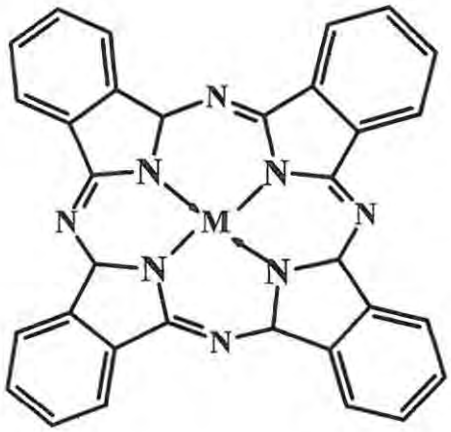

Figure 1.6 Structure of metallophthalocyanine (MPc)

Phthalocyanines were discovered during the production of phthalamide in 1928 at the Grangemouth plant of Scottish Dye [23]. The reactors' glass lining cracked exposing the outer steel casing to the reaction mixture. This resulted in the formation of a blue impurity, which was

isolated and called phthalocyanine by Linstead [23]. Phthalo is named after the precursor phthalic acid and cyanine originates from the Greek word for blue [23].

Linstead was the first to elucidate the structure of phthalocyanine in the early 1930`s. The study revealed that the phthalocyanines contain a ring system of eight isoindole units, linked by aza nitrogen atoms. The phthalocyanine`s eighteen π electron aromatic macrocycle structure proved to be related to the naturally occurring porphyrins. Both phthalocyanine and porphyrin central cavities can host a variety of metal cations and metalloids [23]. They are both macrocyclic, differing only in the components linking the rings. Thus, due to such great similarities in structure, porphyrins and phthalocyanines share similar chemical and physical properties.

Since the discovery of phthalocyanines, thousands of tons are produced to satisfy the worldwide demand. Phthalocyanines have diverse applications ranging from dyes to drugs (for the treatment of cancer) [23].

Phthalocyanines have been employed as catalysts for the oxidation of many reactions. Kaliya *et al.* [22] reported on the possible improvement of the triarylmethanic dye industry by replacing the existing heavy metal oxidants with phthalocyanines using dioxygen as an oxidant. They also developed a new heterogeneous CoPc-based catalyst for the cleaning up of wastewater through oxidation. They improved an already existing phthalocyanine based 'Merox' process (hydrocarbon oxidation) by developing a more stable and catalytically active substituted CoPc catalyst.

With colleagues from Milan University, Kaliya *et al.* [22] also showed that the epoxidation of olefins by peracetic acid in the presence of phthalocyanine solutions were molecular and 100% chemiselective. They oxidized naphthalene, naphthalene methyl derivatives and phenols to 1,4 quinones with yields of up to 60% [22].

Halogen and cyano peripherally substituted phthalocyanines have been used as heterogeneous catalyst for the oxidation of cyclohexane. Using these MPcs, Ratnasamy and Raja [24] reported cyclohexanol, cyclohexanone and adipic acid as oxidation products with conversions ranging between 6% and 24%wt.

The use of supported PdPc as a catalyst for the partial oxidation of methane resulted in the formation of ethane rather than methanol, whereas when RuPc, or CoTPP and MnTPP were employed, methanol was produced [25]. The only observable products for the oxidation of methane using FeTPP, RuTPP, FePc and CoPc as catalysts were carbon dioxide and water [25].

Raja and Ratnasamy [26] encapsulated iron, copper and cobalt phthalocyanines into zoelites X and Y for the conversion of methane to methanol and formaldehyde. They used molecular oxygen and *tert*-butylhydroperoxide (TBHP) as an oxidant and reported the formation of low amounts of carbon dioxide, at high conversion rates [26].

Parton *et al.* [27] and Vankele *et al.* [28] encapsulated Fe(II)Pc into zoelite Y pores and used it as a catalyst by employing TBHP as oxidant for the oxidation of cyclohexane. They reported a conversion of up to 25% with a 95% selectivity towards cyclohexanone [27,28]. Balkus *et al.*

[29] reported that zoelite encapsulated ruthenium perfluorophthalocyanine was an active catalyst towards the oxidation of cyclohexane [29].

Alumino silicate supported perfluorinated CoPc was found to be more active and selective for cyclohexane oxidation than unsupported species [30]. Higher activity and selectivity were also observed when CuPc was incorporated into a Y zeolite [27]. Carbon black supported FePc has been employed for selective oxidation of cyclohexane [31].

The use of MPc complexes as catalysts for chlorinated phenols, using oxidants such as hydrogen peroxide, has received considerable attention in recent years [32-38]. Iron(II) tetrasulfophthalocyanine $[FeTSPc]^{4-}$ was in particular found to efficiently catalyze the oxidation of trichlorophenol with high turnover rates [35].

Thus phthalocyanines have shown remarkable diversities within the catalytic domain. They have proved to be stable, catalytically active and selective. However, these complexes have been used only as heterogeneous catalysts for alkane oxidation, and in this thesis their use as homogeneous catalysts for cyclohexane oxidation was explored. Cyclohexane was used as a general model for alkane oxidation.

$FePc(Cl)_{16}$, $[FeTSPc]^{4-}$, $[MnTSPc]^{4-}$ and $[CoTSPc]^{4-}$ are employed as homogeneous catalyst for the oxidation of cyclohexane using oxidants H_2O_2, TBHP and *m*-chloroperoxybenzoic acid (CPBA). **Figure 1.7** shows the structures of the above mentioned catalysts.

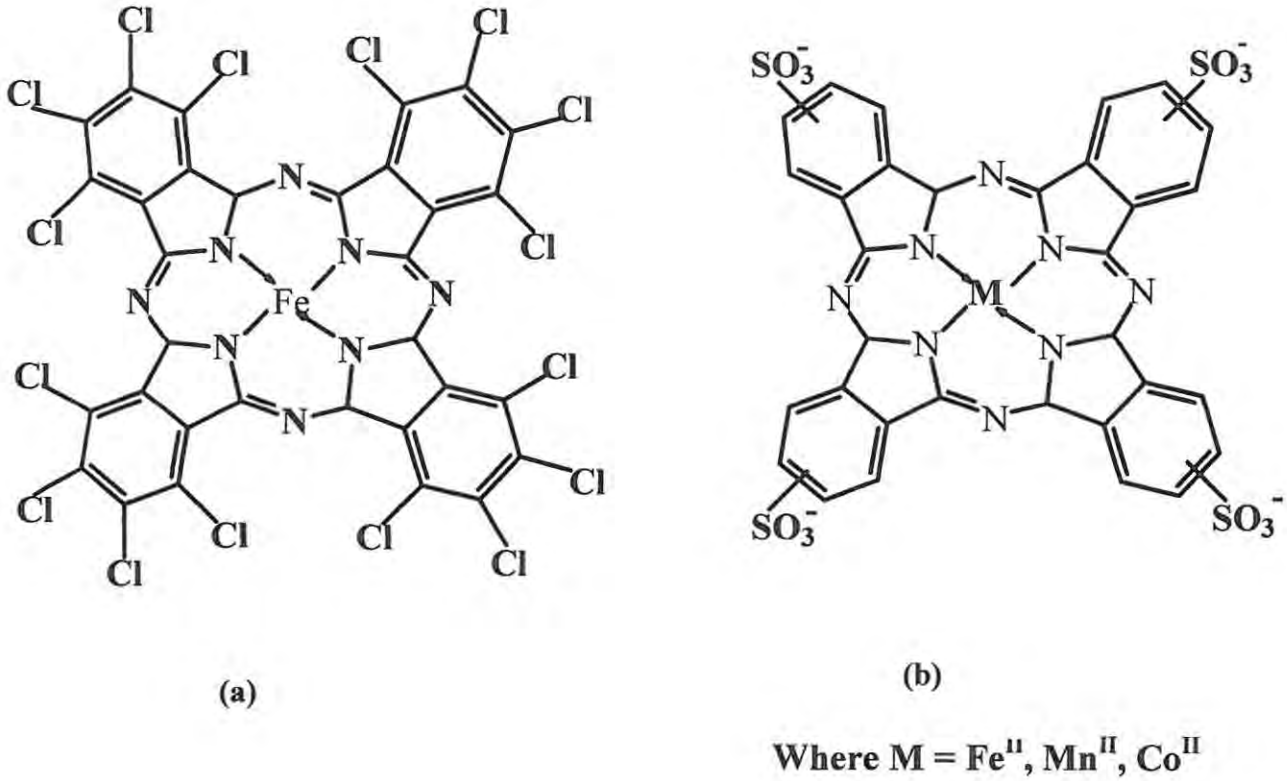

(a) (b)

Figure 1.7 Structures of **(a)** iron hexadecachlorophthalocyanine, $FePc(Cl)_{16}$ and **(b)** tetrasulfophthalocyanine, $[MTSPc]^{4-}$

Aims of thesis

To use MPc complexes, $FePc(Cl)_{16}$, $[FeTSPc]^{4-}$, $[MnTSPc]^{4-}$ and $[CoTSPc]^{4-}$ as homogeneous catalysts for the oxidation of cyclohexane using three different oxidants, H_2O_2, TBHP and CPBA.

To use $[CoTSPc]^{4-}$ as a homogeneous electrocatalyst for oxidation of an alkene with the aim of establishing conditions for possible electrocatalytic oxidations of alkanes.

To study the stability of $FePc(Cl)_{16}$, $[FeTSPc]^{4-}$, $[MnTSPc]^{4-}$ and $[CoTSPc]^{4-}$ catalysts during catalysis using the UV/Visible spectroscopy (UV = ultra violet). These catalysts were chosen because they have active central metals, which may generate reactive intermediates needed for the oxidation reactions.

1.6 MPc complexes as homogeneous electrocatalysts

MPc complexes are excellent electrochemical catalysts due to the accessibility of a range of oxidation states of the Pc ring and the central transition metal [39-46]. MPc complexes have been well studied as heterogeneous electrochemical catalysts, and less as homogeneous catalysts.

In homogeneous catalysis, the catalyst and substrate are in a single phase. During the catalytic process, the catalyst and substrate form an adduct which is transported to the electrode surface where charge transfer occurs. After the formation of product the catalyst-substrate adduct spontaneously decomposes, regenerating the catalyst. Examples of the use of MPc complexes as homogeneous catalysts include, reduction of nitrite [47] and the oxidation and reduction of nitric oxide [48].

In heterogeneous catalysis, the catalyst is adsorbed onto the electrode surface. The adsorbed catalyst is believed to form an adduct with the substrate at the surface of the electrode. The catalyst act as a mediator via which charge is transferred between the electrode and the substrate. Many heterogeneous catalytic examples are known such as, (1) oxygen reduction [49, 50], (2) oxidation of cysteine and other thiols [51-53], (3) reduction of carbon dioxide [54-56], (4)

reduction of thionyl chloride [46], (5) reduction of nitrite [57, 58] and (6) oxidation of cysteine-containing proteins [43]. The proposed electrocatalytic mechanisms for CoPc catalyzed cysteine oxidation in acid media is shown in **Scheme 5** [58].

$$Co^{II}Pc \longrightarrow Co^{III}Pc + e^-$$

$$Co^{III}Pc + RSH \longrightarrow Co^{II}Pc + RS^{+\cdot} + H^{+\cdot}$$

$$2RS^{+\cdot} \longrightarrow RSSR$$

Where RSH = cysteine

RSSR = cystine

Scheme 5 Mechanism of electrocatalytic oxidation of cysteine by cobalt phthalocyanine

No examples for the electrocatalysis of alkanes and alkenes employing MPc complexes as catalysts are known. Water soluble manganese(III)tetrakis(N-methyl-4-pyridyl)porphin (MnTMPyP) electrocatalysized the oxidation of cyclopent-2-ene-1-acetic acid to cyclopent-2-ene-4-one-1-acetic acid. Manganese(III)tetrakis(sulfonatomesityl)porphin (MnTSMP) oxidized cyclopent-2-ene-1-acetic acid to cyclopent-2-ene-4-one-1-acetic acid and cyclopent-2,3-diol-1-acetic acid [59,60]. FeTSMP and ZnTSMP were also employed for the preceding electrocatalytic

oxidation. The proposed electrocatalytic mechanism for porphyrin catalyzed oxidation of alkenes is shown in **Scheme 6** [59].

$$(H_2O)M^{III}P \rightleftharpoons O{=}M^{IV}P + e^- + 2H^+$$

$$O{=}M^{IV}P + \text{alkene} \xrightarrow[H_2O,\ O_2]{} (H_2O)M^{III}P + \text{oxidation products}$$

Scheme 6 Mechanism of electrocatalytic oxidation of alkenes employing metalloporphyrins

The advantages of the above electrocatalytic oxidation system are: (1) water is the source of oxygen and it is plentiful, (2) it is possible to produce different products at different potentials and hence 100% selectivity can be achieved by such a system [59] and (3) there is no need for the employment of expensive oxidants and therefore the possibility of by-products is minimized.

Other electrocatalytic systems exist, such as the hydroxylation of benzene to phenol and hydroquinone. In this system Pd-black was added to a carbon whisker cathode and Fe_2O_3 salt was added to the reaction mixture. In this catalytic process O_2 is reduced at the carbon whisker cathode resulting in the formation of H_2O_2. The redox couple of Fe^{III}/ Fe^{II} enhances the generation of OH radicals from H_2O_2, which attacks the benzene ring [1].

When cyclohexane was used instead of benzene no oxidation was observed. Ethylene can also be electrocatalytically oxidized to acetaldehyde using the redox couples Pd^{2+}/ Pd^{0} and Cu^{2+}/ Cu^{+} as catalysts in HCl solution [1].

In this thesis, water-soluble $[CoTSPc]^{4-}$ has been investigated as a possible homogeneous electrocatalyst for the oxidation of 4-pentenoic acid. This study is essential so as to eventually design a system for alkane electrocatalysis.

1.7 Review of the properties of MPcs

1.7.1 Spectra

Since spectra of MPcs will be used to characterize complexes formed following catalytic oxidation of cyclohexane, it is important to understand the spectra of the neutral, reduced or oxidized MPc species.

The origin of the phthalocyanine absorption spectra can be explained in terms of a combination of metal and ring molecular orbitals. The highest occupied molecular orbital (HOMO) of the phthalocyanine ring is a_{1u} (π) and the next low-lying orbital is a_{2u} (π). The lowest unoccupied molecular orbital (LUMO) is doubly the degenerate e_g (π^*) orbitals [61].

Phthalocyanines have a D_{4h} symmetry configuration, with π to π^* transition between 230 nm and 800 nm. There are two distinct π to π^* transitions, the a_{1u} (π) to e_g (π^*) transition which produces an intense band in the visible region called the Q band and a_{2u} (π)/ b_{2u} (π) to e_g (π^*) called the Soret or B band as shown in **Figure 1.8**.

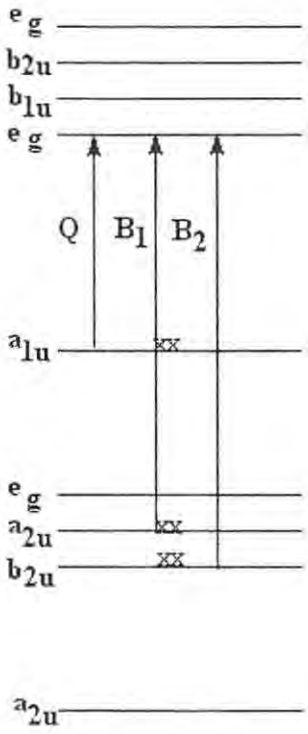

Figure 1.8 Molecular orbital diagram of metallophthalocyanine

The Q band absorbs strongly in the red region between 600nm and 700nm, and the B band absorbs weakly between 300 nm and 450 nm in the blue region, **Figure 1.9**. Thus, due to the strong Q band absorption, phthalocyanine complexes in solutions or solid state

show the characteristic blue and green colours which makes them to be in demand for the dye industry [23].

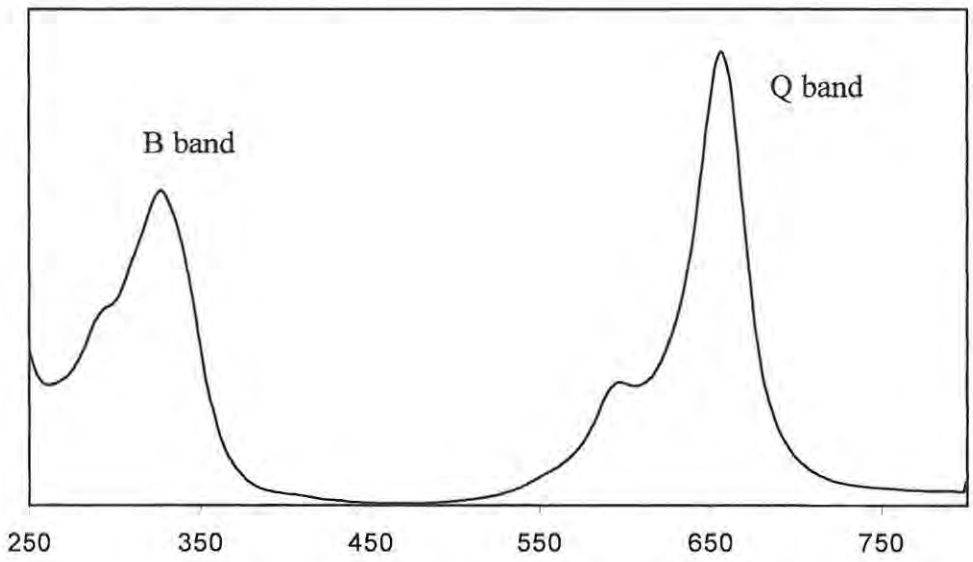

Figure 1.9 General spectra of MPc

Charge transfer (CT) transition also occur within the same region as the phthalocyanine ring π to π^* transitions [62]. The most well known CT bands lie between 450nm and 600nm and the weaker CT bands occur between 700nm and 1500nm. The direction and resultant energies of the CT transitions are dependent on the spin and the oxidation state of the central metal. The CT bands are not distinct and they generally mix with the bands resulting from π to π^* transitions. The CT transitions are assigned as either metal to ligand charge transfer (MLCT) and ligand to metal charge transfer (LMCT). The charge

transfer transitions occur between the phthalocyanine ring π system and the d orbitals of the central metal, with exception to metal of the d^0 and d^{10} group.

Unsubstituted MPc complexes are insoluble. Addition of positively or negatively charged substituents results in improved solubility. Sulfonated Pcs in particular are water-soluble and are known to form aggregated species in solution even at low concentrations.

1.7.2 Electrochemistry

Redox processes of MPc complexes may occur at the Pc ring or at the central metal. Metal oxidation or reduction occurs only if the d orbitals (b_{2g}, e_g, a_{1g} and b_{1g}) of the metal, as shown in **Figure 1.10,** are buried inside the filled Pc orbitals or lie within the HOMO-LUMO gap [63].

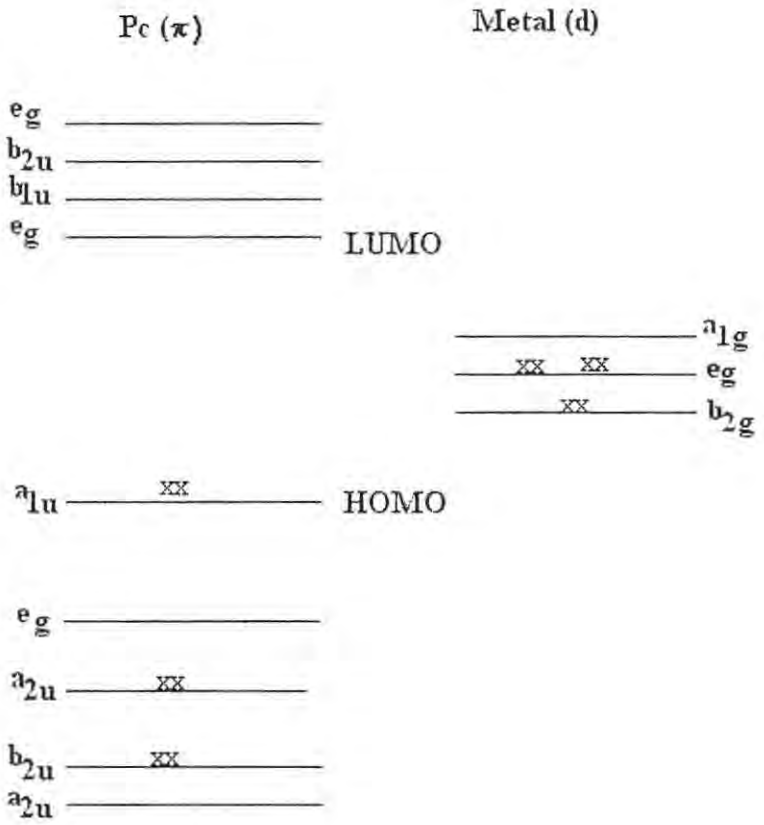

Figure 1.10 A simplified energy-level diagram of a typical metallophthalocyanine. A d^6 central metal is used as an example.

The redox potentials depend on: (1) the nature and oxidation state of the central metal, (2) the nature of the substituents on the Pc ring and (3) the nature of the axial ligands and solvents [63].

The site of MPc redox activities is greatly affected by the nature of the axial ligands. π-Acceptor axial ligands such as CO tend to lower the energies of the metal d orbitals

resulting in a shift of redox activity from the metal to the ring exclusively. σ-Donors increase the energies of the metal d orbitals resulting in redox activities on both ring and the metal [63].

If metal processes occur at potentials lying between the phthalocyanine oxidation and reduction, it is believed that the d orbitals of the metal lie between the Pc HOMO(π) and LUMO(π^*) orbitals [64]. Therefore the number of redox couples observed in a cyclic voltammogram depends on the energy levels of the metal d orbitals with respect to the energy levels of the Pc ring. **Figure 1.11** illustrates a typical MPc cyclic voltammogram.

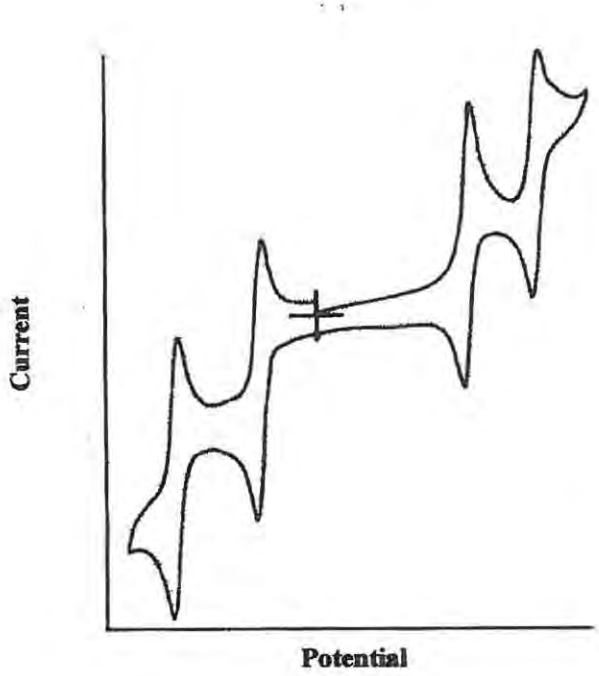

Figure 1.11 Typical cyclic voltammogram of MPc

Redox processes occurring on the metal do not significantly affect the colour or spectra of MPc complexes. Metal oxidation and reduction is characterized by a shift in the wavelength of the Q band without changes in intensity [62].

The phthalocyanine dianion is represented by (Pc^{2-}), $Pc^{2-}M$ complex may be reduced up to four times by successive addition of electrons to the e_g (π^*) LUMO energy level in **Figure 1.10**, forming $[MPc(3-)]^{1-}$, $[MPc(4-)]^{2-}$, $[MPc(5-)]^{3-}$ and $[MPc(6-)]^{4-}$. Ring oxidation of $Pc^{2-}M$ complexes occur by the removal of one or two electrons from the a_{1u} HOMO energy level, forming $[MPc(-1)]^{+}$ and $[MPc(0)]^{2+}$ respectively [62].

Each one-electron ring oxidation or reduction process is characterized by the distinct electronic absorption spectrum. The singly ring oxidized species is purple in colour and has a characteristic broad band near 500 nm. The singly reduced $[MPc(3-)]^{1-}$ species is purple-blue in colour with two weak bands between 500 nm and 600 nm. Whereas the $[MPc(4-)]^{2-}$ species is characterized by the disappearance of one of the reduction bands of $[MPc(3-)]^{1-}$ and the formation of a new band near 520 nm [65]. Redox processes based on the ring result in the decrease of the Q band intensity. Thus, electronic absorption spectra can be used to differentiate between ring and metal based redox processes.

1.8 Background on electrochemistry

Since cyclic voltammetry (CV) was employed to follow catalytic activity, a brief review of CV theory follows.

1.8.1 Cyclic voltammetry

In cyclic voltammertry an applied potential is scanned from an initial potential, E_I, to a final potential, E_f, and back to E_I completing one cycle (see **Figure 1.12.**).

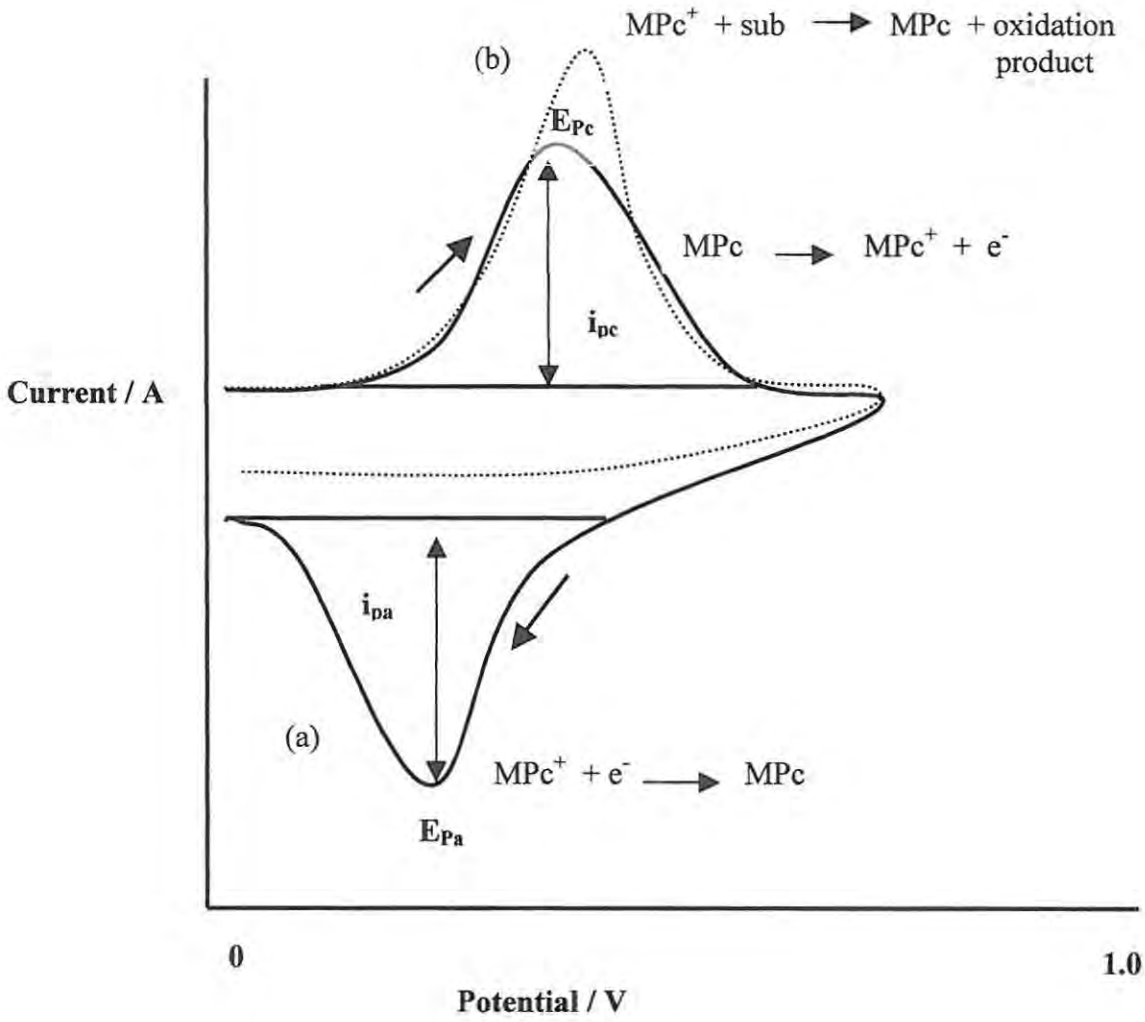

Figure 1.12 (a) Typical cyclic voltammogram (solid line) and **(b)** changes expected on the cyclic voltammogram of a catalyzed reaction (dotted line)

During a positive scan the substrate is oxidized to form an electro-generated product. On the return of the scan the electro-generated product is reduced back to the starting material. Similarly for the negative scan the reduction product formed on forward scan is re-oxidized on return. Cyclic voltammertry is therefore generally used for determining redox couples of systems.

Electrocatalysis is characterized by: (1) an enhancement in peak current, (2) sometimes a shift to less positive potentials and (3) at times a complete disappearance in the return peak. **Figure 1.12** illustrates the effects of electrocatalysis on cyclic voltammograms.

Three processes exist in cyclic voltammatry: reversible, irreversible and quasi-reversible. A redox couple is termed an electrochemically reversible couple if both species rapidly exchange electrons with the working electrode. A reversible couple can be identified by measuring the potential differences between the cathodic and anodic components of a couple. **Equation 4**, applies to both electrochemical and chemically reversible systems.

$$\Delta E_p = E_{pa} - E_{pc} = 2.3RT/nF \approx 0.059V/n \text{ at } 25^{\circ}C \quad \text{.....(4)}$$

Where,

n = number of electrons transferred
E_{pa} = anodic peak potential
E_{pc} = cathodic peak potential
R = gas constant
F = Faraday constant

The formal reduction potential, which is approximately equal to the half-wave potential of the couple, can be calculate by **equation 5.**

$$E_{1/2} \approx E^{o'} = E_{pa} + E_{pc} / 2 \quad \text{.....(5)}$$

The peak current for reversible systems are described by the Randle-Sevick **equation 6.**

$$i_p = 2.69 \times 10^5 \times n^{3/2} AD^{1/2}Cv^{1/2} \quad \text{.....(6)}$$

Where,

n = number of electrons transferred

A = the electrode surface area

D = the diffusion coefficient

C = concentration of the electroactive species in solution

v = scan rate

For reversible systems, when the scan rate is increased both, i_{pa}, (anodic peak current) and i_{pc} (cathodic peak current), **Figure 1.12,** increase linearly with the square root of the scan rate ($v^{1/2}$). If i_{pa} and i_{pc} versus $v^{1/2}$ adheres to a linear relationship, it indicates that diffusion controlled mass transportation occurs.

The values of i_{pa} and i_{pc} for a reversible couple are similar in magnitude. That is,

$$i_{pa} / i_{pc} \approx 1 \quad \text{.....(7)}$$

A redox couple is termed electrochemically irreversible if both species sluggishly exchange electrons with the working electrode. An electrochemically irreversible redox couple is characterized by the separation of peak potentials that are much greater than 0.059V/n, or by lack of return peaks, and by peak potentials which are dependent on the scan rate [66].

A quasi-reversible process is characterized by both charge and mass transport occurring simultaneously. In general, they show more drawn out cyclic voltammograms which have large peak potential separations (ΔE_p), and the peaks are more broad as compared to a reversible process. For a quasi-reversible redox couple, **equation 6** does not hold and no linearity exists between i_p and $v^{1/2}$ [67].

1.8.2 Spectroelectrochemistry

Spectroelectrochemistry was employed to monitor the products of catalysis of alkenes. Spectroelectrochemistry couples electrochemical and spectroscopic techniques for observation of electrogenerated products in homogenous reactions, without the interference from the starting material [66]. In optically transparent thin layer electrochemistry (OTTLE), cell metal minigrids are used for working electrodes, allowing transmittance of the optical beam through the electrode. The minigrids are easily incorporated into a thin layer cell [66].

1.9 Summary of aims:

Biomimetic homogeneous oxidation of cyclohexane using metallophthalocyanines as catalysts.

Electrocatalytic oxidation of an alkene using water-soluble metallophthalocyanines as homogeneous catalysts.

2 Experimental

2.1 Synthesis

2.1.1 Synthesis of iron hexadecachlorophthalocyanine ($FePc(Cl)_{16}$), Scheme 7

Iron hexadecachlorophthalocyanine, $FePc(Cl)_{16}$, was prepared according to the method outlined by Mezt *et al.* [68]. Urea (19.4g), 24.16g of tetrachlorophthalic anhydride **(1)**, 4.04g of $FeCl_2.4H_2O$ and 0.19g ammonium molybdate were finely pulverised and stirred into 150ml of nitrobenzene. The suspension was heated to 180°C - 190°C for $^1/_2$ hour and maintained at the temperature for $4^1/_2$ hours. The reaction pathway is outlined below, **Scheme 7**.

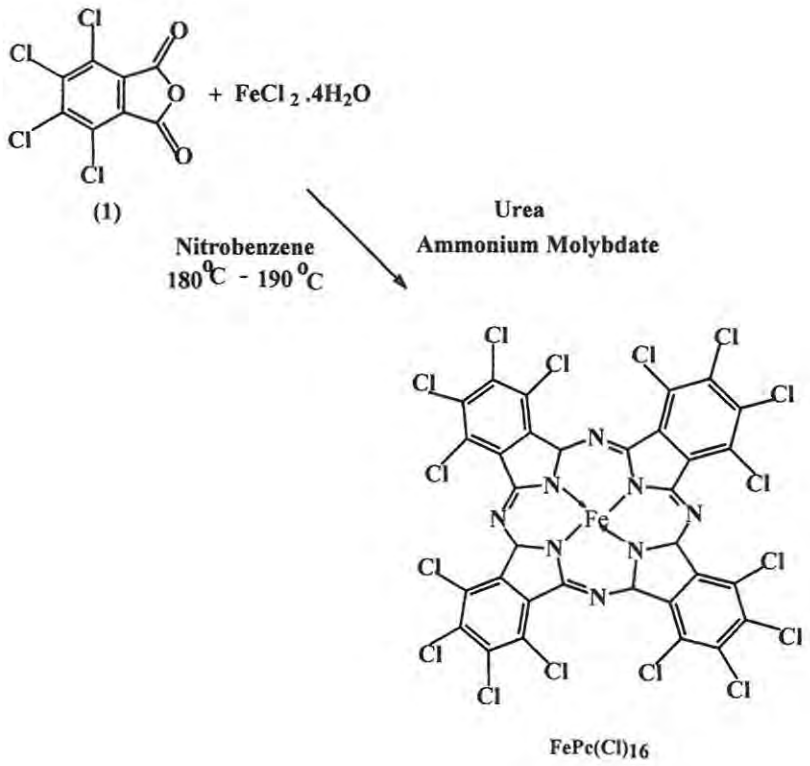

Scheme 7 A simplified synthetic route for $FePc(Cl)_{16}$

The viscous green suspension was cooled to 90°C and diluted with an equal volume of absolute ethanol. This was followed by boiling the crude product with a 1% HCl solution (10min) and a 1% NaOH solution (10min). The crude product was treated with acetone and petroleum ether on a sintered glass until the filtrate was clear. The resultant crude product obtained in this way was Soxhlet extracted an additional three days into chlorobenzene [68]. Yield = 90%. IR (KBr pellets) 1722w, 1652w, 1597w, 1563w, 1544w, 1503w, 1440vw, 1391m, 1304s, 1274m, 1212s, 1159s, 1094w, 954m, 773m, 605vw, 507w. UV/Visible spectra (DMF:dichloromethane): (λ max) 623 nm, 343 nm, and 312 nm. Molar extinction coefficient was determined to be 7.4 x 10^4 dm^3 mol^{-1} cm^{-1}.

2.1.2 Synthesis of iron (II) 4, 4`, 4``, 4```-tetrasulfophthalocyanine [FeTSPc]$^{4-}$, Scheme 8

The monosodium salt of iron(II)4, 4`, 4``, 4```-tertasulfophthalocyanine $Na_4[FeTSPc]^{4-}$ was synthesized according to Weber and Busch [69]. 10.8g of monosodium salt of 4-sulfophthalic acid **(2)**, 1.2g ammonium chloride, 14.5g urea, 0.2g ammonium molybdate and 3.4g ferrous chloride were ground together until a homogeneous mixture was obtained. A 100ml three-necked flask, fitted with thermometer, a condenser and a cork was used for the reaction. 10ml of nitrobenzene was added to the flask and heated to 180°C. The homogeneous mixture was added slowly with continuous stirring while keeping the reaction temperature between 160°C - 190°C. The reaction pathway is outlined below, **Scheme 8**.

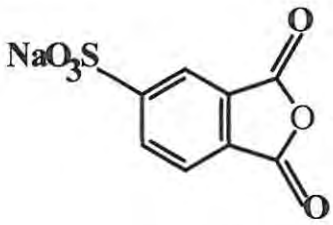

(2) + **metal salt**

Urea

Nitrobenzene → **Ammonium molybdate**
180°C - 190°C → **Ammonium chloride**

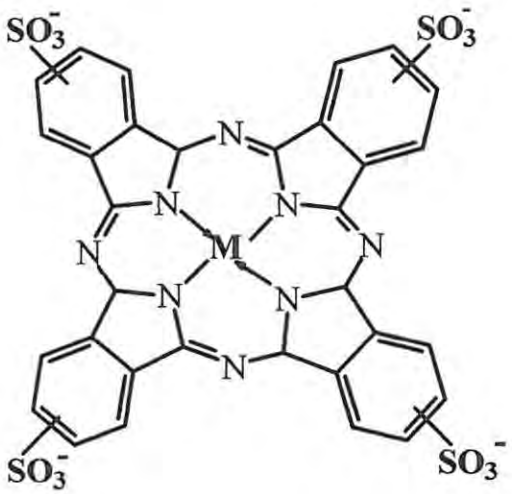

M = Fe = $[FeTSPc]^{4-}$
Co = $[CoTSPc]^{4-}$
Mn = $[MnTSPc]^{4-}$

Scheme 8 A simplified synthetic route for metallotetrasulfophthalocyanine $[MTSPc]^{4-}$

The heterogeneous reaction mixture was heated at 180°C for 6 hours. The end crude product was ground and washed with methanol until the odour of nitrobenzene could no

longer be detected. The remaining product was added to 275ml of HCl (1M) solution saturated with NaCl. This step ensures the removal of excess Fe(II) traces in the end product. The solid product and HCl solution were briefly heated to boiling, cooled to room temperature and filtered.

The filtrate was dissolved in 175ml of 0.1M NaOH, which was heated to 80°C. All insoluble impurities were immediately separated by filtration. 67,5g sodium chloride was added to the solution, resulting in some precipitation of the solid product. The slurry mixture was heated and stirred at 80°C until the ammonium evolution stopped. The product was obtained by filtration and the initial reprecipitation process (using NaOH and HCl) was repeated for two additional times.

The product was separated and washed with 80% aqueous ethanol and refluxed for 4 hours in 200ml absolute ethanol [69]. The product was filtered and left to dry over P_2O_5. Yield = 50% . IR (KBr pellets) 1736w, 1707w, 1605w, 1509w, 1329w, 1364m, 1190s, 1146w, 1109w, 1030s, 8231m, 746w, 694m, 631w, 594w, 559w. UV/Visible spectra (methanol:water): (λ max) 663 nm, 496 nm, 338 nm, 274 nm. The published molar extinction coefficient, 4.8×10^4 dm^3 mol^{-1} cm^{-1}, was used [70].

2.1.3 Synthesis of the monosodium salt of 4-sulfophthalic acid

The monosodium salt of the 4-sulphthalic acid was prepared according to the method outlined by Rollman *et al.* [71], by reacting a 1:1 molar ratio of sodium hydroxide with a 30% sulfophthalic acid solution. The evaporation of the solution overnight in the fume hood resulted in the formation of pinkish-white crystals.

2.1.4 Synthesis of cobalt (II) 4, 4`, 4``, 4```- tetrasulfophthalocyanine [CoTSPcf^{4-}, Scheme 8

The tetrasodium salt of cobalt(II) 4, 4`, 4``, 4```-tetrasulfophthalocyanine, Na_4[Co(II)TSPc], was synthesized following a similar detailed procedure to that above for Na_4[Fe(II)TSPc] but cobalt (II) sulfate 7-hydrate was used instead of ferrous chloride [69]. Yield = 80%. IR (KBr pellets) 1645m, 1525w, 1404w, 1366w, 1330m, 1189s, 1151m, 1112m, 1075w, 1059m, 1031s, 935vw, 833m, 763vw, 750s, 700s, 650s, 594m, 569vw. UV/Visible spectra (methanol:water): (λ max) 657 nm, 597 nm, 327 nm. The published molar extinction coefficient, 5.6 x 10^4 dm^3 mol^{-1} cm^{-1}, was used [72].

2.1.5 Synthesis of manganese (II) 4, 4`, 4``, 4```- tetrasulfophthalocyanine [MnTSPc]$^{4-}$, Scheme 8

The tetrasodium salt of manganese(II) 4, 4`, 4``, 4```-tetrasulfophthalocyanine, Na_4[Mn(II)TSPc], was synthesized following a similar detailed procedure to that above for Na_4[Fe(II)TSPc] but manganese(II) sulfate 7-hydrate was used instead of ferrous chloride [69]. Yield = 30%. IR (KBr pellets) 1617m, 1499w, 1403w, 1318m, 1194s, 1142w, 1109w, 1032s, 745w, 696m, 675m, 594w. UV/Visible spectra (water): (λ max) 716 nm, 636 nm, 511 nm, 342 nm, 274 nm.

2.2 Reagents

Hydrogen Peroxide (33%) was purchased from SAARTECH, *m*-chloroperoxybenzoic acid (CPBA), *tert*-butylhydroperoxide (TBHP, 70%), cyclohexane, cyclohexanone, cyclohexanol and 1,4-cyclohexanediol were purchased from Aldrich and used as received. Dimethylformamide (DMF), dichloromethane and methanol were of gas chromatography (GC) or high pressure liquid chromatography (HPLC) grade. Triply deionized Millipore water was employed.

4-Pentenoic acid was purchased from Aldrich and freshly prepared phosphate buffer of pH 7 was employed in electrocatalytic reactions and spectroelectrochemistry. Triply deionized Millipore water was employed.

Urea, tetrachlorophthalic anhydride, ferrous chloride, ammonium molybdate, 30% 4-sulphthalic acid, cobalt sulphate and manganese sulphate were all purchased from Aldrich.

2.3 Catalytic methods

2.3.1 Biomimetic catalysis

The oxidation reactions were performed at room temperature (20 to 25°C). When $FePc(Cl)_{16}$ was employed as a catalyst, a solvent mixture containing DMF and dichloromethane was employed. The ratio of DMF to dichloromethane which gave the highest yields of products was found to be 3:7 and this solvent mixture was used for subsequent studies. The $FePc(Cl)_{16}$ complex and cyclohexane were dissolved in the solvent mixture, the respective oxidant (H_2O_2, CPBA or TBHP) was then added and the reaction monitored with time using gas chromatography and UV/Visible absorption spectroscopy. The water: methanol (1:9) solvent mixture was employed when $[FeTSPc]^{4-}$, $[CoTSPc]^{4-}$ and $[MnTSPc]^{4-}$ were used as catalysts. All the reactions were run at least in triplicates and not always using the same batches of the catalyst, oxidants or substrates.

The homogeneous reactions run at 80°C employed a silicone oil bath to ensure an even distribution of heat. The reaction was performed using a round bottom flask connected to a reflux condenser.

The molar extinction concentration of $FePc(Cl)_{16}$ catalyst was determined in DMF/CH_2Cl_2 mixture to be 7.4 x 10^4 dm^3 mol^{-1} cm^{-1} and used for the determination of concentration. The published [70] molar extinction coefficient, 4.8 x 10^4 dm^3 mol^{-1} cm^{-1}, for $[FeTSPc]^{4-}$ and 5.6 x 10^4 dm^3 mol^{-1} cm^{-1} for $[CoTSPc]^{4-}$ were used for the determination of concentration.

The oxidation products were identified by spiking with standards and by measurements of retention times in gas chromatography. The nature of the products was also determined by gas chromatography connected to a mass spectrometer (GCMS).

All the yields were based on the % weight of the products. The equations used for the determination of conversion, yield and selectivity are shown below:

$$\%\text{Conversion} = \frac{\text{intial substrate - substrate remaining}}{\text{initial substrate}} \times 100$$

$$\%\text{Yield} = \frac{\text{product obtained}}{\text{initial substrate}} \times 100$$

$$\%\text{Selectivity} = \frac{\text{product obtained}}{\text{initial substrate - final substrate}} \times 100$$

Amounts obtained were calculated relative to GC % peak area.

2.3.2 Electrocatalytic reactions

The experiments were performed under homogeneous conditions. For electrocatalytic experiments, a solution of 4-pentenoic acid (Aldrich) in pH 7 buffer solution was prepared before use. The 4-pentenoic acid solution was added to a freshly prepared solution of $[CoTSPc]^{4-}$ in pH 7 buffer. Cyclic voltammetry was carried out in a three electrode cell and nitrogen was bubbled through the solution before CV and a nitrogen atmosphere was maintained throughout the CV scan. The electrodes were, a glassy carbon working ($0.07cm^2$ area), Ag/AgCl (3M NaCl) reference and a Pt wire counter, **Figure 2.1**. The ions of the phosphate buffer, pH 7 (purchased from BDH) act as the electrolyte.

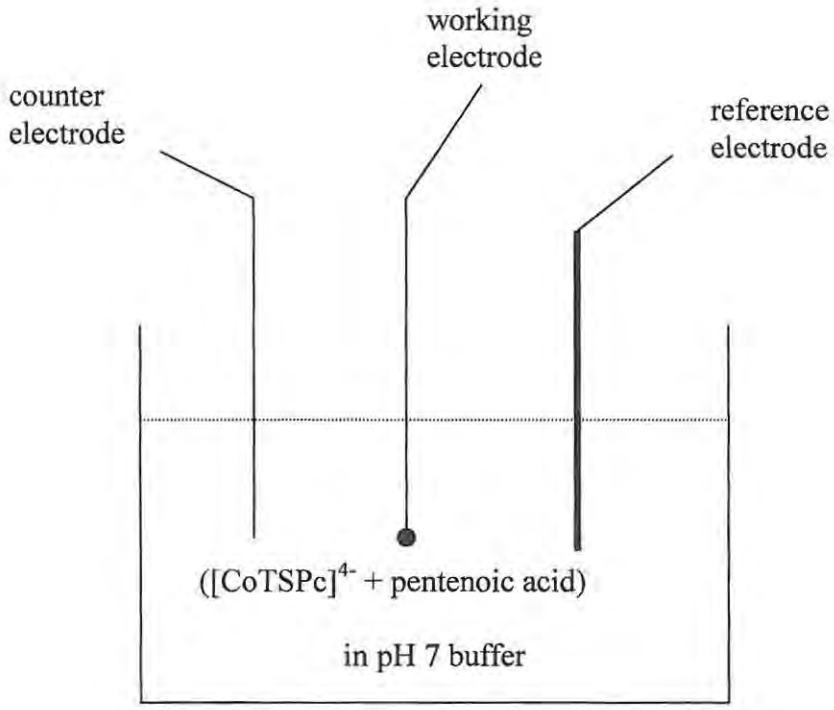

Figure 2.1 A typical three electrode system

The glassy carbon electrode was cleaned by polishing it with alumina on a Buehler felt pad, and rinsed in a dilute solution of nitric acid followed by the buffer. Spectroelectrochemistry was performed in an optically transparent thin layer electrochemistry cell (OTTLE) consisting of a platinum mesh working and counter electrodes and a Ag wire pseudo reference electrode. Freshly prepared solutions containing $[CoTSPc]^{4-}$ complex and 4-pentenoic acid in pH 7 buffer were employed.

Following the spectroelectrochemical experiments attempts were made to generate the oxidation products for identification using bulk electrolysis. Bulk electrolysis was carried out in a three electrode cell with two compartments separated by a glass frit, **Figure 2.2**.

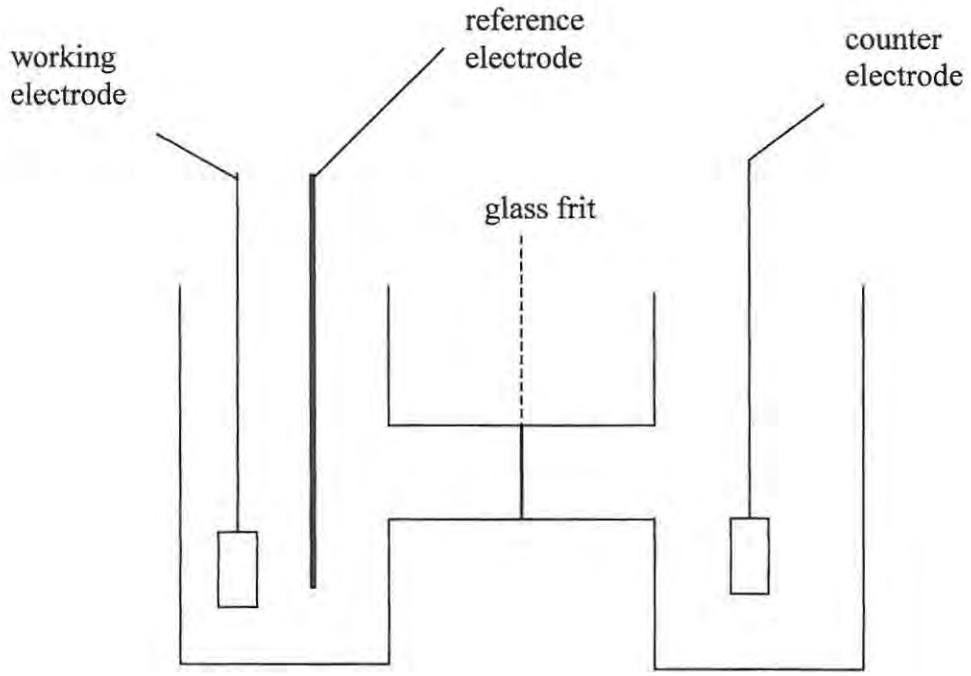

Figure 2.2 A typical bulk electrolysis cell

One component contains $[CoTSPc]^{4-}$ and 4-pentenoic acid in pH 7 buffer, the other component contains only the pH 7 buffer. The platinum plate working and Ag/AgCl reference electrodes are housed in the former compartment and the platinum plate counter electrode in the latter compartment.

2.4 Instrumentation

Gas chromatograph (GC) was recorded with a Hewlett-Packard HP 5890. The gas chromatograph was fitted with FID detector, using a cross-linked siloxane capillary column (30m length, 0.32mm internal diameter and 0.25μm film thickness). The parameters for analysis were: carrier gas nitrogen at 30.7cm s^{-1}, injector temperature = 225°C, detector temperature = 280°C. Mass spectra was recorded with Finnigan LCQ-MS coupled with J& W Scientific column of 30m length, 0.312mm and 0.25μm film thickness. UV/Visible spectra was recorded with the Cary 500 UV/Visible/NIR Spectrophotometer. Electrochemical data were collected by the BioAnalytical system (BAS) model CV-100W Voltammetric Analyser. All the electrochemical data was carried under nitrogen atmosphere. The nitrogen was purchased from MG Fed gas, purified by passing through drierite self-indicating mesh 8 (unhydrous $CaSO_4$) purchased from SAARTECH. Spectroelectrochemistry data was collected with BAS CV-27 Voltammograph analyser and the Cary 500 UV/Visible/NIR Spectrophotometer. The infrared data (KBr pellets) were recorded with a Perkin-Elmer Fourier Transform Infrared (FTIR) spectrophotometer Spectrum 2000.

3. Results and Discussion

3.1 Characterization of MPc complexes

3.1.1 Spectroscopic characterization of [FeTSPc]$^{4-}$

Metallotetrasulfophthalocyanines, ([MTSPc]$^{4-}$), are in general known to exist as dimers in equilibrium with monomers in aqueous solutions [72,73]. Their UV/Visible spectra thus consists of two peaks in the Q band region. The lower energy absorption band near 670 nm is associated with the monomeric species while the high energy absorption band near 620 nm is due to the dimeric species [72]. The ratio of monomer to dimer is dependent of many factors including the ionic strength, the pH and the temperature.

The nature of the [FeTSPc]$^{4-}$ complex has been subject of several investigations. Like all [MTSPc]$^{4-}$ complexes, the spectra of [FeTSPc]$^{4-}$ in aqueous solutions consists of a dimer in equilibrium with a monomer. In the presence of non-aqueous solvents, the monomeric species predominates. Thus, since the solvent mixture used for the catalytic studies in this work contained methanol, the absorption band at 663 nm is associated with the monomeric [FeTSPc]$^{4-}$ species, as shown below in **Figure 3.1**.

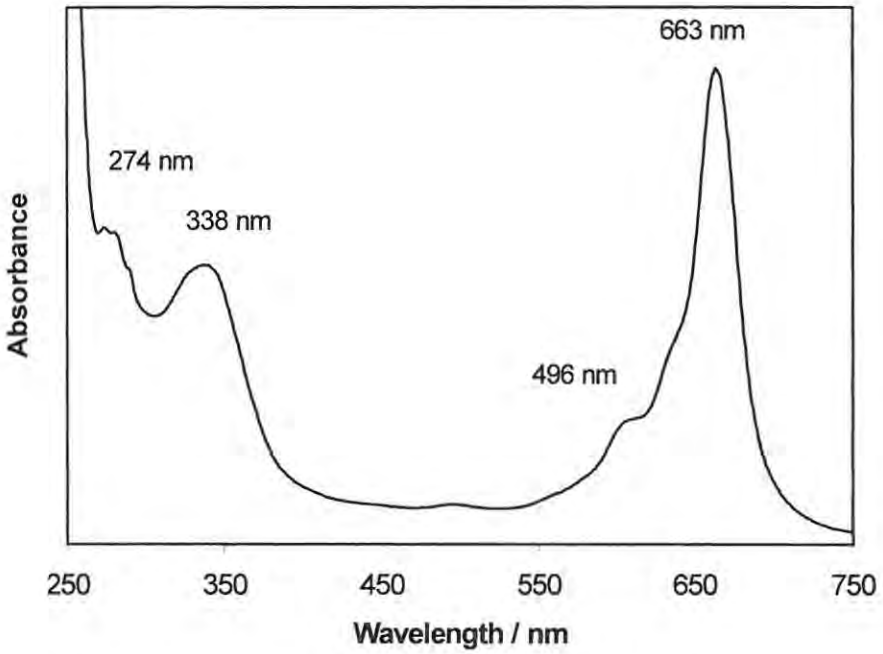

Figure 3.1 Spectra of iron tetrasulfophthalocyanine, $[FeTSPc]^{4-}$ in water:methanol solvent mixture

The Soret or B band peak was observed at 338 nm. The UV/visible data are listed in **Table 2.**

The nature of $[FeTSPc]^{4-}$ species prepared according to the Weber and Busch [69] has been found to vary with each preparation batch. A wide range of iron phthalocyanine complexes have been obtained with different preparation batches [35], with some authors reporting on the formation of μ-oxo complexes, while other authors found no evidence of the dimeric μ-oxo species. The formation of $[Fe^{III}TSPc]^{3-}$ is common in many preparations [35,69].

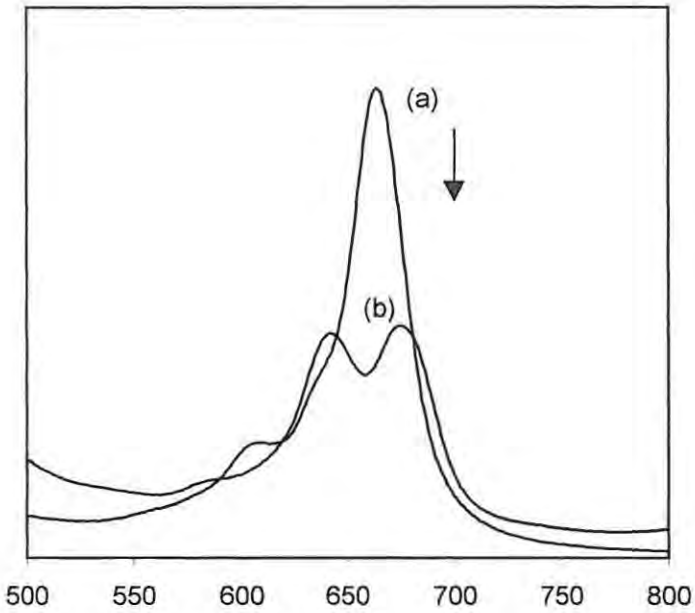

Figure 3.2 Electronic absorption spectral changes observed. Spectra **(a)** before and **(b)** on addition of ferric chloride to $[Fe^{II}TSPc]^{4-}$ in water:methanol solvent mixture.

In order to confirm the nature of the species prepared in this work, i.e. $[Fe^{II}TSPc]^{4-}$ or $[Fe^{III}TSPc]^{3-}$, chemical oxidation was employed. Spectral changes observed on addition of ferric chloride to solutions of FeTSPc in a methanol:water solvent mixture are shown in **Figure 3.2.** Oxidation of $[Fe^{II}TSPc]^{4-}$ complex using ferric chloride resulted in the formation of a split Q band and a shifting of one of the Q band components to longer wavelengths, as is typical of the oxidation of Fe(II)Pc to Fe(III)Pc [61].

Chemical oxidation of $[FeTSPc]^{4-}$ give spectral changes typical of the formation of $Fe^{III}Pc$ species, **Figure 3.2**, hence confirming that the iron is in the +2 oxidation state in the original complex prepared in this work.

The IR spectra of $[Fe^{II}TSPc]^{4-}$, was typical for metallophthalocyanines with the aromatic C-H stretching vibrations observed at 3190 cm^{-1}, C-H out-of-plane bending at 746 and 694 cm^{-1}, C-C benzene ring skeletal stretching vibration at 1605 and 1509 cm^{-1}.

The absence of strong vibrational bands at 715 and 1000 cm^{-1} is an indication that the complex is free of metal free phthalocyanine contamination [74].

3.1.2 Spectroscopic characterization of $[CoTSPc]^{4-}$

$[CoTSPc]^{4-}$ like other $[MTSPc]^{4-}$ complexes exists as a dimer in equilibrium with a monomer in water, **Figure 3.3 (a)**. **Figure 3.3 (b)** shows the UV/visible spectra of $[CoTSPc]^{4-}$ in a solvent mixture of methanol and water, and as discussed above for the $[FeTSPc]^{4-}$ species, in the presence of organic solvents the monomeric species predominates as seen in **Figure 3.3 (b).**

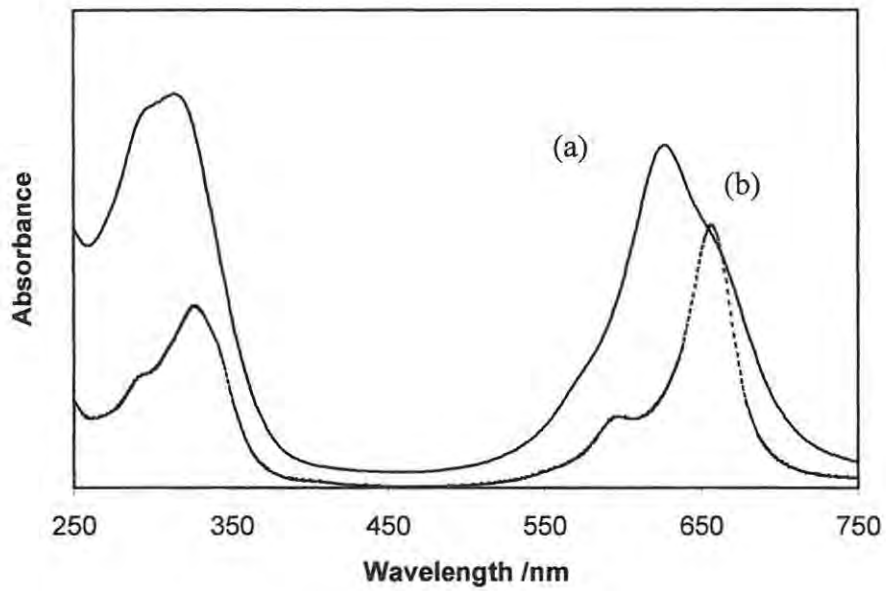

Figure 3.3 (a) Spectra of cobalt tetrasulfophthalocyanine $[CoTSPc]^{4-}$ in water (solid line) and **(b)** in water:methanol solvent (dotted line).

The Q band at 657 nm (**Figure 3.3 (b)**) is associated with the monomeric $[Co^{II}TSPc]^{4-}$ species. The peak at 597 nm is a vibronic band and the absorption band at 327 nm is assigned as the Soret or B band (**Figure 3.3 (b)**). In **Figure 3.3 (a)** the Q band at 624 nm is associated with the dimeric species and the band at 312 nm is assigned as the B band. **Table 2** shows the Q and B band for $[CoTSPc]^{4-}$ are observed at shorter wavelengths than for $[FeTSPc]^{4-}$.

Unlike $[FeTSPc]^{4-}$ where various other species can be synthesized from the Weber and Busch method [69], $[Co^{II}TSPc]^{4-}$ is known to be the only possible species obtained by

this method. The IR spectra of [Co TSPc]$^{4-}$ is similar to the IR spectra of [FeTSPc]$^{4-}$ as expected.

3.1.3 Spectroscopic characterization of [MnTSPc]$^{4-}$

Again [MnTSPc]$^{4-}$ like all [MTSPc]$^{4-}$ also exist as a dimer in equilibrium with a monomer in water. **Figure 3.4(a)** shows the UV/visible spectra of [MnTSPc]$^{4-}$ in an aqueous solution.

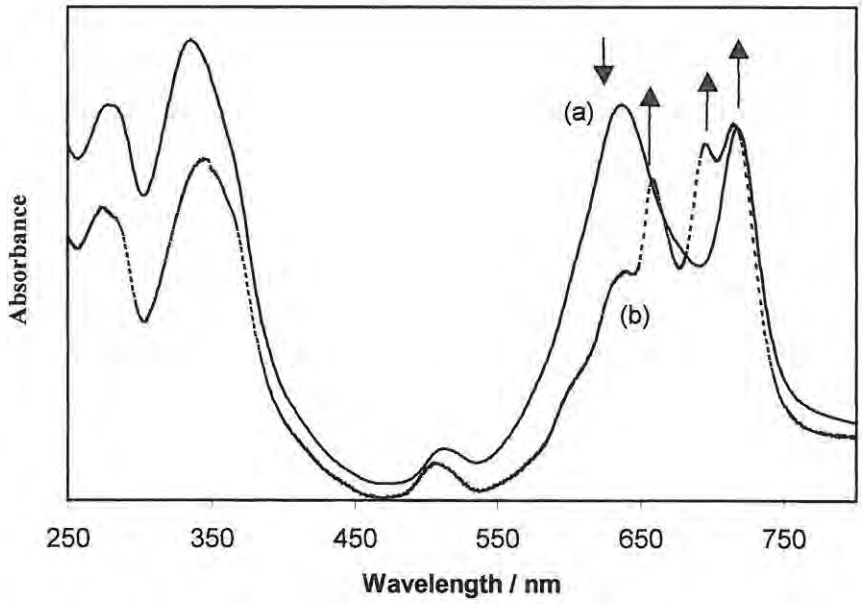

Figure 3.4 (a) Spectra of manganese tetrasulfophthalocyanine ([MnTSPc]$^{4-}$) in water

(b) after the addition of methanol

There are two peaks in the Q band region as expected for [MTSPc]$^{4-}$ complexes in aqueous solutions, **Figure 3.4 (a)**. The lower energy absorption band at 716 nm is

associated with the monomeric species and the higher energy absorption band at 636 nm is associated with the dimeric species. These observations are similar to those reported in literature [75]. The Soret or B band was observed at 342 nm, in **Figure 3.4 (a)**. **Table 2** shows that the Q and B bands for $[MnTSPc]^{4-}$ occur at a longer wavelengths than for $[FeTSPc]^{4-}$, which also occurs at a longer wavelength than for $[CoTSPc]^{4-}$.

After the addition of methanol to solutions of $[MnTSPc]^{4-}$, **Figure 3.4 (b)** two new bands in the Q band region appear at 655 nm and at 691 nm. The absorption band at 636 nm which is associated with the dimeric species, disappears as expected in the presence of organic solvents. There was also a slight increase in the absorption band at 716 nm which is associated with the monomeric species.

The two bands at 655 nm and 691 nm are associated with H_2TSPc i.e. the demetallated phthalocyanine species [61]. Thus in the presence of a methanol and water solvent mixture, both $[MnTSPc]^{4-}$ and H_2TSPc species were present in solution.

The IR spectra of $[MnTSPc]^{4-}$ was similar to the IR spectra of $[FeTSPc]^{4-}$ as expected.

Table 2 Spectroscopic characteristic of $[MTSPc]^{4-}$ and $FePc(Cl)_{16}$.UV/visible data taken from spectra of $[MTSPc]^{4-}$ in a solvent mixture of methanol and water (9:1) and $FePc(Cl)_{16}$ in DMF/CH_2Cl_2. IR KBr pellets.

Catalyst	**λ max, nm (log Є)**	**Characteristic IR bands/cm^{-1}**
$[FeTSPc]^{4-}$	663 (4.7), 496 (4.5), 338 (4.3), 274 (4.3)	694m *v*(S-O)
$[CoTSPc]^{4-}$	657 (4.7), 597 (4.7) , 327 (4.4)	700s *v*(S-O)
$[MnTSPc]^{4-}$	716, 691, 655, 511, 342, 274	694m *v*(S-O)
$FePc(Cl)_{16}$	623 (4.9), 343 (5.6), 312 (5.5)	1094w *v* (C-Cl)

3.1.4 Spectroscopic characterzation of $FePc(Cl)_{16}$

$FePc(Cl)_{16}$ like all $MPc(Cl)_{16}$ has low solubilities in essentially all solvents. It is however soluble in DMF after sonication, resulting in moderately strong coloured solutions.

$FePc(Cl)_{16}$ unlike $CoPc(Cl)_{16}$ and $ZnPc(Cl)_{16}$ do not easily aggregate in solution [76]. However the Q band wavelength for $FePc(Cl)_{16}$ is different for each preparation batch as has been reported before [76]. **Figure 3.5** shows the spectra of $FePc(Cl)_{16}$ in a DMF: dichloromethane (3:7) solvent mixture.

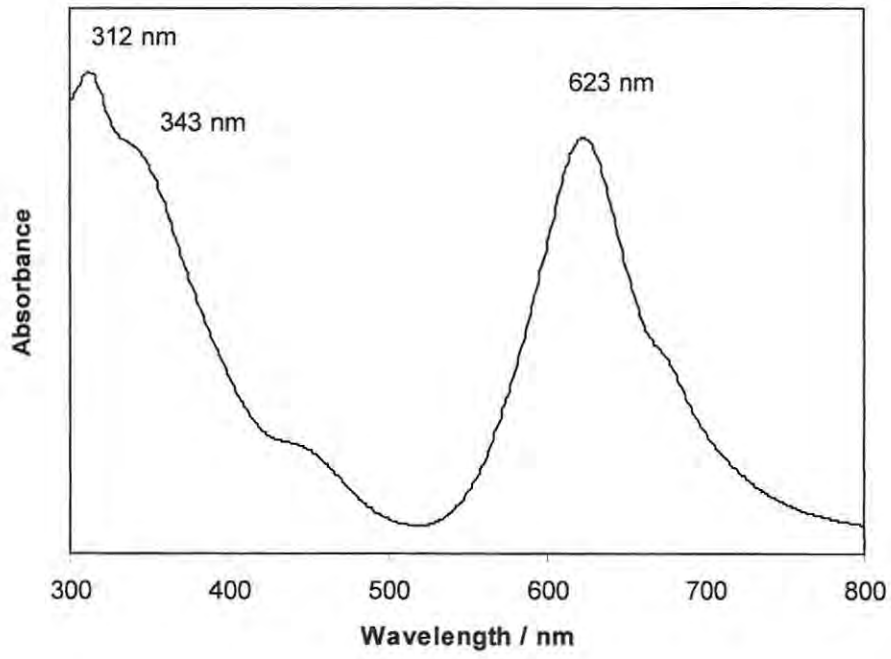

Figure 3.5 Spectra of $FePc(Cl)_{16}$ in a DMF:CH_2Cl_2 solvent mixture

The Q band in **Figure 3.5** for $FePc(Cl)_{16}$ is observed at 623 nm and it is associated with the $Fe^{II}Pc(Cl)_{16}$ species. The Soret or B band is observed at 343 nm.

The IR spectra of $FePc(Cl)_{16}$, **Figure 3.6**, is typical of metallophthalocyanines as expected. With C-C stretch vibration of the benzene ring being observed at 1652 and 1440 cm^{-1}. The C-Cl stretch vibration was observed at 1094 cm^{-1}.

The absence of strong vibrational bands at 715 and 1000 cm^{-1} again indicates that the complex is free of metal free phthalocyanine contamination.

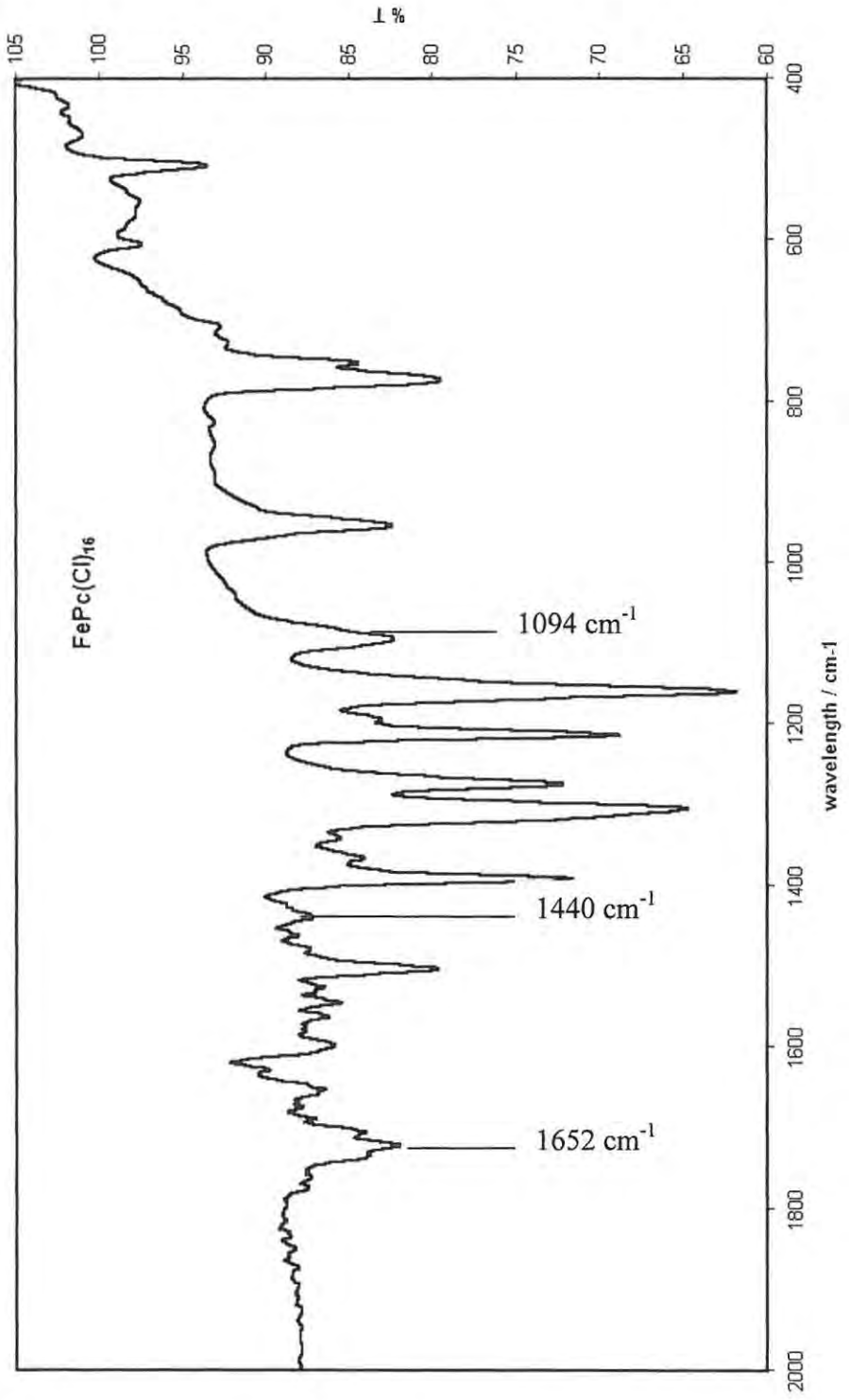

Figure 3.6 The IR spectra of $FePc(Cl)_{16}$

*3.2 Catalytic oxidation of cyclohexane using $[FeTSPc]^{4-}$ catalyst

Phthalocyanine complexes are more stable and readily available catalysts compared to porphyrins. However, the former have relatively lower solubility. This may explain why there has been less attention of the use of phthalocyanine as homogeneous catalysts.

3.2.1 Effects of oxidants on stability of $[FeTSPc]^{4-}$

$[FeTSPc]^{4-}$, **Figure 3.7**, like all $[MTSPc]^{4-}$ complexes is soluble in water .

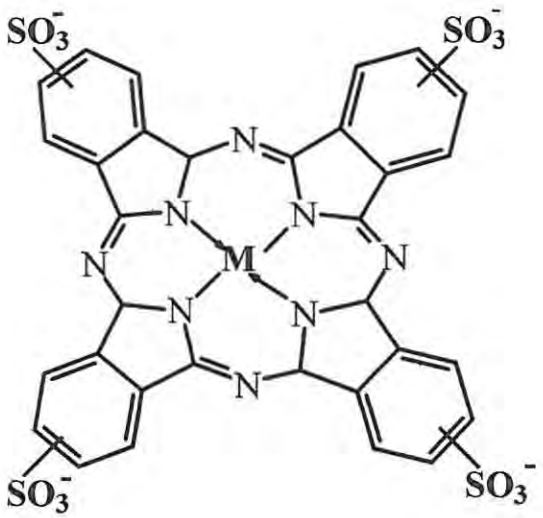

Figure 3.7 The structure of $[FeTSPc]^{4-}$

* Parts of Sections 3.2 and 3.3 have been published as N. Grootboom and T. Nyokong 'Iron perchlorophthalocyanine and tetrasulfophthalocyanine catalysed oxidation of cyclohexane using hydrogen peroxide, chloroperoxybenzoic acid and *tert*-butlyhydroperoxide as oxidants' J. Mol. Cat. A. Chemical (2002) in press.

In order to get all the components of the reaction mixture (oxidant, $[FeTSPc]^{4-}$ and cyclohexane) into solution, it was necessary to use a methanol:water solvent mixture. The three oxidants (H_2O_2, TBHP and CPBA), (**Figure 3.8**) were tested for cyclohexane oxidation using $[FeTSPc]^{4-}$ as a catalyst. Solutions containing appropriate concentrations of $[FeTSPc]^{4-}$ and cyclohexane was prepared and then a known amount of the appropriate oxidant was added and the reaction monitored with time using GC and UV/visible spectra.

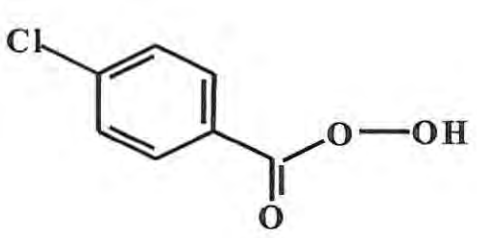

***m*-Chloroperoxybenzoic Acid**

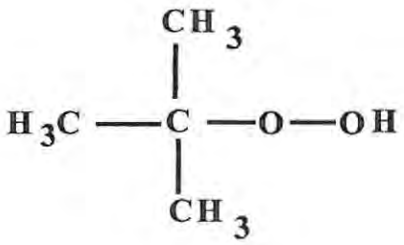

***Tert*-butylhydroperoxide**

Figure 3.8 The structure of *m*-chloroperoxybenzoic acid (CPBA) and *tert*-butylhydroperoxide (TBHP)

Fast degradation of the phthalocyanine ring in $[FeTSPc]^{4-}$ was observed when CPBA was employed as an oxidant. In fact, the solution went from the blue-green colour of the $[FeTSPc]^{4-}$ catalyst to colourless, immediately following addition of this oxidant, hence oxidation using this oxidant and $[FeTSPc]^{4-}$ catalyst was not studied. A degradation of the ring was also observed for hydrogen peroxide, though to a lesser extent compared to

CPBA. Less degradation of the phthalocyanine ring was observed when TBHP was employed as an oxidant, but some degradation was still evident. TBHP has been reported before [30] to be a more convenient oxidant for MPc catalyzed oxidation of cyclohexane.

3.2.2 Reaction products obtained

Varying amounts of cyclohexanol, cyclohexanone and cyclohexanediol were identified from gas chromatography analysis, **Figure 3.9**, as the products obtained on the oxidation of cyclohexane using $[FeTSPc]^{4-}$ catalyst.

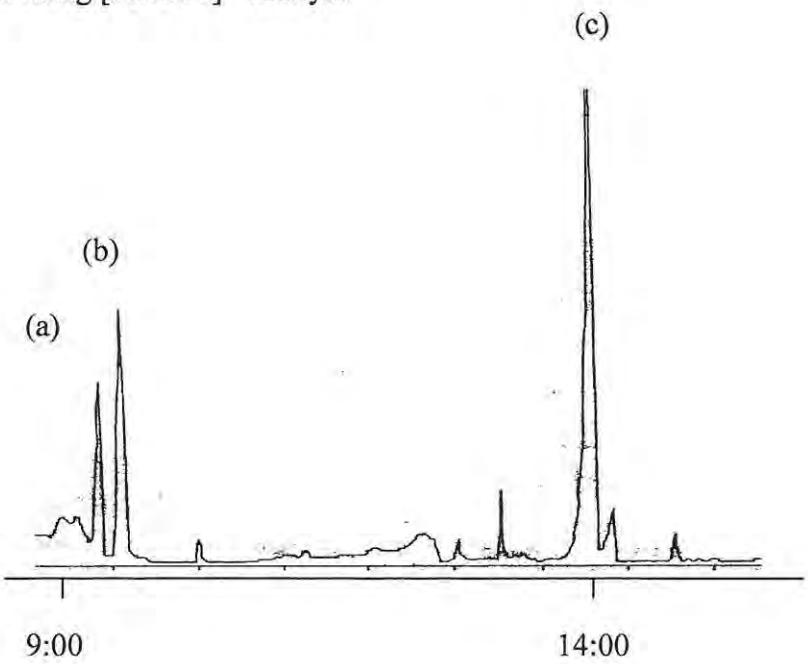

Figure 3.9 Typical GC trace obtained for reaction mixture employing 0.2 mol dm^{-3} cyclohexane in the presence of 1.4×10^{-3} mol dm^{-3} $[Fe^{II}TSPc]^{4-}$ catalyst. Oxidant = 0.8 mol dm^{-3} TBHP. **(a)** cyclohexanone, **(b)** cyclohexanol and **(c)** cyclohexanediol

Mass spectroscopy was used to confirm the products identified by using standards and spiking of GC peaks. **Figure 3.10** shows typical mass spectrum obtained for cyclohexanol, showing M-1 at 99 hence confirming that the product is cyclohexanol. The rest of the peaks are due to fragments from cyclohexanol.

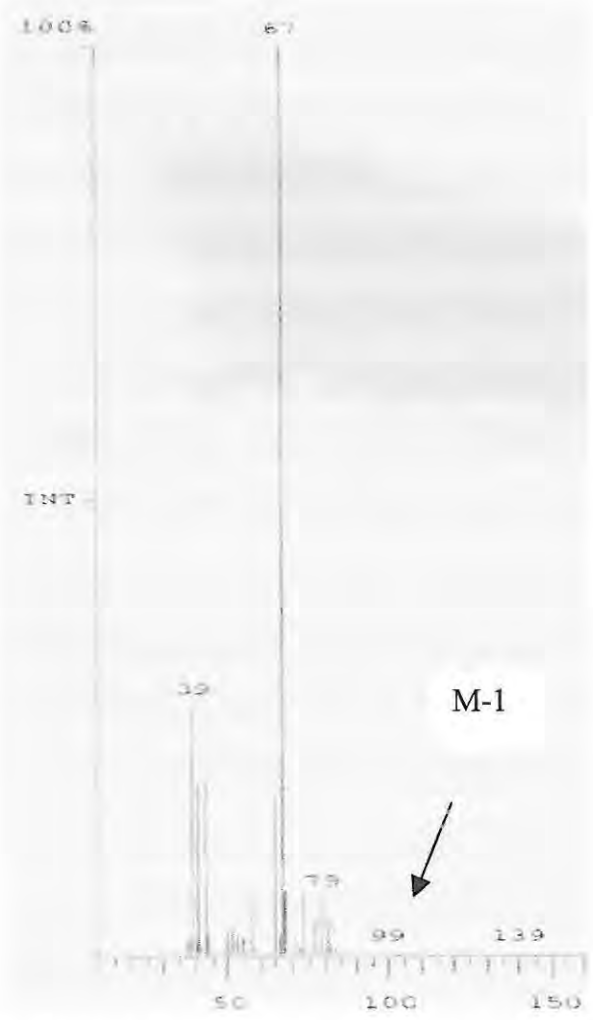

Figure 3.10 Mass spectrum obtained for reaction mixture employing 0.2 mol dm^{-3} cyclohexane in the presence of 1.4×10^{-3} mol dm^{-3} $[Fe^{II}TSPc]^{4-}$ catalyst. Oxidant = TBHP (0.8 mol dm^{-3}). Cyclohexanol (peak **(b)** in **Figure 3.9**) is used as an example.

To the author's knowledge, this is the first time that cyclohexanediol has been reported as one of the products of cyclohexane oxidation by phthalocyanines. There have been reports of the formation of adipic acid, cyclohexanol and cyclohexanone, from cyclohexane using halogenated phthalocyanine complexes as heterogeneous catalysts [24]. The results of the catalytic oxidation of cyclohexane by TBHP in the presence of $[FeTSPc]^{4-}$ catalyst are shown in **Figure 3.11**, which shows the variation of product percent yield with reaction time.

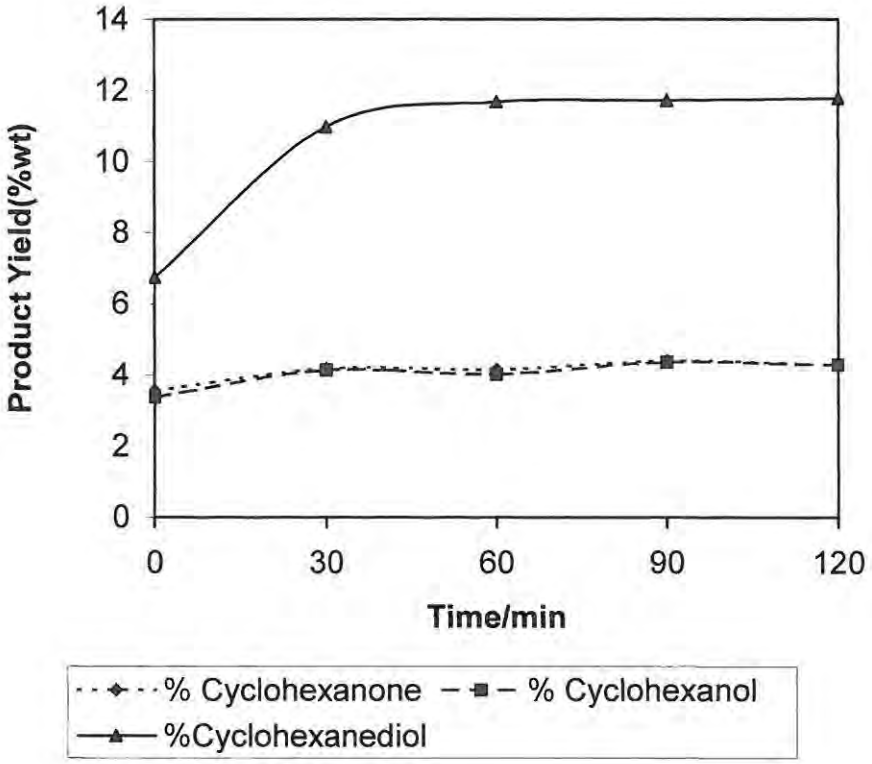

Figure 3.11 Variation of product %yield with time for the oxidation of 0.2 mol dm^{-3} cyclohexane in the presence of 1.4 x 10^{-3} mol dm^{-3} $[Fe^{II}TSPc]^{4-}$ catalyst. Oxidant = TBHP (0.8 mol dm^{-3})

According to **Figure 3.11**, the yield of the three products increases relatively fast initially but soon level off with time. The leveling off in **Figure 3.11** is most likely due to the degradation of the phthalocyanine catalyst by the TBHP oxidant, with time.

Higher percent yields and percent selectivities were obtained for cyclohexanediol than for cyclohexanol or cyclohexanone. The percent yields and percent selectivity for cyclohexanol and cyclohexanone were similar (**Table 3**).

Product percent yields reported in **Figure 3.11** and **Table 3**, are slightly higher (in some cases) than those reported for perhaloginated iron phthalocyanine as heterogeneous catalysts and oxygen as an oxidant [24]. Iron tetradecabromophthalocyanine yielded an overall percent conversion of 8% and iron tetradecachlorophthalocyanine yielded an overall percent conversion of 22%.

Table 3. Product %yields and %selectivities for the oxidation of 0.2 mol dm^{-3} cyclohexane by 0.8 mol dm^{-3} TBHP in the presence of the 1.4 x 10^{-3} mol dm^{-3} $[FeTSPc]^{4-}$ complex as catalyst. Water:methanol (1:9) solvent mixture was employed. Product yield based on the substrate.

Product	Selectivity (%)	Yield (%)
Cyclohexanol	21.0	4.3
Cyclohexanone	21.0	4.3
Cyclohexanediol	58.0	11.8
Overall conversion		20.4

3.2.3 Effects of catalyst loading on overall percent conversion, percent yield and percent selectivity

Figure 3.12 shows the effect of $[FeTSPc]^{4-}$ catalyst loading on the percent conversion of cyclohexane, for a reaction mixture consisting of a constant concentration of cyclohexane (0.2 mol dm^{-3}) and 0.8 mol dm^{-3} of the TBHP oxidant.

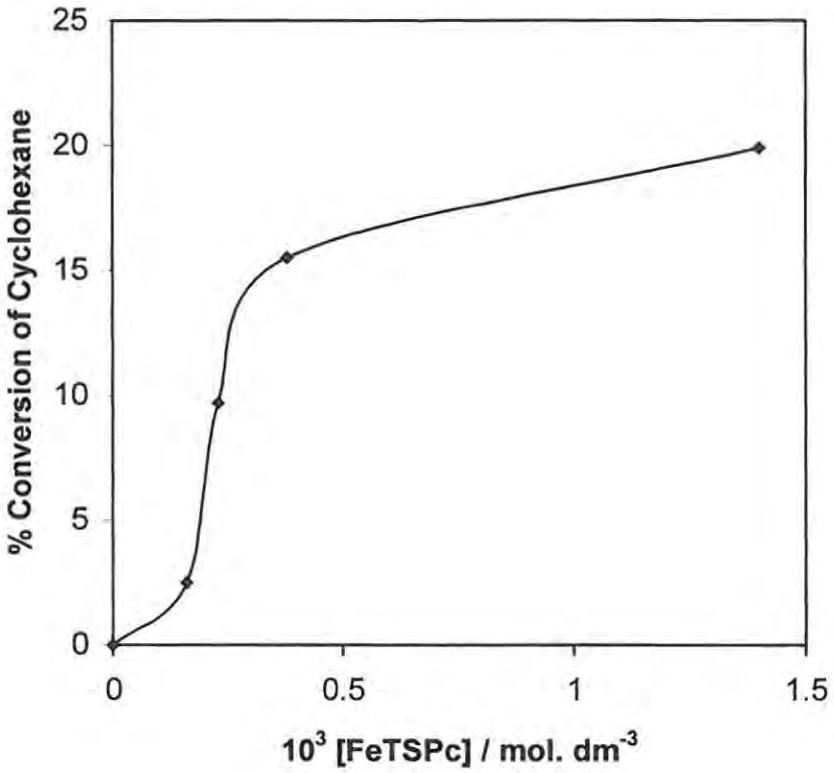

Figure 3.12 The effect of $[FeTSPc]^{4-}$ catalyst loading of the overall percentage conversion of 0.2 mol dm^{-3} cyclohexane after 2hrs. Oxidant = TBHP (0.8 mol dm^{-3}). Water:methanol solvent mixture.

There is an increase in the overall percent conversion with increase in the concentration of the catalyst within the concentration range shown in **Figure 3.12.** There is a fast increase in percent conversion at low concentrations of the catalyst, and a more gradual increase at higher concentrations.

Aggregation of the phthalocyanine complexes is known to occur at high concentrations, lowering the catalytic activity of the catalyst at high concentrations, hence the leveling

off of percent conversion in **Figure 3.12**. It has also been reported [11] for porphyrins that at high catalyst concentrations, the catalyst effectively competes with the substrate for oxidation. This possibility for the MPc catalysts cannot be ruled out.

As the catalyst concentration increases there is a general increase in the percentage yields and a decrease in percentage selectivity for cyclohexanol and cyclohexanone, **Table 4**. Low selectivity between cyclohexanol and cyclohexanone was also observed at high catalyst concentration. For cyclohexanol and cyclohexanone, the percent yield also increase to a certain level then begins to decrease, for example there is a an increase in percent yield for catalyst concentration ranging from 1.6×10^{-4} mol dm^{-3} to 3.8×10^{-4} mol dm^{-3}, but a decrease at 1.4×10^{-3} mol dm^{-3}. There is also an increase in the percentage yield and percentage selectivity towards cyclohexanediol with an increase in the catalyst concentration. A 58% selectivity towards cyclohexanediol was obtained at 1.4×10^{-3} mol dm^{-3}.

Table 4. %Yields and %selectivities for the oxidation of 0.2 mol dm^{-3} cyclohexane by 0.8 mol dm^{-3} TBHP in the presence of the $[FeTSPc]^{4-}$ complex as catalyst. A water:methanol (1:9) solvent mixture. All readings were taken after 2 hour reaction period. Selec. = selectivity

$[FeTSPc]^{4-}$	**0.16 x 10^{-3} mol.dm^{-3}**		**0.23 x 10^{-3} mol.dm^{-3}**		**0.38 x 10^{-3} mol.dm^{-3}**		**1.40 x 10^{-3} mol.dm^{-3}**	
Product	**Selec. %**	**Yield %**	**Selec. %**	**Yield %**	**Selec. %**	**Yield %**	**Selec. %**	**Yield %**
Cyclohexanol	43.1	1.1	31.3	3.2	28.0	4.5	21.0	4.3
Cyclohexanone	45.3	1.4	34.7	3.5	33.0	5.3	21.0	4.3
Cyclohexanediol	11.6	0.3	34.0	3.5	39.0	6.2	58.0	11.8

3.2.4 Effects of temperature on overall percent conversion, percent yield and percent selectivity

Table 5 shows the effect of temperature on the overall percentage conversion of the reaction employing 0.38 x 10^{-3} mol dm^{-3} $[FeTSPc]^{4-}$ and 0.8 mol dm^{-3} of TBHP.

Table 5 The effect of temperature on overall %conversion, %yields and %selectivity of a reaction mixture of 0.2 mol dm^{-3} cyclohexane, 0.38 x 10^{-3} mol dm^{-3} $[FeTSPc]^{4-}$ and 0.8 mol dm^{-3} of TBHP. A 1:9 water to methanol solvent was employed.

Temp. (°C)	**25**		**80**	
Product	**Selectivity (%)**	**Yield (%)**	**Selectivity (%)**	**Yield (%)**
Cyclohexananol	28.0	4.5	34.0	6.5
Cyclohexanone	33.0	5.3	34.0	6.5
Cyclohexanediol	39.0	6.2	31.0	5.9
Conversion (%)	16.0		19.0	

At 80°C there is a 3% increase in overall conversion compared to the reaction done at 25°C. With an increase in temperature there is a loss of specific selectivity towards either cyclohexanol or cyclohexanone with 34 % selectivity for both at 80°C. There is a decrease in the yield for cyclohexanediol with an increase in temperature.

3.2.5 Effects of substrate loading on overall percent conversion, percent yield and percent selectivity

Figure 3.13 shows the variation of the overall percent conversion of cyclohexane with time for three different concentrations of this substrate (cyclohexane) for a reaction mixture containing 0.8 mol dm^{-3} of the TBHP oxidant and 3.8 x 10^{-4} mol dm^{-3} $[FeTSPc]^{4-}$

.

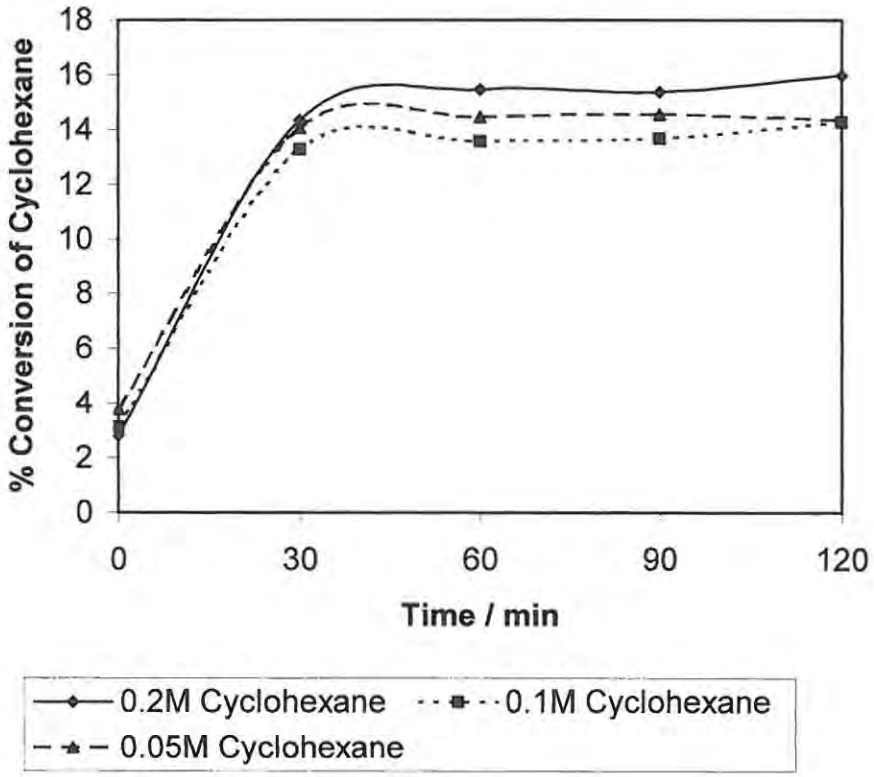

Figure 3.13 Effect of substrate (cyclohexane) concentration the overall %conversion in the presence of $[FeTSPc]^{4-}$ catalyst. Oxidant = TBHP (0.8 mol dm^{-3}). Water:methanol solvent mixture.

The overall percent conversion is not affected much by changes in the concentration of the substrate for the concentration employed in **Figure 3.13**. Oxidation of cyclohexane was not observed in the absence of the $[FeTSPc]^{4-}$ catalyst, confirming that the catalyst plays a prominent role in the oxidation process.

The observed lack of change of the overall percent conversion with changes in the oxidant:substrate ratio, is due to the fact that the catalyst concentration was kept constant as this ratio was changed. After 30 minutes of the reaction an additional 0.8 mol dm^{-3} of oxidant was added to the reaction. No further oxidation occurred, indicating that the leveling off of the oxidation was not due to the complete decomposition of the oxidant, but rather due to the decomposition and inactivation of the catalyst.

Table 6 shows the effect substrate (cyclohexane) loading had on the percentage yields and percentage selectivity of the products.

Table 6 The effect of substrate loading on %yields and %selectivity for a reaction mixture of cyclohexane, 0.38 x 10^{-3} mol dm^{-3} $[FeTSPc]^{4-}$ and 0.8 mol dm^{-3} of TBHP. A 1:9 water to methanol solvent was employed. Reaction time = 2 hours

[Substrate] (cyclohexane)	**0.2 mol.dm^{-3}**		**0.1 mol.dm^{-3}**		**0.05 mol.dm^{-3}**	
Products	**Selectivity %**	**Yield %**	**Selectivity %**	**Yield %**	**Selectivity %**	**Yield %**
Cyclohexanol	28.0	4.5	33.0	4.7	33.0	4.7
Cyclohexanone	33.0	5.3	34.0	4.8	34.0	5.0
Cyclohexanediol	39.0	6.2	34.0	4.8	33.0	4.7

Although there is no significant change in the overall percent conversion of cyclohexane with a decrease in the concentration of substrate (cyclohexane), **Figure 3.13**, there are changes in the percentage selectivity of products. As the concentration of substrate decreases there is an overall increase in percentage selectivity towards cyclohexanol and cyclohexanone and a decrease towards the percentage selectivity of cyclohexanediol. There is a small increase in the percentage yield for cyclohexanol with a decrease in

substrate (cyclohexane) concentration. For cyclohexanone and cyclohexanediol there is a decrease in percentage yield with a decrease in substrate (cyclohexane) concentration.

3.2.6 Spectral changes observed during the reaction

Figure 3.14 shows the spectral changes observed for the $[FeTSPc]^{4-}$ catalyst during the course of the oxidation of cyclohexane in the presence of the TBHP oxidant.

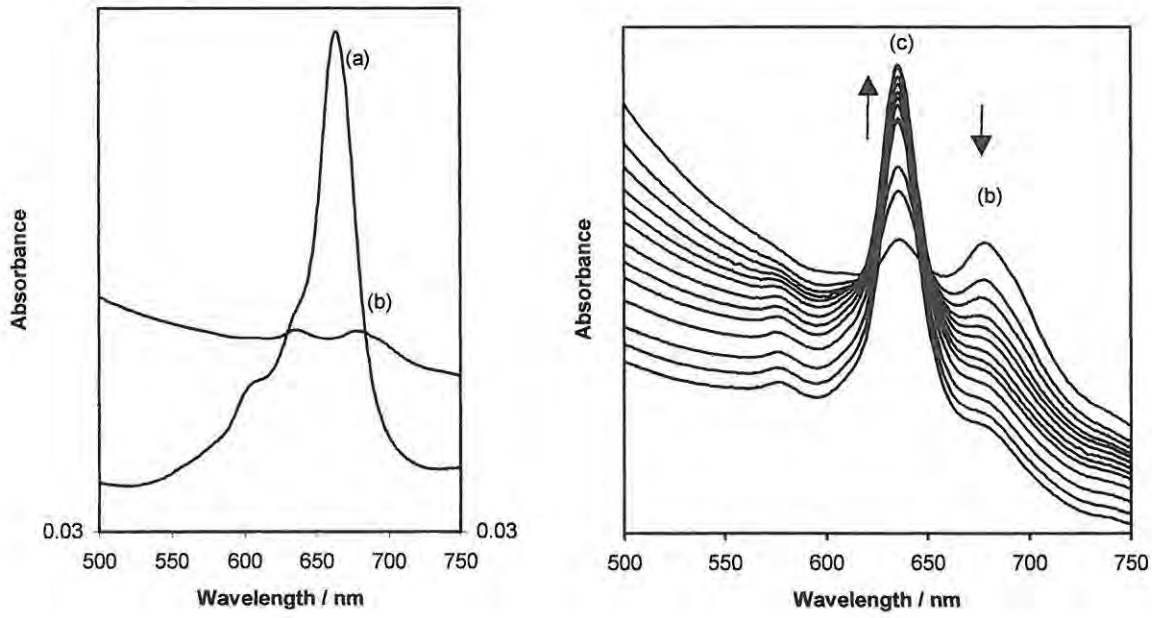

Figure 3.14 Electronic absorption spectral changes observed on addition of TBHP oxidant (0.8 mol dm^{-3}) to a reaction mixture containing 3.8 x 10^{-4} mol dm^{-3} $[Fe^{II}TSPc]^{4-}$ catalyst and 0.2 mol dm^{-3} cyclohexane. Spectra **(a)** before, **(b)** immediately after and **(c)** 2 hours after, addition of TBHP oxidant.

The reaction was exothermic; the temperature of the solution was found to increase by 40 ^{0}C immediately following addition of the oxidant to solutions containing the catalyst and the substrate.

The spectra of $[FeTSPc]^{4-}$ has been discussed above, **Section 3.1.1**, it consists of an intense band called the Q band at 663 nm, and a B band at 338 nm. The spectral changes following addition of oxidant (**Figure 3.14)** consisted of a drastic decrease in both the Q and B bands (only the Q band area shown in **Figure 3.14**) and the splitting of the Q band. No changes in the spectra of $[FeTSPc]^{4-}$ were observed in the absence of the oxidant. The lower energy band in **Figure 3.14(b)** was observed at 678 nm and the higher energy band at 636 nm.

The 636 nm band increased in intensity with time as shown in **Figure 3.14(c)**, as the band at 678 nm decreased. The band at 636 nm has been observed before and has been associated with the formation of stacked monomers [35]. The absorption at 636 nm is not due to the original $[FeTSPc]^{4-}$ species as the Q band for this species was located at 663 nm.

As discussed above the spectra of $[FeTSPc]^{4-}$ in aqueous solutions consists of a dimer in equilibrium with a monomer.

The ratio of monomer to dimer is dependent of many factors including, the ionic strength, pH and temperature. In the presence of non-aqueous solvents, the monomeric species

predominates. Thus, since the solvent mixture used for the catalytic studies in this work contained methanol, the spectra shown before addition of the oxidant in **Figure 3.14** is that of the monomeric $[FeTSPc]^{4-}$ species, as discussed above in **Section 3.1.1**. The spectral changes observed in **Figure 3.14(b)** are similar to those observed for the chemical oxidation of $[Fe^{II}TSPc]^{4-}$ and the formation of $[Fe^{III}TSPc]^{3-}$, **Figure 3.2**, hence confirming the formation of the latter during the catalytic oxidation of cyclohexane.

The spectral changes observed for the $[Fe^{II}TSPc]^{4-}$ catalyst during the oxidation of cyclohexane using the TBHP oxidant, suggest that the mechanism for the transformation of the catalyst is as outlined in **Scheme 9**.

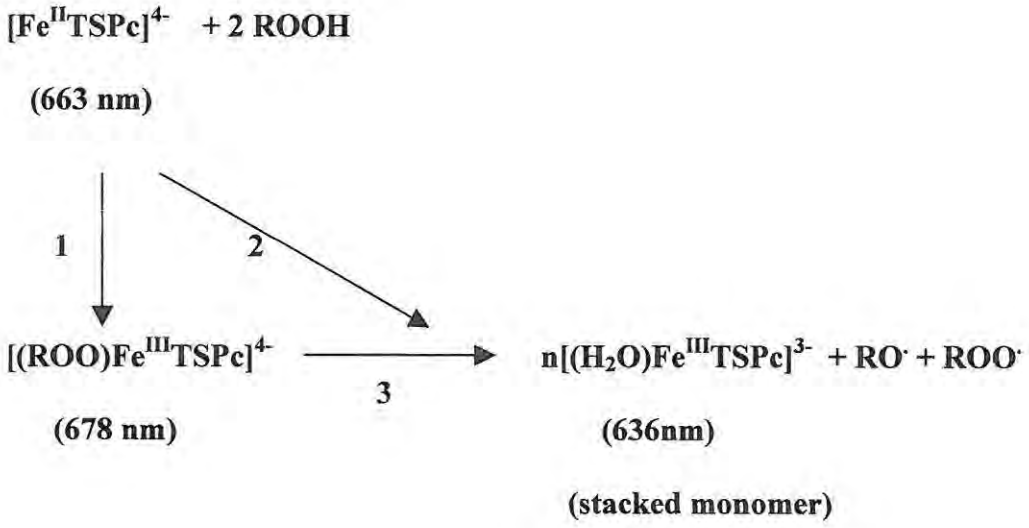

Scheme 9 Mechanism of $[FeTSPc]^{4-}$ transformation

Routes 1 and **2** are proposed on the basis of the split in the Q band on addition of the oxidant, with the formation of bands at 678 and 636 nm. **Route 3** is proposed on the basis of the observation of a decrease in the band at 678 nm and the increase with time (**Figure 3.14(c)**) in the band at 636 nm which has been associated with the formation of the stacked monomer.

The suggested presence of the $[(ROO)Fe^{III}TSPc]^{4-}$ intermediate is based on the fact that the Fe(III)(OOR) phthalocyanine species has been proposed as a key species for the ring cleavage of chlorophenols [35]. Recently many authors have reported the existence of Fe(III)(OOR) porphyrins, which have the ability to oxidize alkanes [6-8]. Also oxidation of alkanes catalyzed by iron porphyrin have been described as being mediated by porphyrin species containing oxo iron porphyrin species and a high oxidation state iron [11, 77, 78].

The $RO^{\cdot}$ and $ROO^{\cdot}$ radicals formed in **Scheme 9** then react with cyclohexane according to **Scheme 10** [16].

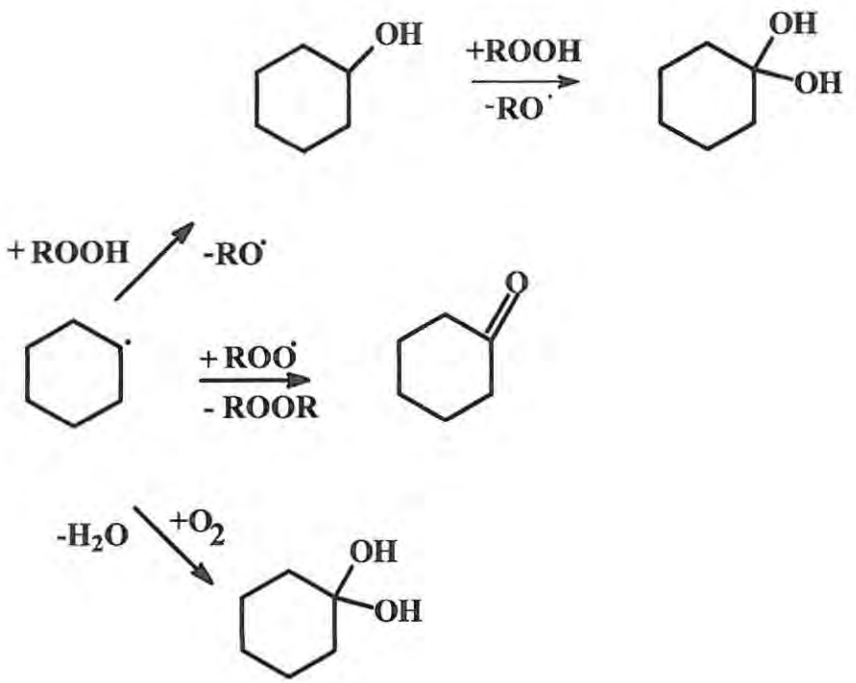

Scheme 10 Overall mechanism for cyclohexane oxidation by metallophthalocyanine

The cyclohexyl radical is formed by the homolytic fission induced by RO· radical producing ROH. Cyclohexanol is produced by the reaction of ROOH and the cyclohexyl radical. Cyclohexanone is formed by the reaction between the cyclohexyl radical and ROO· radical. It is also possible for the ketone to be formed as a secondary product from the alcohol due to the reaction being radically based. Cyclohexanediol may be formed via the alcohol and as a primary product by direct reaction of the cyclohexyl radical in the presence of residual oxygen and oxygen produced from ROOH [2].

3.2.7 Effect of central metals on the catalytic activity of metallotetrasulfophthalocyanine

Co and Mn have also been employed as central metals in tetrasulfophthalocyanine and used as catalysts for cyclohexane oxidation. Co(II) and Mn(II) 4, 4`, 4``, 4```tertrasulfophthalocyanine performed poorly compared to Fe(II) 4, 4`, 4``, 4```tertrasulfophthalocyanine, yielding an overall percent conversion of less than 1% compared to the 21% overall conversion of $[FeTSPc]^{4-}$ as shown in **Table 7,** values obtained for $[MnTSPc]^{4-}$ were similar to those shown in **Table 7** for $[CoTSPc]^{4-}$.

The percentage selectivity and percentage yields of cyclohexanol and cyclohexanone decreases when $[MnTSPc]^{4-}$ and $[CoTSPc]^{4-}$ are used as central metals when compared to the same concentration of $[FeTSPc]^{4-}$. The percentage selectivity and percentage yield of cyclohexanediol increases on the other hand, **Table 7**.

Table 7 The effect of central metals on %yields and %selectivity of a reaction mixture of cyclohexane, 0.38 x 10^{-3} mol dm^{-3} $[MTSPc]^{4-}$ and 0.8 mol dm^{-3} of TBHP. A 1:9 water to methanol solvent was employed. Selec.= Selectivity

Catalyst	**$[FeTSPc]^{4-}$**		**$[CoTSPc]^{4-}$**	
Product	**Selec. %**	**Yield %**	**Selec. %**	**Yield %**
Cyclohexanol	28.0	4.5	19.5	0.2
Cyclohexanone	33.0	5.3	28.6	0.2
Cyclohexanediol	39.0	6.2	52.0	0.4
Conversion	16.0		0.8	

The catalytic reaction employing $[CoTSPc]^{4-}$ was monitored by UV/visible spectroscopy, **Figure 3.15**, to determine whether the Co(III) species was involved in the reaction and the extent of catalyst decomposition.

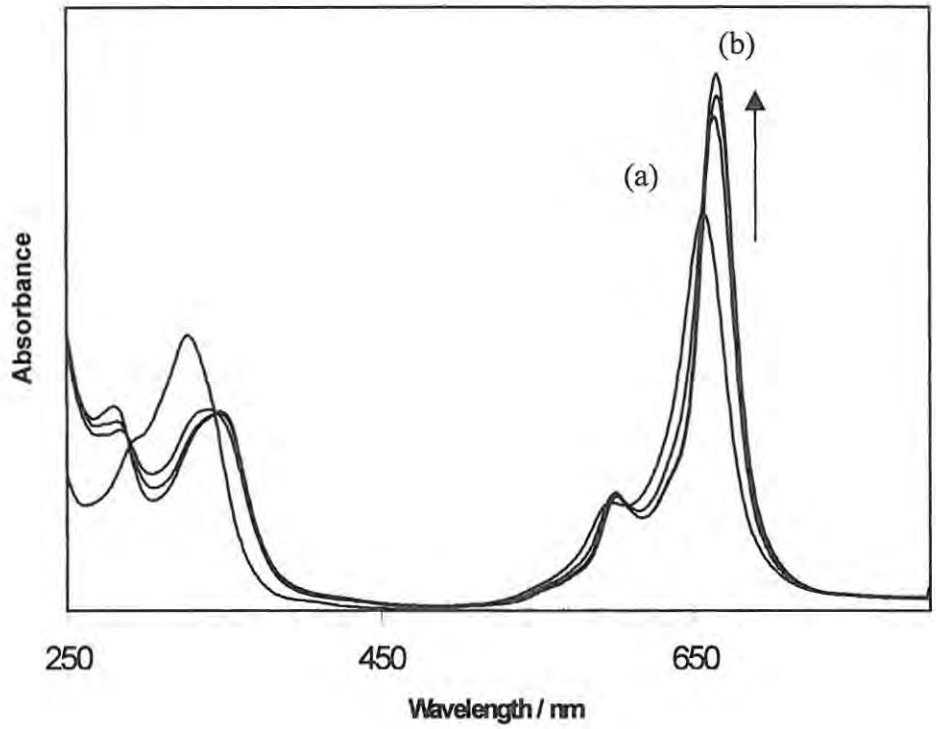

Figure 3.15 Electronic absorption spectral changes observed on addition of TBHP oxidant (0.8 mol dm^{-3}) to a reaction mixture containing 3.8 x 10^{-4} mol dm^{-3} $[Co^{II}TSPc]^{4-}$ catalyst and 0.2 mol dm^{-3} cyclohexane. Spectra **(a)** before and **(b)** after 2 hours. A solvent mixture of 1:9 water:methanol was employed.

Figure 3.15 (a) shows the spectra of the monomeric species with a Q band at 657 nm, at the start of the reaction. Immediately after the addition of TBHP there is a shift in the Q band to higher wavelengths, **Figure 3.15 (b)** and an increase in absorption. This type of observation is typical for either metal oxidation or reduction (as discussed in **Section 1.7.2**).

To confirm oxidation of the central metal, $[Co^{II}TSPc]^{4-}$ was chemically oxidized by ferric chloride. The chemical oxidation of $[Co^{II}TSPc]^{4-}$ gave a spectra similar to that of **Figure 3.15**, therefore proving that the central metal is oxidized from $[Co^{II}TSPc]^{4-}$ to $[Co^{III}TSPc]^{3-}$ species. In the absence of TBHP no spectral changes were observed for a two hour period and no oxidation of cyclohexane was observed.

A split in the B band upon the addition of TBHP was also observed simultaneously with the shift in the Q band to higher wavelengths. The splitting of the B band is usually indicative of strong axial ligation to the central metal of MPcs [61]. The splitting of the B band is well known for the ligation of cyanide to the central metals of MPc complexes. Therefore strong ligation of TBHP or cyclohexane to $[Co^{II}TSPc]^{4-}$ could explain the low overall percent conversion of the catalytic reaction.

According to **Scheme 9** axial ligation of the TBHP is essential for the production of RO· and ROO· radicals. The radicals may form from the ligation of two TBHP molecules to the central metal after which fission occurs forming the radical, and the central metal site becomes available for the ligation of two new TBHP molecules [22]. Therefore if strong ligation of TBHP or cyclohexane occurs in $[CoTSPc]^{4-}$ as the split in the B band indicates it hinders the formation of radicals and hence the significant drop in overall percent conversion with the change in central metal form Fe to Co. The split in B band was not observed for $[FeTSPc]^{4-}$ hence showing a less strong axial ligation compared to $[CoTSPc]^{4-}$, hence higher percent conversion for the former.

The fate of $[Mn^{II}TSPc]^{4-}$ catalyst during catalysis was also monitored by UV/Visible spectroscopy, **Figure 3.16.**

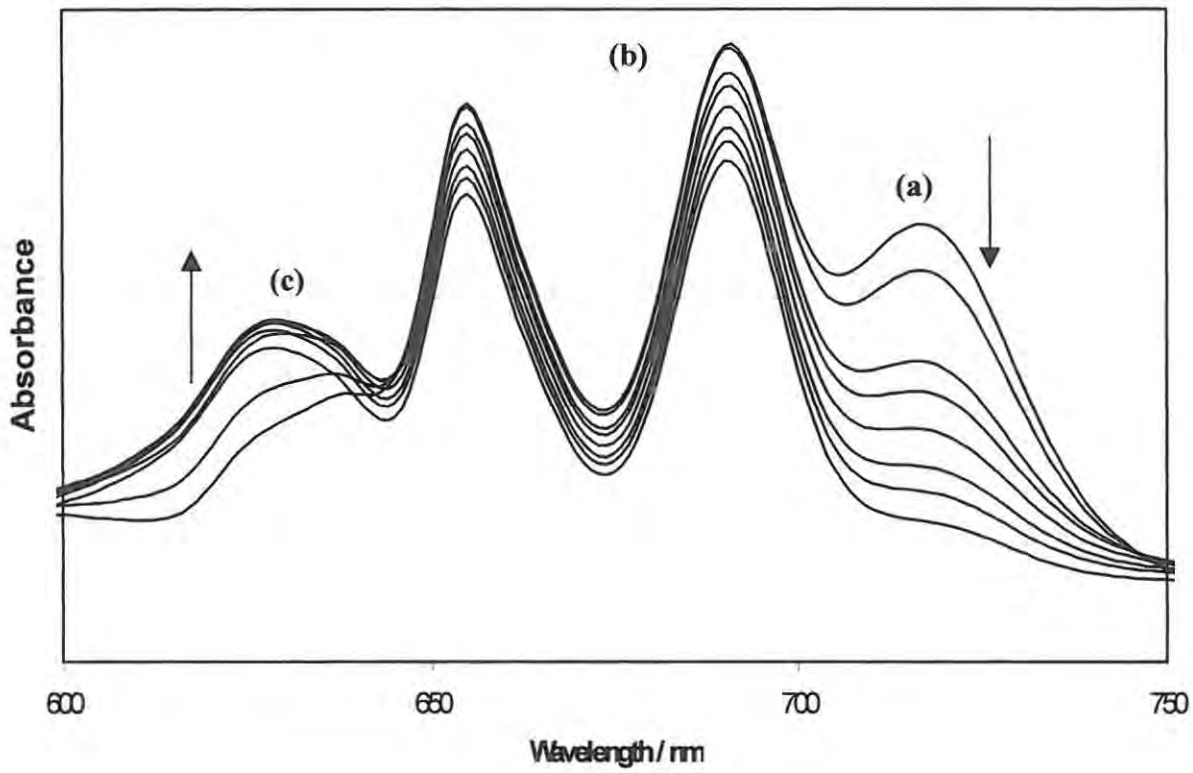

Figure 3.16 Electronic absorption spectral changes observed on addition of TBHP oxidant (0.8 mol dm^{-3}) to a reaction mixture containing 3.8 x 10^{-4} mol dm^{-3} $[Mn^{II}TSPc]^{4-}$ catalyst and 0.2 mol dm^{-3} cyclohexane.

The same conditions for catalysis were employed for $[Mn^{II}TSPc]^{4-}$ catalyst as for $[Co^{II}TSPc]^{4-}$ and $[Fe^{II}TSPc]^{4-}$ catalytic reactions. The initial spectra of $[Mn^{II}TSPc]^{4-}$ in the presence of water and methanol is not like the typical $[MTSPc]^{4-}$ complexes as discussed above (**Section 3.1.3**), due to the presence of H_2TSPc species. Immediately after the addition of TBHP no change in the spectra was observed. The reaction was

monitored for a period of two hours, a significant decrease in the peak at 716 nm **(a)** and an increase in the peak at 636 nm **(c)** was observed. Splitting in the B band for $[Mn^{II}TSPc]^{4-}$ catalyst was not observed. The peaks at 655 nm and 691 nm also decreased in intensity.

The peaks at **(a)** 716 nm and **(c)** 636 nm have been [75] assigned before as being due to the monomeric and dimeric species respectively [75]. The two intense peaks at **(b)** 655 nm and 691 nm were found to increase with the percentage methanol in solution (as discussed in **Section 3.1.3)**. These two peaks are characteristic of demetallated Pcs. In the absence of methanol the only two peaks observed are the **(c)** dimeric and **(a)** monomeric species (as discussed in **Section 3.1.3)**.

From the relative intensities of 655nm and 691 nm (H_2TSPc) compared to 636 nm and 716 nm ($[MnTSPc]^{4-}$), it is clear that most of the $[Mn^{II}TSPc]^{4-}$ species in the reaction mixture has demetallated. This observation would explain the low overall percent conversion observed for $[MnTSPc]^{4-}$ compared to $[FeTSPc]^{4-}$. The $[Mn^{II}TSPc]^{4-}$ was oxidized using ferric chloride and resulted in a single peak absorbing at 716 nm. This suggested that the monomeric species and the oxidized species of $[Mn^{II}TSPc]^{4-}$ absorb at the same wavelength, hence it could not unequivocally confirm the involvement of $[Mn^{III}TSPc]^{4-}$ species in the catalytic oxidation.

Thus $[Mn^{II}TSPc]^{4-}$ is not a good catalyst because, it is easily demetallated under the reaction conditions used in this work.

3.3 Catalytic oxidation of cyclohexane using $FePc(Cl)_{16}$ catalyst

3.3.1 Solvent effects

Dichloromethane has been used successfully as a solvent for the catalytic oxidation of cyclohexane using metalloporphyrins [11,79]. However the $FePc(Cl)_{16}$ catalyst shown in **Figure 3.17** is not soluble in dichloromethane (as discussed in **Section 3.1.4**), but is more soluble in DMF. Thus, a DMF: dichloromethane solvent mixture was employed for studies involving the $FePc(Cl)_{16}$ catalyst. The catalytic reactions were performed by dissolving appropriate concentration of $FePc(Cl)_{16}$ species and cyclohexane in DMF:CH_2Cl_2 mixture, and recording the spectra, then adding the appropriate oxidant and monitoring the GC and UV/visible spectra with time.

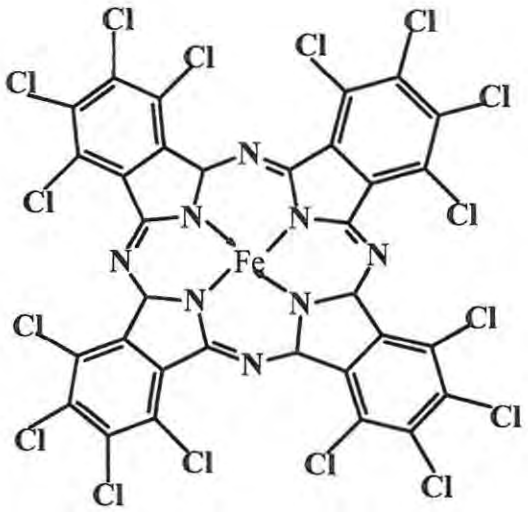

Figure 3.17 The structure of $FePc(Cl)_{16}$

When DMF was employed in the absence of dichloromethane, for the catalytic oxidation of cyclohexane in the presence of any of the oxidants (CPBA, TBHP or H_2O_2) employed in this work, no oxidation products were obtained. The percentage yield of oxidation products increased with the dichloromethane content of the solvent mixture, however, the solubility of the catalyst decreased with decrease in the DMF content. The best results in terms of product percentage yield and solubility were obtained with a DMF:CH_2Cl_2 ratio of 3:7.

Unlike when $[FeTSPc]^{4-}$ was employed as a catalyst, all three oxidants could individually be used for the oxidation of cyclohexane in the presence of $FePc(Cl)_{16}$ without drastic destruction of catalyst observed for $[FeTSPc]^{4-}$ in the presence of H_2O_2 and CPBA. Thus this section reports on the catalytic oxidation of cyclohexane in the presence of each of the oxidants H_2O_2, TBHP and CPBA.

The main reaction products were cyclohexanol and cyclohexanone, as the GC trace, **Figure 3.18**, shows.

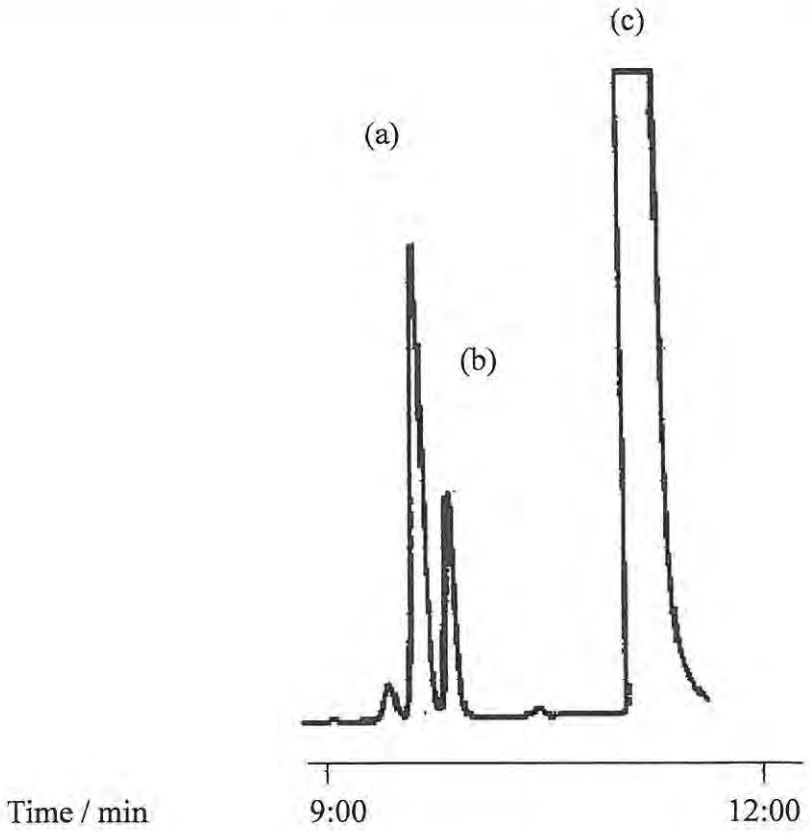

Figure 3.18 Typical GC trace obtained for reaction mixture of 0.2 mol dm^{-3} cyclohexane in the presence of 1.4 x 10^{-3} mol dm^{-3} $[Fe^{II}TSPc]^{4-}$ catalyst. Oxidant = TBHP (0.8 mol dm^{-3}). Reaction time = 2 hours **(a)** cyclohexanone, **(b)** cyclohexanol and **(c)** solvent peak

Insignificant amounts of cyclohexanediol were detected compared to cyclohexanol and cyclohexanone for $FePc(Cl)_{16}$ catalyst with the three oxidants. The products were again confirmed using Mass spectroscopy discussed above.

3.3.2 Effect of oxidants on overall percent conversion and percent yield

Figure 3.19 shows the variation of the product yields for a reaction mixture consisting of a constant concentration of the $FePc(Cl)_{16}$ catalyst (6 x 10^{-6} mol dm^{-3}), 0.2 mol dm^{-3} cyclohexane and varying amounts of the CPBA oxidant in a 3:7 DMF:CH_2Cl_2 solvent mixture.

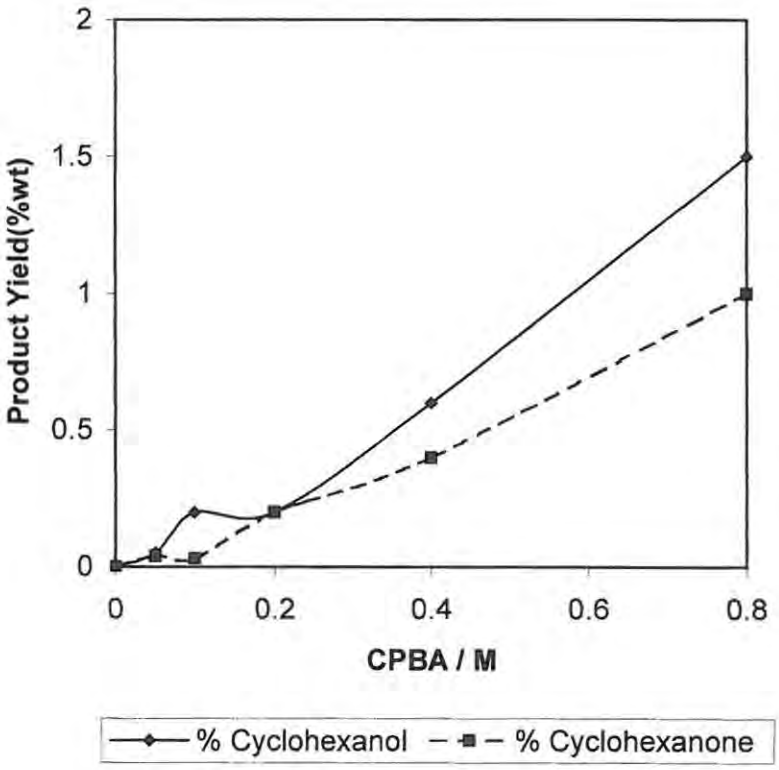

Figure 3.19 Variation of product %yield with CPBA oxidant concentration for the oxidation of 0.2 mol dm^{-3} cyclohexane in the presence of 6 x 10^{-6} mol dm^{-3} $FePc(Cl)_{16}$ catalyst

As the concentration of CPBA was increased, the percentage yields of cyclohexanone and cyclohexanol increased. The percentage yields shown in **Figure 3.19** are smaller than those reported above for the $[FeTSPc]^{4-}$ catalyst. This is most likely due to the low solubility of $FePc(Cl)_{16}$ compared to $[FeTSPc]^{4-}$. Product yields of 3% have been reported using halogenated MPc complexes as heterogeneous catalysts and oxygen as an oxidant [24].

The product percentage yields are highly dependent on the nature of the oxidant. **Figure 3.20** shows the variation of overall percent conversion of cyclohexane with increase in the concentration of the oxidant for the three oxidants under consideration in this work.

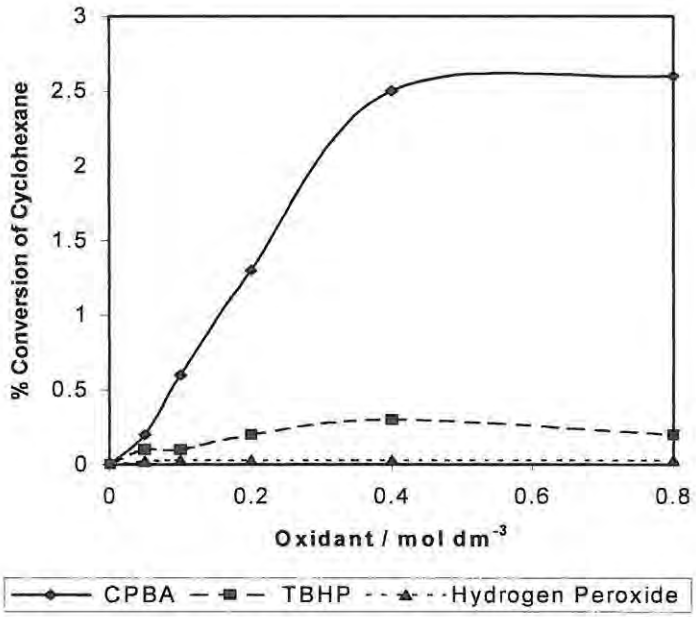

Figure 3.20 Variation of percentage conversion of 0.2 mol dm^{-3} cyclohexane with oxidant concentration, for 6 x 10^{-6} mol dm^{-3} $FePc(Cl)_{16}$ catalyst.

A relatively high increase in overall percent conversion of cyclohexane was observed as the concentration of the CPBA oxidant was increased, but leveled off at high concentrations of the oxidant. The overall percent conversion was the lowest for hydrogen peroxide, with TBHP showing a slightly higher overall percent conversion compared to hydrogen peroxide, as shown in **Figure 3.20.**

Table 8 shows that the percentage selectivity for the cyclohexanol was slightly higher than for cyclohexanone using the CPBA oxidant. **Table 8** also shows that even though the product percentage yields using TBHP oxidant were lower than for CPBA, much higher percentage selectivity for one of the products (cyclohexanone) was obtained for TBHP oxidant compared to either CPBA or hydrogen peroxide.

Table 8. Product %yields and %selectivities for the oxidation of cyclohexane by three different oxidants, CPBA, TBHP and H_2O_2 in the presence of the $FePc(Cl)_{16}$ complex as a catalysts. A DMF:dichloromethane (3:7) was employed. Product yield based on the substrate. Reaction time = 2hours. Selec. = Selectivity

Product	Oxidant					
	CPBA		TBHP		H_2O_2	
	Selec. (%)	Yield (%)	Selec. (%)	Yield (%)	Selec. (%)	Yield (%)
Cyclohexanol	54.0	1.6	10.0	0.02	40.0	0.01
Cyclohexanone	38.0	1.0	90.0	0.2	60.0	0.02
Cyclohexanediol	-	-	-	-	-	-

The percentage selectivity towards cyclohexanone was also higher for hydrogen peroxide when compared to CPBA. Selectivity of the products was found not to vary with the solvent in that when methanol or acetonitrile were employed instead of dichloromethane in the solvent mixture, no changes in selectivity were observed.

The results presented here show that of the three oxidants chosen, CPBA, TBHP and hydrogen peroxide, CPBA is the most efficient in the presence of the $FePc(Cl)_{16}$ catalyst, in terms of giving higher yields of the products. Hydrogen peroxide gave the lowest yields. Hydrogen peroxide dismutates in the presence of MPcs, to oxygen and water,

resulting in small amounts of radicals being formed for oxidations. Hydrogen peroxide is also known to attack MPc rings resulting in a more rapid decomposition of the MPc ring.

3.3.3 Effects of oxidants on catalyst stability

Figure 3.21 shows electronic spectral changes of the $FePc(Cl)_{16}$ catalyst observed during the course of the oxidation of cyclohexane in the presence of the CPBA oxidant.

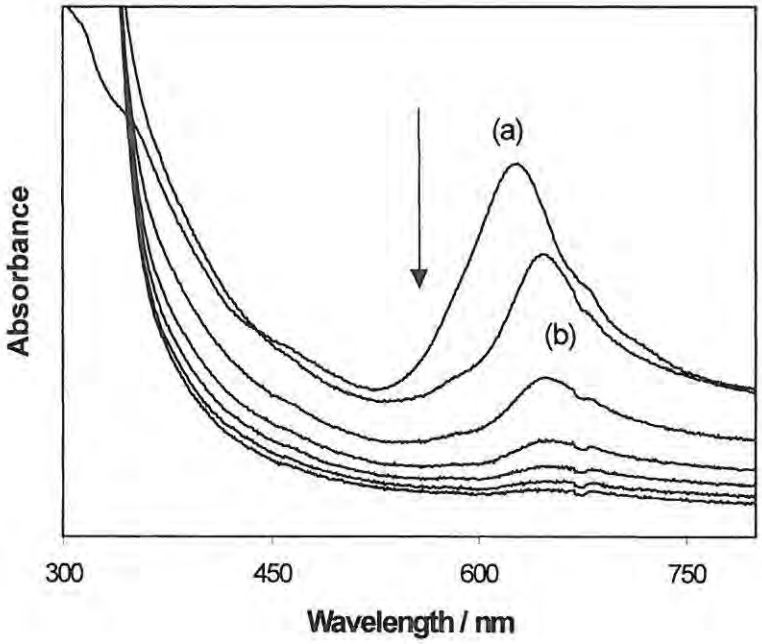

Figure 3.21 Electronic absorption spectral changes observed on addition of CPBA oxidant (0.8 mol dm^{-3}) to a reaction mixture containing 2 x 10^{-6} mol dm^{-3} $FePc(Cl)_{16}$ catalyst and (0.2 mol dm^{-3}) cyclohexane. Spectra **(a)** before and **(b)** immediately after the addition of oxidant.

The Q band of the $FePc(Cl)_{16}$ catalyst in the DMF:CH_2Cl_2 solvent mixture was observed at 629 nm, **Figure 3.21(a)**, the wavelength is different from the one reported in **Section 3.1.4.**, (623 nm) since as reported before [76], the Q band shifts with each preparation. On addition of the CPBA oxidant to solutions of $FePc(Cl)_{16}$ catalyst and 0.2 mol dm^{-3} of the substrate (cyclohexane), the Q band maxima of $FePc(Cl)_{16}$ catalyst shifted from 629 to 647 nm, **Figure 3.21(b)**. The new spectra is similar to the spectra obtained following chemical oxidation of $FePc(Cl)_{16}$ using bromine, hence confirms the involvement of an $Fe^{III}Pc(Cl)_{16}$ species. Oxidation of iron phthalocyanine complexes occurs at the central metal prior to ring-based oxidation. Shifts of the Q band to higher wavelengths occur following the central metal oxidation in FePc complexes [61]. Following the formation of the Fe(III) perchlorophthalocyanine complex in **Figure 3.21**, a decrease in the Q band is observed without any new bands being formed, showing that the phthalocyanine complex degrades as the oxidation proceeds. Decomposition of the phthalocyanine ring was not observed in the absence of the oxidant.

As discussed above, a split in the Q band and its shifting to longer wavelengths following oxidation of Fe(II)Pc to the Fe(III)Pc species has been reported [61]. The splitting is not observed in **Figure 3.21 (b)**, and was also not observed when other oxidants, such as bromine, were employed. The split in the Q band was however observed for the oxidations employing $[Fe^{II}TSPc]^{4-}$ catalyst as discussed above, **Figure 3.14.**

As mentioned above for the $[Fe^{II}TSPc]^{4-}$ catalyst, it is proposed that the Fe(III)(OOR) phthalocyanine species is an intermediate in the oxidation of cyclohexane catalyzed by

$FePc(Cl)_{16}$ complex. The decomposition of the phthalocyanine complex during the oxidation of cyclohexane, **Figure 3.21**, is a result of the attack of the phthalocyanine ring by the $RO^{\cdot}$ and $ROO^{\cdot}$ radicals.

When TBHP was used as an oxidant, the formation of the Fe(III) phthalocyanine complex was not observed, as shown in **Figure 3.22**.

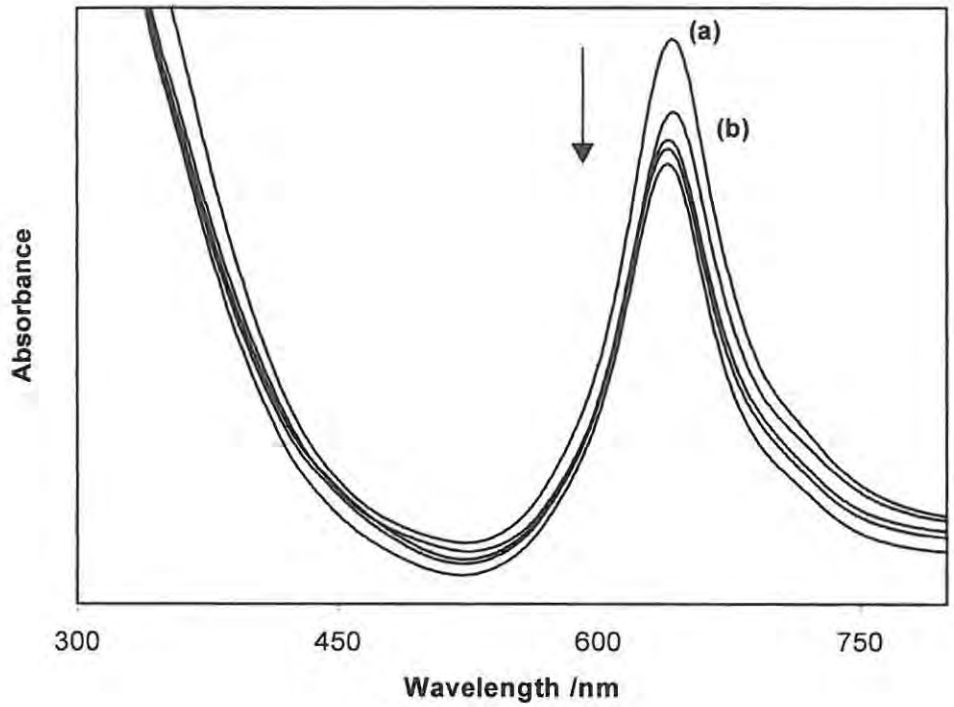

Figure 3.22 Electronic absorption spectral changes observed on addition of TBHP oxidant (0.8 mol dm^{-3}) to a reaction mixture containing 2 x 10^{-6} mol dm^{-3} $FePc(Cl)_{16}$ catalyst and (0.2 mol dm^{-3}) cyclohexane. Spectra **(a)** before and **(b)** immediately after the addition of oxidant.

Spectral changes for $FePc(Cl)_{16}$ observed during the oxidation of cyclohexane by TBHP consisted of a small decrease in the Q band without much shift of the wavelength. As discussed above, shifts to longer wavelength shown in **Figure 3.21** are associated with central metal oxidation and the formation of an Fe(III) phthalocyanine species. Such shifts were not observed when using TBHP as an oxidant as shown in **Figure 3.22.**

It is possible that the Fe(III)(OOR) phthalocyanine intermediate is formed as proposed above when CPBA is employed as an oxidant, but that this intermediate is readily reduced back to an Fe(II) phthalocyanine species when TBHP was employed as an oxidant.

Also the phthalocyanine ring is not significantly destroyed by the radicals when TBHP is employed as an oxidant as judged by lack of a significant decrease in the Q band even after prolonged reaction times. The TBHP oxidant contains electron-donating methyl groups whereas the CPBA oxidant contains electron-withdrawing groups in its molecule, **Figure 3.23**. Ring destruction in phthalocyanines has been reported to be through oxidative degradation [80].

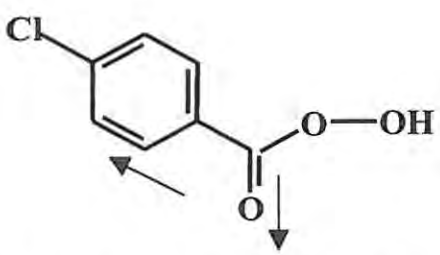

m-Chloroperoxybenzoic Acid

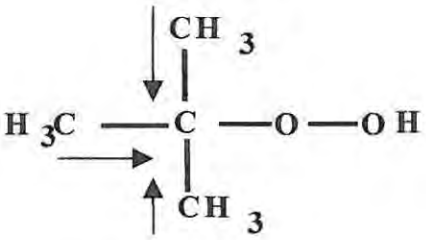

Tert-Butylhydroperoxide

Figure 3.23 The structure of *tert*-butylhydroperoxide (TBHP) and *m*-chloroperoxybenzoic acid (CPBA)

The RO· and ROO· radicals generated from the TBHP oxidant contain electron-donating groups hence these radicals are less destructive to the phthalocyanine ring. Whereas the radicals from the CPBA oxidant contain electron-withdrawing substituents, hence the phthalocyanine ring is more readily degraded through an oxidative mechanism.

The fact that the spectra for the Fe(III) phthalocyanine species is not observed when TBHP is employed as an oxidant, suggests that this intermediate is not stable in the presence of the electron-donating TBHP oxidant, but is stable in the presence the electron-withdrawing CPBA oxidant.

When hydrogen peroxide was employed as an oxidant, total destruction of the phthalocyanine ring was observed with time, without formation of the intermediate

Fe(III) phthalocyanine species, when using the $FePc(Cl)_{16}$ catalyst. Thus this catalyst is not stable to hydrogen peroxide and to a lesser extent, to CPBA oxidants, but is stable to TBHP.

3.4 Electrocatalytic oxidation using $[CoTSPc]^{4-}$

$[FeTSPc]^{4-}$, $[MnTSPc]^{4-}$ and $[CoTSPc]^{4-}$ were tried as electrocatalysts for the oxidation of 4-pentenoic acid but only $[CoTSPc]^{4-}$ showed some catalytic behavior, hence only the discussion of this complex is included in this chapter. $[CoTSPc]^{4-}$ complex is water-soluble and therefore it was ideal for homogeneous catalytic oxidation of 4-pentenoic acid. **Figure 3.24** shows the structure of 4-pentenoic acid. This complex was chosen for this study because of water solubility. The study was undertaken as a first step in establishing conditions for possible use of Pcs as electrocatalysts for alkane and alkene oxidations.

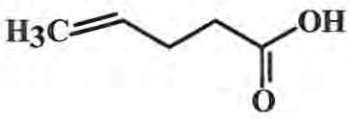

Figure 3.24 Structure of 4-pentenoic acid

Figure 3.25 (a) shows the cyclic voltammogram of the solution of $[CoTSPc]^{4-}$ in pH 7 buffer obtained on a glassy carbon electrode (GCE). Two processes (**I** and **II**) are observed. These are assigned to $Co^{III}Pc(-2)/Co^{II}Pc(-2)$ and $Co^{III}Pc(-1)/Co^{III}Pc(-2)$, (where Pc (-2) = phthalocyanine dianion) oxidations following the literature [81]. On the addition of 0.1×10^{-3} mol dm^{-3} 4-pentenoic acid, there was a significant enhancement of anodic peak currents for both process **I** and **II** at 716 mV and 898 mV. There was also an

improvement in the reversibility, in that there are return peaks following the addition of 4-pentenoic acid, **Figure 3.25 (b)**. There was no significant shift in oxidation potentials.

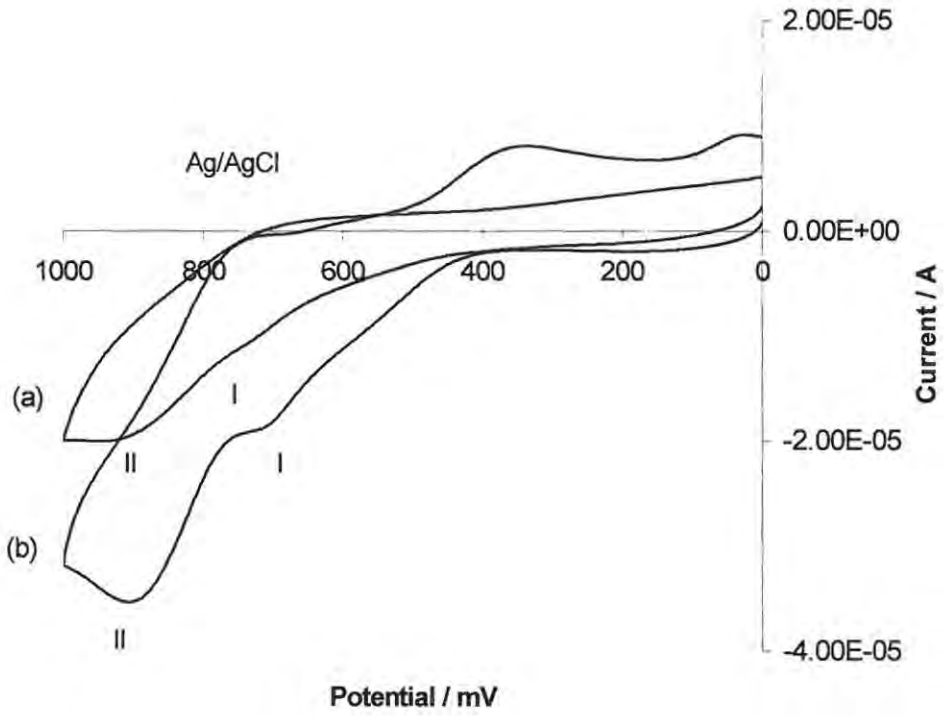

Figure 3.25 (a) Cyclic voltammogram of $[CoTSPc]^{4-}$ in blank (pH 7 buffer). **(b)** Cyclic voltammogram of $[CoTSPc]^{4-}$ in the presence of 4-pentenoic acid, 0.1 x 10^{-3} mol dm^{-3}. Scan rate 100mVs^{-1}.

As the concentration of 4-pentenoic acid is increased there is an increase in the anodic peak currents, **Figure 3.26,** showing that $[CoTSPc]^{4-}$ does electrocatalyze the oxidation of 4-pentenoic acid. Both processes **I** and **II** showed an increase in currents but larger increases in currents were observed for process **II,** involving the ring oxidation, suggesting that both $Co^{III}Pc(-2)$ and $Co^{III}Pc(-1)$ species may be involved in the catalytic

processes. The increase of currents in the presence of analyte is typical of catalytic processes.

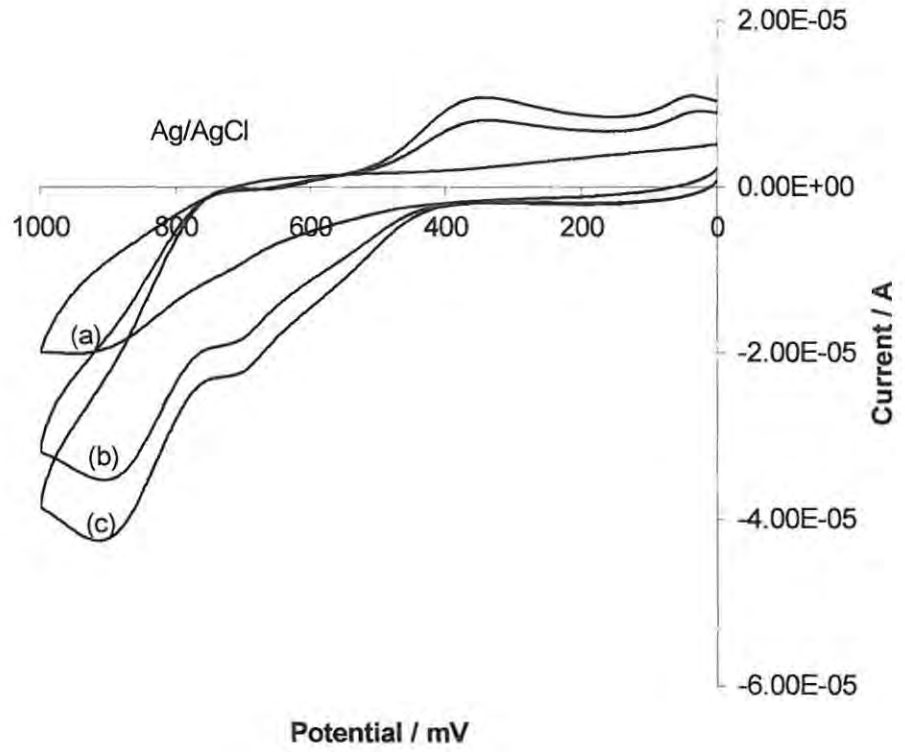

Figure 3.26 Cyclic voltammogram of $[CoTSPc]^{4-}$ in **(a)** blank (pH 7 buffer) and in the presence of **(a)** 4-pentenoic acid, **(b)** 0.1 x 10^{-3} mol dm^{-3} and **(c)** at 0.2 mol dm^{-3}. Scan rate 100mVs^{-1}.

The plot of the square root of scan rate versus peak currents, on GCE in $[CoTSPc]^{4-}$ in pH 7 buffer solution, is nearly linear at scan rates ranging from 50 to 400 mV/sec which indicates diffusion control, **Figure 3.27.**

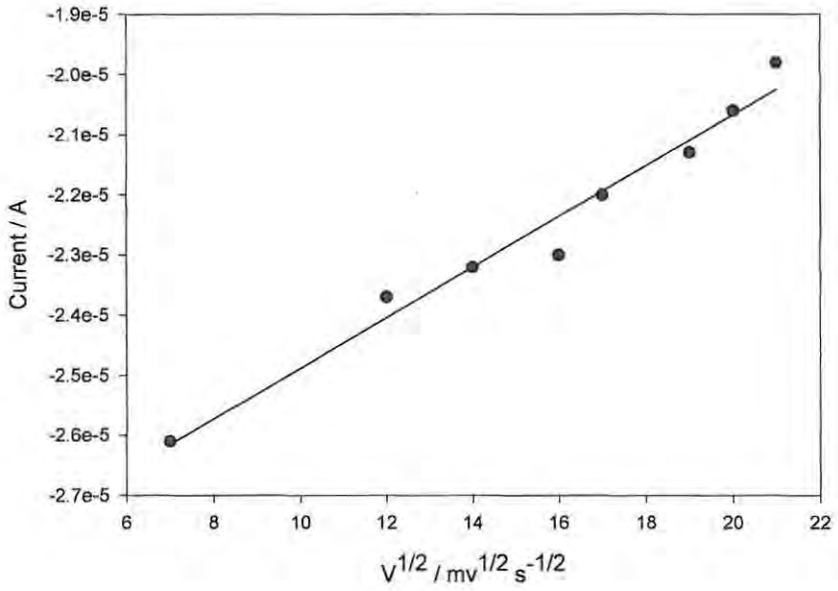

Figure 3.27 Variation of peak currents for 4-pentenoic acid oxidation with the square root of scan rate on GCE. 4-Pentenoic acid concentration 0.3×10^{-3} mol dm^{-3}.

The electrocatalytic oxidation of 4-pentenoic acid using $[CoTSPc]^{4-}$ catalyst was followed spectroscopically using an OTTLE cell. As mentioned before, $[M^{II}TSPc]^{4-}$ exists in a dimer-monomer equilibrium in an aqueous medium. At the start of the electrocatalytic reaction $[CoTSPc]^{4-}$ complex exists mainly as a dimer in pH 7 buffer and in the presence of 0.1 mol dm^{-3} 4-pentenoic acid, **Figure 3.28 (a)**. The Q band of the

dimer was observed at 625 nm under these conditions and the peak due to the monomer was not clearly evident. As explained before the monomer-dimer equilibrium in MTSPc species depends on conditions such as pH, electrolytes and solvent.

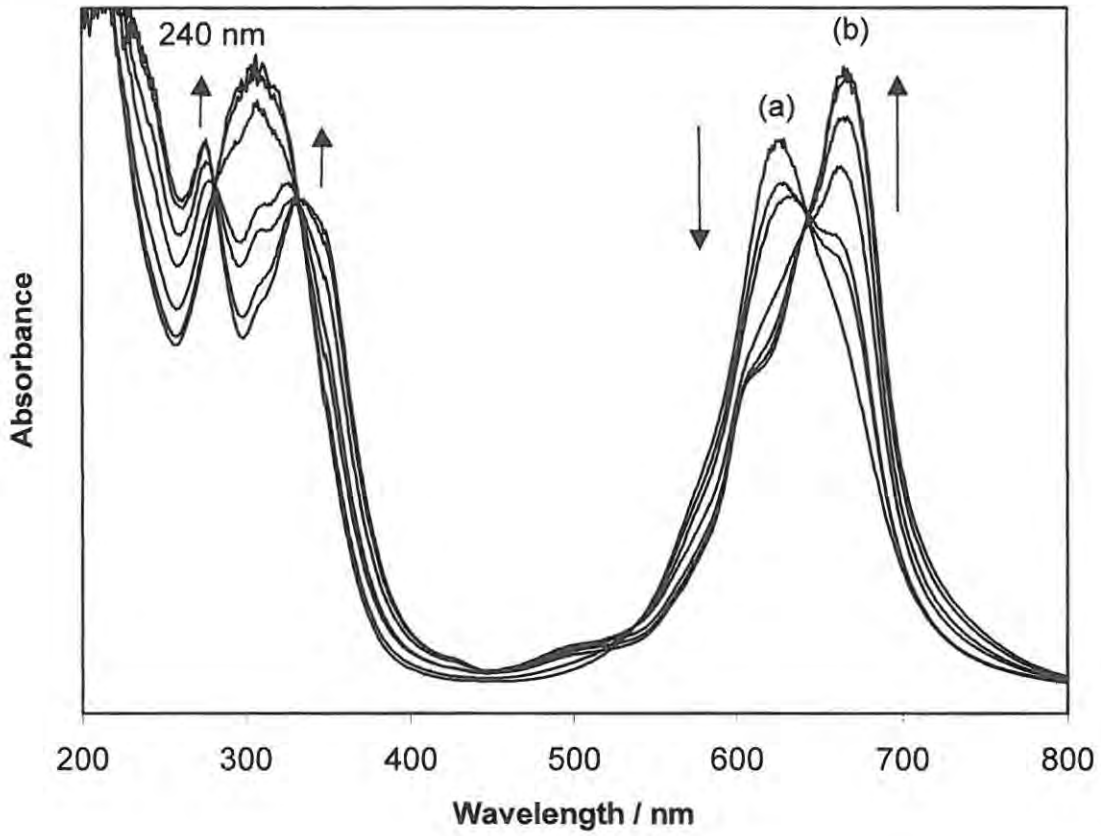

Figure 3.28 Thin-layer spectra of $[CoTSPc]^{4-}$ containing 0.1 mol dm^{-3} 4-pentenoic acid at an applied potentials of process **I, Figure 3.25(a)** before electrolysis and **(b)** after electrolysis. In pH buffer 7.

Following application of potential for the first oxidation of $[Co^{II}TSPc]^{4-}$ (process **I**), this complex undergoes one-electron oxidation from $[Co^{II}TSPc]^{4-}$ (Q band at 625 nm) to $[Co^{III}TSPc]^{3-}$ (Q band at 671 nm), **Figure 3.28**. The confirmation of the formation of $[Co^{III}TSPc]^{3-}$ comes from the fact that spectral changes similar to those shown in **Figure**

3.15 were observed when $[Co^{II}TSPc]^{4-}$ was chemically oxidized, forming $[Co^{III}TSPc]^{3-}$. As the reaction proceeds, there is a decrease in $[Co^{II}TSPc]^{4-}$ at 625 nm and an increase in the oxidized species $[Co^{III}TSPc]^{3-}$ at 671 nm. The final spectra in **Figure 3.28** is typical of monomeric species. In addition a split in the B band and an increase in absorption in the 240 nm region were observed. The split in the B band is typical of axial ligation to MPc complexes, as discussed above.

Similar increase in a band in the 240 nm region was reported by Liu and Su [59] and they assigned the band to the production of the oxidized enone product. In a similar manner the band at 240 nm is assigned to the formation of enone product from 4-pentenoic acid , see **Scheme11** (later).

Spectral changes in **Figure 3.28** show that $[Co^{III}TSPc]^{3-}$ still remains at the end of the reaction, this is unexpected. If this species, catalyzed oxidation of alkenes it would be expected to be reduced back to $[Co^{II}TSPc]^{4-}$ by **equation 8**, and there would be no spectral changes.

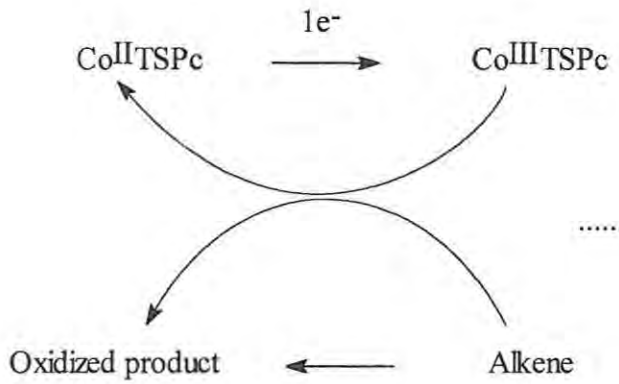

.....**Equation (8)**

The observed presence of $[Co^{III}TSPc]^{3-}$ suggested that it is the ring oxidized $[Co^{III}TSPc(-1)]^{2-}$ which is involved in catalysis, confirming CV data which shows a greater enhancement of the ring oxidation process.

A solution of 4-pentenoic acid and $[Co^{II}TSPc]^{4-}$ was left in a sample holder for some time without electrochemical oxidation and spectral changes shown below, **Figure 3.29** were observed after a prolonged time.

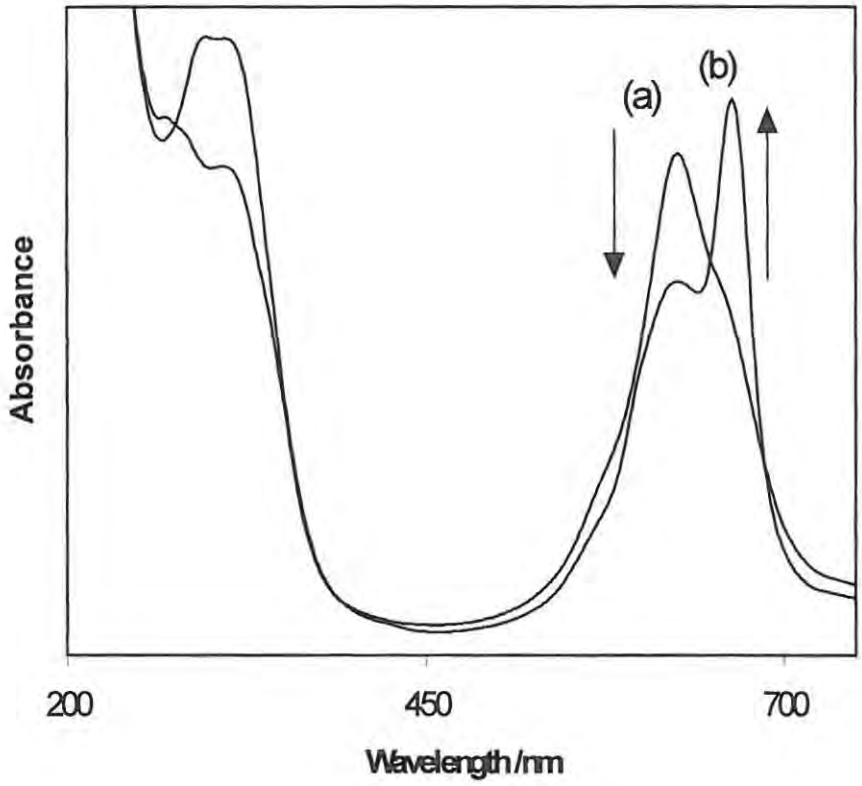

Figure 3.29 Solution of $[CoTSPc]^{4-}$ containing 0.1 mol dm^{-3} 4-pentenoic acid

(a) at zero and **(b)** after 64 hours

These changes are similar to those shown in **Figure 3.28**, except the 240 nm band was not observed, hence 4-pentenoic acid was not oxidized. But a split in the B band was observed. The Q band shifted to 669 nm, a wavelength slightly different from the one observed in **Figure 3.28** for $[Co^{III}TSPc]^{3-}$ formation.

These changes may be supported either by air oxidation of $[Co^{II}TSPc]^{4-}$ or axial ligation of 4-pentenoic acid to $[Co^{II}TSPc]^{4-}$. Axial ligation would also result in the formation of the monomeric species. However no spectral changes were observed with time when $[Co^{II}TSPc]^{4-}$ was left in air, hence proving that spectral changes shown in **Figure 3.29** are not due to air oxidation of $[Co^{II}TSPc]^{4-}$, but most likely due to axial ligation of 4-pentenoic acid. As discussed above (**Section 3.1.7**) a split in the B band is observed on axial ligation of species to MPc complexes, which is observed in **Figure 3.29.**

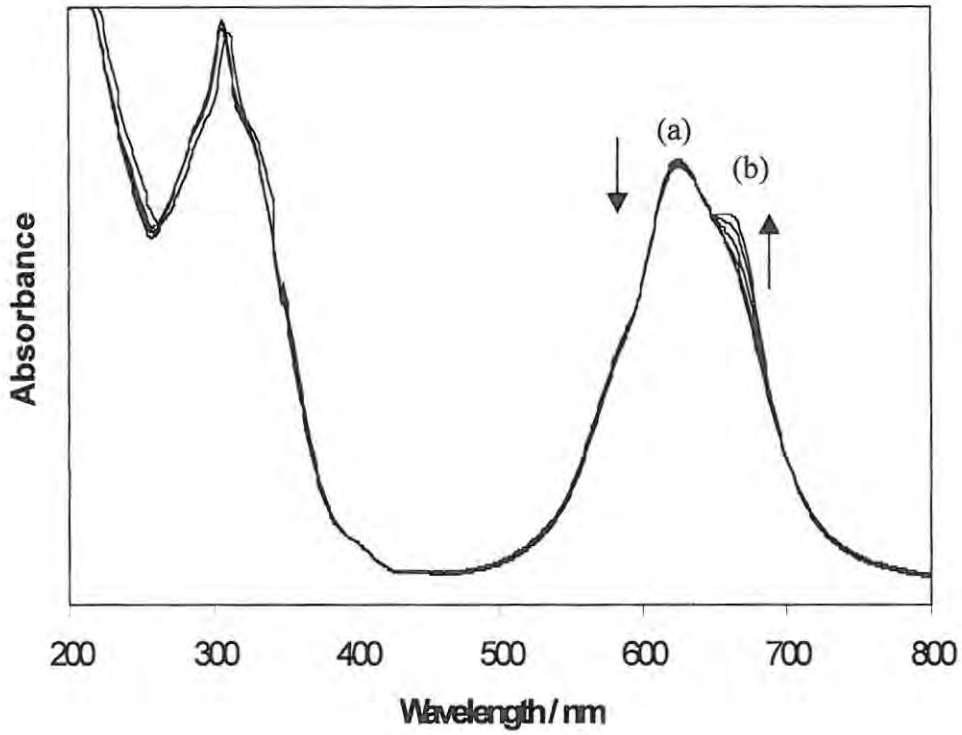

Figure 3.30 Thin-layer spectra of $[CoTSPc]^{4-}$ on application of potentials for first oxidation of MTSPc. Spectra (a) before electrolysis (b) after electrolysis

Electrolysis of $[Co^{II}TSPc]^{4-}$ in the absence of 4-pentenoic acid, as shown in **Figure 3.30** show no splitting in the B band and no formation of a band in the 240 nm region. A very slow oxidation of $[CoTSPc]^{4-}$ was evident by a gradual increase in the band near 669 nm.

The mechanism proposed for the electrocatalytic oxidation of 4-pentenoic acid in the presence of $[Co^{II}TSPc]^{4-}$ is given by **Scheme 11**.

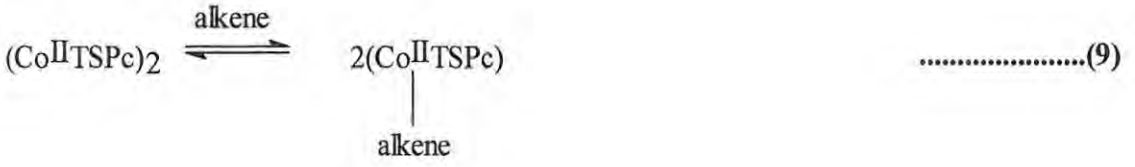

.....(9)

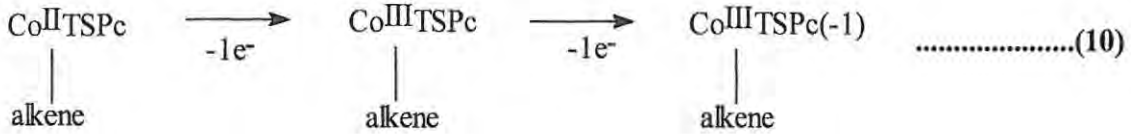

.....(10)

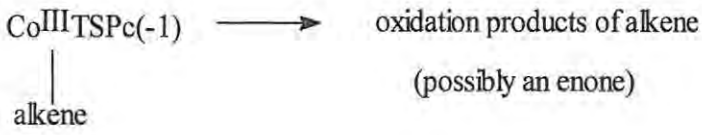

.....(11)

Where alkene = 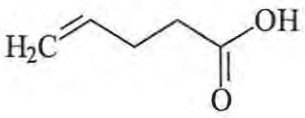

Scheme 11 Proposed mechanism for the electro-oxidation of 4-pentenoic acid

Equation (9) was proved from **Figure 3.29** which shows the monomeric species (accompanied by axial ligation) is formed in the presence of 4-pentenoic acid. **Equation**

(10) is a result of the oxidation of $[Co^{II}TSPc]^{4-}$ to $[Co^{III}TSPc]^{3-}$ during the electrocatalytic process, which was proved by **Figure 3.25** and **Figure 3.28**. The involvement of Pc(-1) by **equation 11** is proved by CV, **Figure 3.25**, where the enhancement of CV peaks due to ring based oxidation process were observed. The nature of the oxidation product was not unequivocally determined, since UV/visible spectroscopy is not a very accurate tool for characterization of species. The formation of an enone derivative is proposed based on literature reports using porphyrin cataysts [59]. Attempts were made to follow the electrolytic reaction by GC. This involved using bulk electrolysis as explained in **Section 2.3.2**. The amounts of oxidation products obtained were not significant enough to be detected by GC. Hence GC/MS was not employed in the analysis of the alkene oxidation products.

4. Conclusion

In conclusion, it has been shown in this work that iron, cobalt and manganese phthalocyanine complexes containing peripheral substituents catalyze the oxidation of cyclohexane through a biomimetic process. The success of the catalytic process depends on the stability and solubility of the catalyst. For some oxidants, the radicals generated during the catalytic process attack the phthalocyanine ring, destroying it. For $FePc(Cl)_{16}$, $[Fe^{II}TSPc]^{4-}$, $[Co^{II}TSPc]^{4-}$ and $[Mn^{II}TSPc]^{4-}$ catalysts, the largest degradation of the ring was observed when the CPBA and hydrogen peroxide oxidants were employed. The stability of the ring in the presence of the TBHP oxidant is attributed to the electron donating nature of the oxidant, which stabilizes the ring from oxidative degradation.

The $[Fe^{II}TSPc]^{4-}$ complex showed higher catalytic activity compared to the perchlorinated iron phthalocyanines. This could be a reflection of the greater solubility of the former. The $[CoTSPc]^{4-}$ and $[MnTSPc]^{4-}$ complexes showed considerably lower catalytic activities when compared to $[FeTSPc]^{4-}$ complex. For $[CoTSPc]^{4-}$ complex this was attributed to the strong ligation of either TBHP or cyclohexane to $[CoTSPc]^{4-}$. For $[MnTSPc]^{4-}$ complex the low catalytic activity was attributed to the formation of H_2TSPc complex in a methanol:water solvent mixture.

The products formed from catalytic oxidation of cyclohexane employing $[MTSPc]^{4-}$ complexes are cyclohexanone, cyclohexanol and cyclohexanediol. For $FePc(Cl)_{16}$ the amount of cyclohexanediol detected was insignificant compared to cyclohexanol and

cyclohexanone. The relative percentage yields, percentage selectivity and overall percentage conversion of each product depended on the type of oxidant, type of catalyst, the concentration of substrate, the concentration of catalyst and lastly the temperature at which the reaction proceeds at. The selectivity in the products generally decreased as the overall percentage conversion increased.

$[CoTSPc]^{4-}$ was the only complex that electrocatalysed the oxidation of 4-pentenoic acid. $[FeTSPc]^{4-}$ and $[MnTSPc]^{4-}$showed no catalytic activity. During the electrocatalytic process no degradation of the $[CoTSPc]^{4-}$ complex was observed.

References

[1] Centri G., Cavani F. and Trifiró F., ***Selective Oxidation by Heterogeneous Catalysis,*** 1st edn, Kuwer Academic Plenum Publishers (New York), 2001,

[2] Hill C.L. (Ed), ***Activation and Functionalization of Alkanes***, 1st edn, John Wiley and Sons (New York),1989, pg1-26, 192-214.

[3] Shriver D.F., Atkins P.W. and Langford C.H., ***Inorganic Chemistry***, 2nd edn, Oxford University Press (U.K), 1994, pg 806, 809-811

[4] Lever A.B.P., ***Adv. Inorg Radiochem.***, **7** (1965) 27

[5] Ah Lee K. and Nam W., ***J. Am. Chem. Soc.,* 119** (1997) 1916

[6] Newcomb M., Shen R., Choi S-Y., Toy P.H., Hollenberg P.F., Vaz A.D.N. and Coon M.J., ***J. Am. Chem. Soc.,* 122** (2000) 2677

[7] Toy P.H., Newcomb M., Coon M.J. and Vaz A.D.N., ***J. Am. Chem. Soc.,* 120** (1998) 9718

[8] Pratt J. M., Ridd T.I. and King L.J., ***J. Chem. Soc. Chem. Commun.,*** (1995) 2297

[9] Nam W., Lim M. H., Moon S.K. and Kim C., ***J. Am. Chem. Soc.,* 122** (2000) 10805

[10] Groves J.T., Nemo T.E. and Myers R. S., ***J. Am. Chem. Soc.,* 101** (1979) 1032

[11] Nappa M. J. and Tolman C.A., ***Inorg Chem.***, **24** (1985) 4711

[12] Mansuy D., Bartoli J. F.and Momenteau M., ***Tetrahedron Lett.***, **23** (1982) 2781

[13] Mansuy D., Bartoli J. F., Chottard J.C. and Lange M., ***Agnew.Chem.*, 19** (1980) 909

[14] Groves J.T. and Nemo T.E., ***J. Am. Chem. Soc*, 105** (1983) 6243

[15] Groves J.T., Kruper W.J. Nemo T.E. and Myers R. S., ***J. Mol. Catal.*,7** (1980) 169

[16] Chang C.K. and Ebina F., ***J. Chem. Soc., Chem. Commun.*,** (1981) 778

[17] Traylor P. S., Dolphin D. and Traylor T.G., ***J. Chem. Soc., Chem. Commun.*,** (1984) 279

[18] Mansuy D, Bartoli J.F and Momenteau M, ***Tetrahedron Lett*, 23** (1982) 2781

[19] Thellend A., Battiono P. and Mansuy D., ***J. Chem. Soc., Chem. Commun.*,** (1994) 1035

[20] Gonsalves A.M.d`A. and Serra A.C., ***J. Porphyrins Phthalocyanines*, 4** (2000) 598

[21] Cortés Corberán V. and Vic Bellón S., ***New development in selective oxidation II***, Elsevier Science Publishers, Amsterdam, 1994

[22] Kaliya O.L., Lukyannets E.A., and Voorozhtsov G.N., ***J. Porphyrins Phthalocyanines*, 3** (1999) 592

[23] McKeown N.B., ***Out of the Blue***, Chem. and Indust., (1999) 92

[24] Ratnasamy P. and Raja R., ***European Patent***, EP 0 784 045 A1

[25] Chan Y.W. and Wilson R.B., ***Jr. ACS National Meeting*, 33** (1998) 453

[26] Raja R. and Ratnasamy P., ***Appl. Catal A:Gen*, 158** (1997) L7-L15

[27] Parton R.F., Peere G.J., Nyeys P.E., Claessens R., Baron G.V. and Jacobs P.A., ***J. Mol. Catal. A:Chem.*, 113** (1996) 445

[28] Vankelecom I.F.J., Parton R.F.,Casselman M.J.A., Uytterhoeven J.B and Jacobs P.A., ***Catal.*, 163** (1996) 457

[29] Balkus K.J., Eissa M. and Lavado R., ***Stud. Surf. Sci. Catal.*, 94** (1995) 713

[30] Armengol E., Corma A., Fornés V., García and Primo J., ***Appl. Cat. A: General*, 181** (1999) 305

[31] Neys P.E., Parton R.F., Jacobs P.A., Sosa R.C., Lardinois O. and Rouxhet P.G., ***J. Mol. A:Chem.*, 110** (1996) 141

[32] Meunier B. and Sorokin A., ***Acc. Chem. Res.*, 30** (1997) 470

[33] Sorokin A., De Suzzoni-Dezard S., Poullain D., Noël J-P. and Meunier B., ***J. Am. Chem. Soc.*, 118** (1996) 7418

[34] Hadasch A., Sorokin A., Rabion A., Fraisse L. and Meunier B., ***Bull. Soc. Chim. Fr.*, 134** (1997) 1025

[35] Hadasch A., Sorokin A., Rabion A., Fraisse L. and Meunier B., ***New J. Chem.*,** (1998) 45

[36] Sorokin A. and Meunier B., ***J. Chem. Soc., Chem. Commun.*,** (1994) 1799

[37] Kasuga K., Mori K., Sugimori T. and Handa M., ***Bull. Chem. Soc. Jpn.*,73** (2000) 939

[38] Sorokin A., Séris J-L. and Meunier B., ***Science,* 268** (1995) 1163

[39] Nyokong T., ***J. Chem. Soc. Dalton Trans.,*** (1994) 1359

[40] Mafatle T. and Nyokong T., ***Anal. Chim. Acta,* 354** (1997) 307

[41] Chebotareva N. and Nyokong T., ***Electrochim. Acta,* 42** (1997) 3519

[42] Mafatle T. and Nyokong T., ***J. Electroanal.Chem.,* 408** (1996) 213

[43] Limson J. and Nyokong T., ***Electroanalysis,*10** (1998) 988

[44] Tse Y.H., Janda P., Lam H. and Lever A.B.P., ***Anal. Chem.,*67** (1995) 981

[45] Halbert M.K. and Baldwin R.P., ***Anal. Chem.,*57** (1985) 591

[46] Zagal J.H., ***Coord. Chem, Rev.,* 119** (1992) 89

[47] Thamae M.and Nyokong T., ***J. Electroanal. Chem.,* 470** (1999) 126

[48] Vilakazi S.and Nyokong T., ***Polyhedron,* 17** (1998) 4415

[49] Zecevic S., Simic-Glavaski B., Yeager E., Lever A.B.P. and Minor P.C., ***J. Electroanal. Chem.,* 196** (1985) 339

[50] Janda P., Kobayashi N., Auburn P.R., Lam H., Leznoff C.C. and Lever A.B.P., ***Can. J. Chem.,* 67** (1989) 1109

[51] Huang X. and Kok W.Th., ***Anal. Chim. Acta,* 273** (1993) 245

[52] Napeir A. and Hart J.P., ***Electroanalysis,* 8** (1996) 1006

[53] Maree S.and Nyokong T., ***J. Electroanal. Chem.,* 492** (2000) 120

[54] Premkumar J. and Ramaraj R., ***J. Photochem.Photobiol. A:Chem.,*110** (1997) 53

[55] Abe T., Yoshid T., Tokita S., Taguchi F., Imaya H. and Kaneo M., ***J. Electroanal. Chem.,*412** (1996) 125

[56] Lieber C.M.and Lewis N.S., ***J. Am. Chem. Soc.,*106** (1984) 5033

[57] Li J.Z., Pang X.Z. and Yu R.Q., ***Anal. Chim. Acta,* 297** (1994) 437

[58] Chebotareva N. and Nyokong T., ***J. Appl. Electrochem.,* 27** (1997) 975

[59] Liu M. and Su Y.O., ***J. Electroanal. Chem.,* 426** (1997) 197

[60] Liu M. and Su Y.O., ***J. Chem. Soc., Chem. Commun.,***(1994) 971

[61] Stillman M.J. and Nyokong T., in Leznoff C C and Lever A.B.P (editors), ***Phthalocyanines: Properties and applications***, Vol 1, VCH publishers (New York)1989.

[62] Minor P.C., Gouterman M. and Lever A.B.P., ***Inorg. Chem.,* 24** (1985) 1894

[63] Nyokong T., ***S. Afr. J. Chem.,* 48** (1995) 23

[64] Lever A.B.P., Pickens S. R., Minor P.C., Licoccia S., Ramaswamy B.S. and Magnell K., ***J. Am. Chem. Soc.,* 103** (1981) 6800

[65] Stillman M.J. and , in Leznoff C C and Lever A.B.P (editors), ***Phthalocyanines: Properties and applications***, Vol 3, Ch .5.1st edn., VCH publishers (New York) 1993.

[66] Kissinger P.T and Heineman W.R., ***Laboratory Techniques in Electroanalytical Chemistry***, 2nd edn, Marcel Dekker, Inc., (U.S.A), 1996, pg 73, pg84-90

[67] Bard A.J.and Faulkner L.R., ***Electrochemical Methods-Fundamentals and Applications***,1st edn, John Wiley and Sons, (USA), 1980, 224

[68] Mezt J., Schneider O. and Hanack M., ***Inorg. Chem.,* 23** (1984) 1065

[69] Weber J.H. and Busch D.H., ***Inorg. Chem.,* 4** (1965) 469

[70] Oni J. and Nyokong T.,***Polyhedron,* 19** (2000) 3125

[71] Rollman L.D. and Iwamoto R.T., ***J. Am. Chem. Soc.,* 90** (1986) 1455

[72] Gruen L.C. and Blagrove R.J., ***Aust. J. Chem.,*26** (1973) 322

[73] Abel E.W., Pratt J.M. and Whelan R., ***J. Chem. Soc., Dalton Trans.,*** (1976) 509

[74] Shurvell H.F. and Pinzuti L., ***Can. J. Chem.,* 44** (1966) 125

[75] Cookson J.D., Smith T.D., Boes J.F. and Pilbrow J.R., ***J. Chem. Soc., Dalton Trans.,*** (1976) 1719

[76] Golovin M.N., Seymour P., Jayaraj K., Fu Y-S. and Lever A.B.P., ***Inorg. Chem.,* 29** (1990) 1727

[77] Nam W., Lee H.J, Oh S.-Y.,Kim C. and Jang H.G., ***J. Inorg. Biochem.,* 80** (2000) 219

[78] Moore K.T., Horváth E.A. and Therien M.J., ***Inorg. Chem.,* 39** (2000) 3125

[79] Battionoi P., Cardin E., Louloudi M., Schöllhorn B., Spyroulias G.A, Mansuy D. and Traylor T.G., ***Chem Commun.,*** (1996) 2037

[80] Borisenkova S.A., Denisova E.P., Batanove E.A., Girenko E.G., Kaliya O., Lukyanets E.A. and Vorozhtsov G.N., ***J. Porphyrins Phthalocyanines,*** **4** (2000) 684

[81] Lever A.B.P., Milaeva E.R. and Speier G., in Leznoff C C and Lever A.B.P (editors), ***Phthalocyanines: Properties and applications***, Vol 3, Ch .1., VCH publishers (New York) 1993.